Pattie Mathieu M.S.

Multipotent Vascular Stem Cells and the Effects of Cyclic Tensile Strain, Collagen Structure and Stenting on Medial Vascular Cell Populations

Trinity College Dublin 2020

A thesis submitted to Trinity College Dublin in partial fulfilment of the requirements for the degree of

Doctor in Philosophy

Supervisors: Prof. Caitríona Lally

Prof. Paul Cahill (DCU)

Internal Examiner: Prof. Conor Buckley

External Examiner: Prof. Abdul Barakat

Declaration

I declare that this thesis has not been submitted as an exercise for a degree at this or any other university and it is entirely my own work.

I agree to deposit this thesis in the University's open access institutional repository or allow the library to do so on my behalf, subject to Irish Copyright Legislation and Trinity College Library conditions of use and acknowledgement.

Pattie Mathieu

Summary

Atherosclerosis is one of the leading causes of mortality worldwide, and presents as a narrowing or occlusion of an artery. Interventions to re-open the arterial lumen (such as stenting) or bypass of the blocked areas (using vascular grafts) can result in re-occlusion through intimal hyperplasia and the formation of a neointima. Historically only de-differentiated vascular smooth muscle cells were thought to contribute to intimal hyperplasia. However recent significant evidence suggests that resident medial multipotent vascular stem cells (MVSC) may also play a role. Therefore the strain response of MVSCs was investigated since these resident cells are also subjected to strain within their native environment.

First, the differences between MVSC and vascular smooth muscle cell (VSMC) strain response were investigated by applying 1 Hz cyclic equiaxial strain for 24 hours, with or without TGF-β1, and evaluating the phenotypic response. In order to investigate a strain environment more similar to the one experienced *in vivo*, uniaxial 1Hz cyclic uniaxial tensile strain was applied at three amplitudes around a mean strain of 5%, (4-6%, 2-8% and 0-10%) for 24 or 72 hours to both cell types. The effect of extracellular matrix (ECM) was assessed by applying 0-10% 1Hz uniaxial tensile strain for 10 days. Finally, MVSC seeded on decellularized porcine carotid arteries were indented with a single wire strut either statically or dynamically to investigate MVSC response to stenting. Cells were evaluated for alignment and proliferation.

In equiaxial strain experiments MVSC became more contractile when exposed to strain, while VSMC showed no phenotypic change. When exposed to uniaxial tensile strain, both cell types respond similarly. While both cell types exhibit strain avoidance after 24 hours, the strain avoidant response was greater for MVSC, while VSMC strain avoid to a greater degree after 72 hours. Both cell types increase strain avoidance as strain amplitude is increased and demonstrate a strain-induced decrease in cell number. When cells are strained on decellularized ECM structures which induce cell alignment, differences between MVSC and VSMC become more apparent. While both MVSC and VSMC align parallel to the collagen fibre direction when left unstrained, when strained parallel to fibre direction, MVSC remained aligned with fibre direction, while in some cases VSMC showed strain avoidant realignment. MVSC aligned in the direction of strain showed increased proliferation, while, conversely, VSMC aligned with strain showed a decreased cell

number. When MVSC were tested with simulated stent strut indentation, they developed patches of dense, highly proliferative cells, mimicking what is seen in in-stent restenosis. These experiments demonstrate for the first time how the mechano-sensitivity of MVSC may play a role in in-stent restenosis. This further emphasizes the importance of strain and ECM structure in controlling the response of vascular cells in tissue engineering applications.

Acknowledgements

I'd like to thank everyone who has been so helpful and supportive throughout my entire PhD. First and foremost, I would like to thank my supervisor Prof. Caitríona Lally for all her help and support throughout my entire PhD. Without her encouragement, none of this would have been possible. I would also like to thank my co-supervisor Prof. Paul Cahill, for all of his expertise and advice on vascular stem cells

I would like to give a special thanks to Dr. Emma Fitzpatrick who worked with me as the other Lally Lab member over in TBSI. Your expertise in cell biology and vascular stem cells was highly appreciated, as was your willingness to be a shoulder to lean on. To all of my fellow students and postdocs in TCBE, I want to thank you for being a welcoming and collaborative community that made it a joy to come in to the lab, even on days when things were going wrong.

I would like to thank my parents for their support and understanding throughout the entire PhD process, and especially for taking my cats, even though I promised when I got them that they never would. Finally, I would like to thank my boyfriend Adam for being there for me through all the ups and downs that come throughout the PhD process. I don’t know how I would have done it without your love and support.

List of Publications and Conference Proceedings

First Author Publications

Mathieu, P.S., Fitzpatrick, E., Di Luca, M., Cahill, P.A., Lally, C. Resident Multipotent Vascular Stem Cells Exhibit Strain Amplitude Dependent Strain Avoidance Similar to that of Vascular Smooth Muscle Cells. Biochemical and Biophysical Research Communications. Available online 6 November 2019

Mathieu, P.S., Fitzpatrick, E., Cahill, P.A., Lally, C. Multipotent Vascular Stem Cells: Insights into Potential Mechanical Responses (*In Preparation*)

Mathieu, P.S., Fitzpatrick, E., Di Luca, M., Cahill, P.A. Lally, C. Multipotent Vascular Stem Cell Strain-Induced Proliferation is Dictated by Orientation of ECM Fibres (*In Preparation*)

Conference Proceedings

Mathieu, P.S., Fitzpatrick, E., Cahill, P.A., Lally, C. (June 2019) The influence of cyclic tensile strain and collagen structure on the alignment and proliferation of multiple vascular cell types. TERMIS European Chapter Meeting 2019. Rhodes, Greece.

Mathieu, P.S., Fitzpatrick, E., Cahill, P.A., Lally, C. (April 2019) Uniaxial Tensile Strain and Collagen Structure Affect Vascular Cell Orientation and Proliferation. 22nd Sir Bernard Crossland Symposium. Belfast, Ireland

Mathieu, P.S., Fitzpatrick, E., Cahill, P.A., Lally, C. (January 2019) Uniaxial Cyclic Tensile Strain and Native Collagen Structure Orientation Play a Critical Role in the Alignment and Proliferation of Vascular Smooth Muscle Cells and Multipotent Vascular Stem Cells. 25th Annual Conference of the Section of Bioengineering of the Royal Academy of Medicine in Ireland (BinI 2019). Limerick, Ireland

Mathieu, P.S., Fitzpatrick, E., Cahill, P.A., Lally, C. (June 2018) Vascular Smooth Muscle Cells and Multipotent Vascular Stem Cells Differ in their Response to Cyclic Tensile Strain. 2018 World Congress of Biomechanics. Dublin, Ireland

Mathieu, P.S., Fitzpatrick, E., Cahill, P.A., Lally, C. (January 2018) Vascular Smooth Muscle Cells and Multipotent Vascular Stem Cells Differ in their Response to Cyclic Tensile Strain. Bioengineering in Ireland 2018 Royal Academy of Medicine in Ireland Section of Bioengineering. Dublin, Ireland

Mathieu, P.S., Cahill, P.A., Lally, C. (January 2016) Strain Mediated Phenotypic Changes in Porcine Smooth Muscle Cells. Bioengineering in Ireland 2016 Royal Academy of Medicine in Ireland Section of Bioengineering. Galway, Ireland

Mathieu P, Cahill P, Mackle J, King J, and Lally C (June 2015). Phenotypic Changes in Rat Smooth Muscles Cells Exposed to Varying Amplitudes of Cyclic Equibiaxial Tensile Strain. UK Society of Biomaterials 2015 Annual Conference. Belfast, UK.

Contents

List of Figures

List of Tables

Chapter 1 Introduction

1.1 Research Motivation

Cardiovascular disease is the leading cause of death in the world with over 17.5 million deaths due to cardiovascular disease every year.[1] Vascular disease can lead to arterial stenosis, which can prevent blood flow to vital organs. Stents are small wire mesh devices that are used to physically open stenosed blood vessels and restore blood flow to these organs. Because of vascular disease, over 640,000 cardiac stents are deployed every year in the United States alone,[2] while stents are also used in other vessels such as the carotid artery. However, stenting can also cause other complications. As of 2015, between 5-10% of all stents failed due to restenosis, the re-occlusion of the vessel from intimal hyperplasia as can be seen in Figure 1.1.[3] Drug eluting stents have been used to try to prevent restenosis, however, these stents increase the risk of thrombosis, which can lead to stroke, heart attack, pulmonary embolism and death.[4] Therefore, there is still a need for improvement in stent designs. There is evidence that stent strut geometry can affect the amount and location of restenosis.[5] Mechanical models have also shown that these different stents result in different strain environments that correlate with the restenotic response of blood vessels.[6] Therefore understanding how these strain environments lead to restenosis will allow for the development of better stent designs, as well as help understand how to design new vascular devices that can limit restenosis or how best to engineer replacement blood vessels.

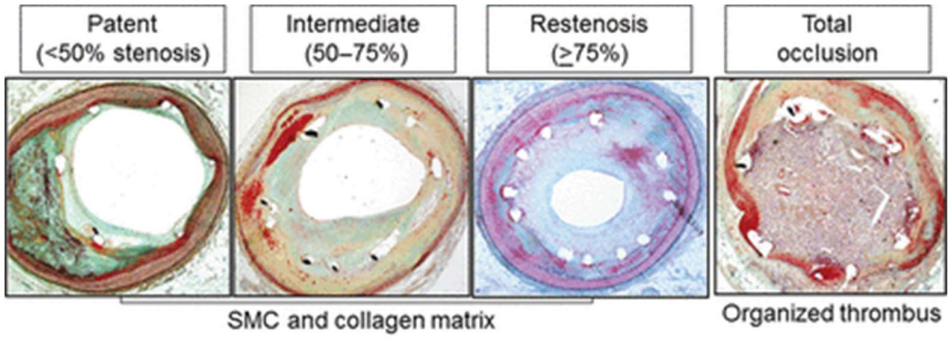

Figure 1.1: Stented blood vessels showing increasing degrees of restenosis., adapted from[7].

Understanding how vessel strain can influence vascular disease within arteries also requires understanding the underlying vascular anatomy. Arteries are composed of three main layers; the intima, the media and the adventitia, shown in Figure 1.2. The medial layer of

arteries is the thickest layer and provides most of the structural support for the vessel. This layer is composed of a collagen and elastin fibre matrix and vascular smooth muscle cells (VSMC). Collagen fibres provide the majority of the mechanical support within the arterial wall.[8] Collagen fibres are oriented in a helical fashion in two families of fibres.[9] However, collagen fibre orientation has also been shown to reorient parallel to stent strut under certain stenting conditions.[10,11]

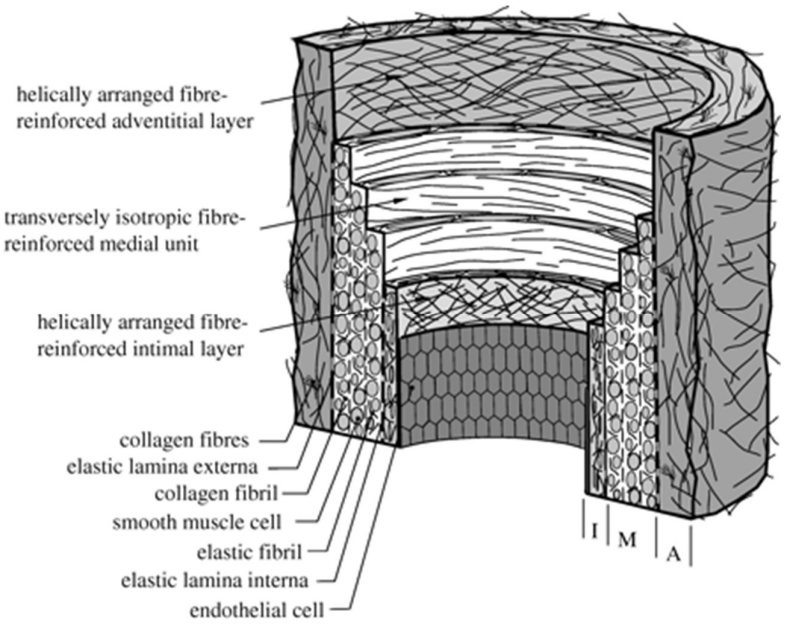

Figure 1.2: Arrangement of extracellular matrix within a vessel wall. Adapted from [9]

Different types of cells have been identified within the medial wall including VSMC and multipotent vascular stem cells (MVSC)[12] located in the vessel as shown in Figure 1.3 VSMC are the predominant cell type in the medial layer and it is traditionally thought that VSMC were the cells that were proliferating in in-stent restenosis. However, recent research has suggested that instead MVSC migrate to the intimal surface and proliferate there.[12] VSMC are known to be a mechanosensitive cell type, with uniaxial tensile strain causing strain-avoidant realignment of cells perpendicular to strain direction.[13-17] *In vivo,* VSMC align parallel to the collagen fibres which is also parallel to the primary strain direction within the vessel. Alignment of VSMC, relative to the strain direction, has been shown to influence how VSMC react to tensile strain.[18] Despite their potential role in causing in-stent restenosis, MVSC response to mechanical forces has not previously been explored. Further exploring these MVSC and their responses to mechanical forces involved in vascular disease and stenting will allow for a better understanding the role they play in vascular disease.

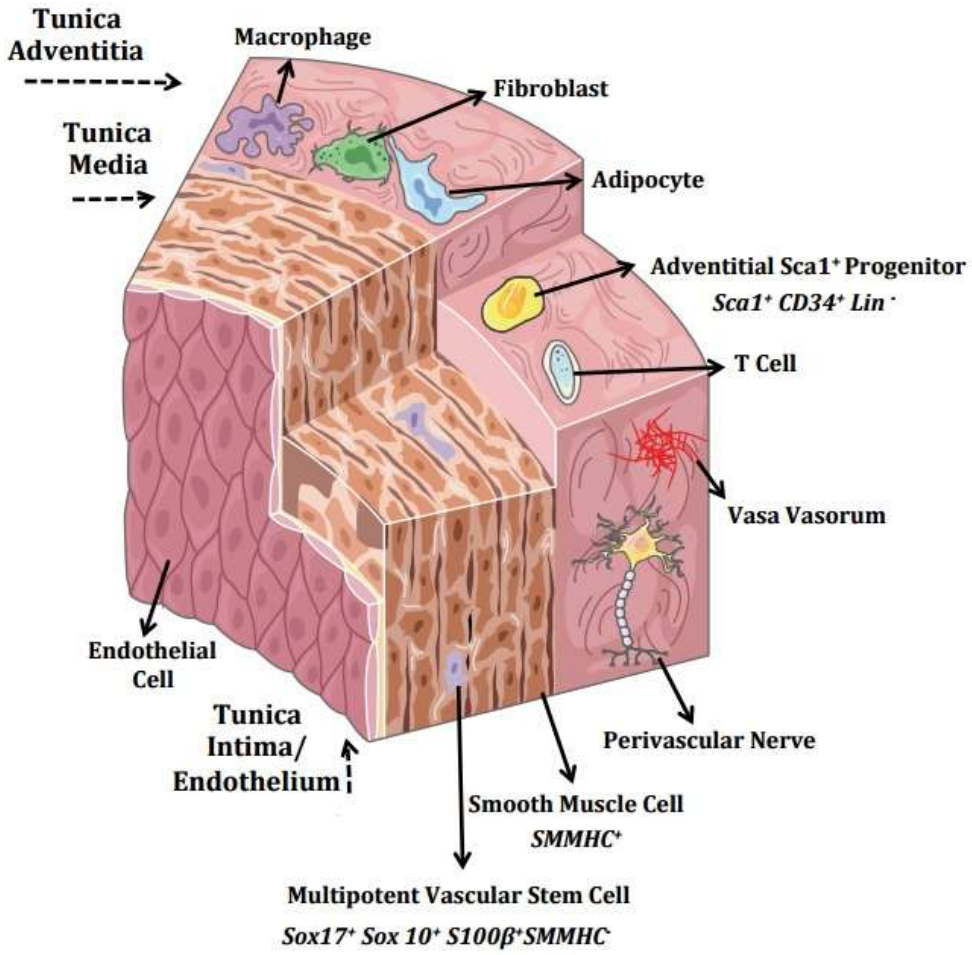

Figure 1.3: Cell populations present within an artery. Adapted from [19]

Despite all the evidence indicating that MVSC could play a critical role in vascular disease, no previous studies have been performed to determine their response to changes in mechanical forces. This population of cells provides a potential new target for preventing the formation of in-stent restenosis, but first these cells require further investigation into the mechanoresponse of this cell type. This thesis aims to understand the role of this key cell type in response to tensile strain, native artery structure, and the complex loading environment of simulated stenting.

1.2 Objectives

The overall objective of this thesis is to explore the mechanobiological response of a newly identified vascular stem cell, MVSC, with or without the presence of a native collagen structure. MVSC and VSMC strain responses will be compared in order to elucidate the role MVSC play in vascular disease caused by altered strain environments. The following specific aims were carried out to achieve these objectives and are summarized in Figure 1.4:

1. Determine the effects of equiaxial tensile strain on both MVSC and VSMC to ascertain differences in cell number and differentiation.
2. Determine the effects of uniaxial tensile strain and strain amplitude on both MVSC and VSMC to determine how uniaxial strain changes cell alignment, proliferation and differentiation.
3. Determine how cell orientation affects how MVSC and VSMC experience uniaxial tensile strain by utilizing native collagen structure to alter initial cell alignment.
4. Develop a system to simulate loading by a single stent strut in order to demonstrate how loading from a stent strut would affect MVSC cell proliferation and collagen structure.

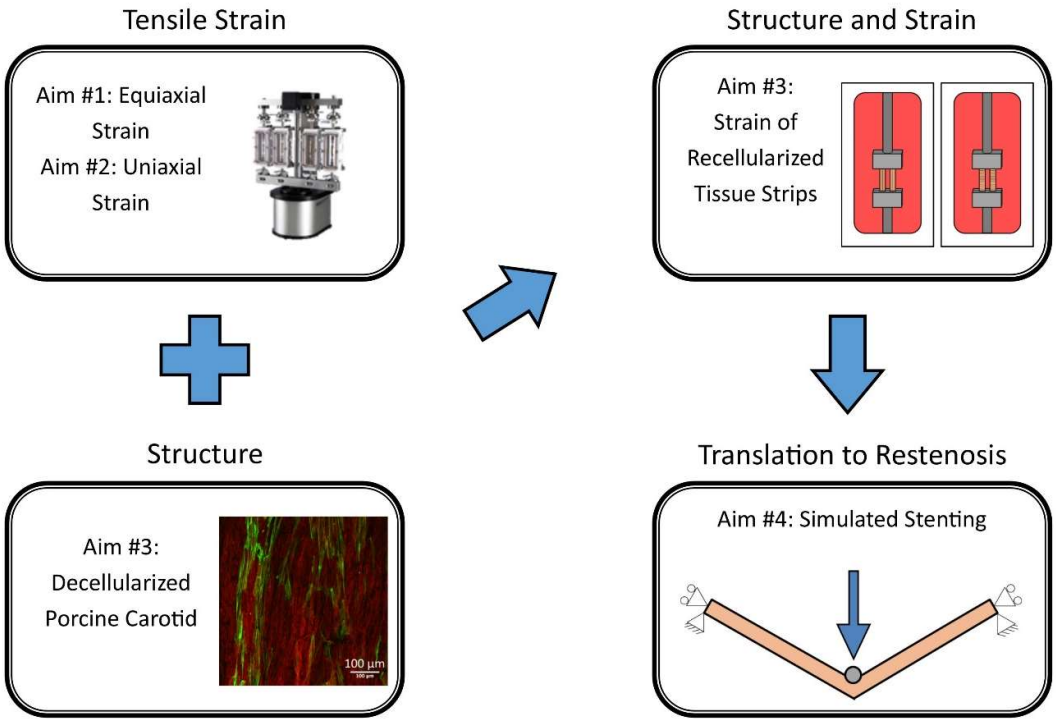

Figure 1.4: Overview of the project aims

1.3 Thesis Structure

This Thesis consists of seven chapters with four main studies. Of these studies, three are being prepared for publication, as well as a section of the literature review. A brief description of each chapter follows:

Chapter 1: Explains the motivation for the work including the prevalence of stenting complications and highlights the existence of a key cell type within the vasculature that has yet to have its mechanosensitivity investigated.

Chapter 2: Reviews the current state of the literature on stent restenosis before covering the cells involved in neointimal formation, highlighting the contributions of MVSC and VSMC. The review then looks at the strain and structure reactions of VSMC and mesenchymal stem cells in order to provide potential insight on how MVSC might react to these stimuli.

Chapter 3: Shows preliminary research on how rat MVSC (rMVSC) and rat aortic VSMC (RASMC) differ in phenotypic response to cyclic equiaxial tensile strain and TGF-β1.

Chapter 4: Demonstrates the effects of different uniaxial strain amplitude on rMVSC and RASMC. It shows how strain amplitude can affect cell alignment, proliferation and differentiation of these two vascular cell types.

Chapter 5: Outlines a study demonstrating the interaction between a decellularized porcine carotid artery substrate and uniaxial tensile strain on rMVSC and RASMC. In this experiment we see clear differences in how rMVSC and RASMC react to uniaxial tensile strain once cells are forced to align parallel to the direction of strain.

Chapter 6: This study looks at how rMVSC respond to the application of indentation by a single wire, designed to simulate a stent strut during intravascular stent deployment. It shows that dynamic loading results in patches of highly proliferative cells that mimic the overproliferation of cells in restenosis.

Chapter 7: Draws conclusions on the implications of the studies on vascular disease and stent design. It also highlights the avenues of further study that these studies suggest.

Chapter 2 Literature Review

2.1 Cardiovascular Mechanical Environment

The cardiovascular system is a vital bodily system which pumps blood throughout the body, supplying oxygen and nutrients to the organs. Arteries carry oxygenated blood away from the heart towards the capillaries. There the oxygen and nutrients diffuse into the surrounding cells, while waste and carbon dioxide diffuse back into the blood. From there veins return the blood to the heart. The cardiovascular system is a mechanically active environment as the heart pumps blood through the vessels within the body.

2.1.1 Mechanical Environment

The vascular environment naturally undergoes mechanical loading. Pulsatile blood flow loads the vessel cyclically, primarily in the circumferential direction, while blood flow causes a fluid shear along the intimal wall (Figure 2.1).

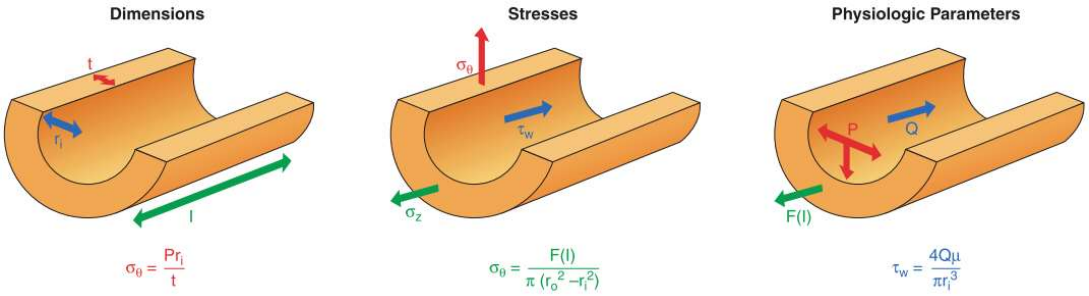

Figure 2.1: A summary of the stresses acting on a blood vessel calculated from the dimensions and physiological parameters of the vessel. σ_θ – Circumferential tensile stress, σ_z – Axial tensile stress, τ_w – Intimal wall shear stress. Adapted from [20]

The heart beat causes a pressure wave form with one large peak as the left ventricle expels blood into the aorta and then a smaller peak after the aortic valve closes These peaks become more distinct as the blood flows away from the heart, and flows into narrower arteries (Figure 2.2). This translates to a similar waveform in the circumferential stresses applied to the vessel wall, which are proportional to blood pressure. The vessel also expands in the axial direction to a lesser degree so that the vessel wall undergoes a small amount of strain in the axial direction. Because of the strain applied in the circumferential and axial directions, the vessel wall experiences a degree of compression in the radial direction. In addition to strains due to pressure within the blood vessel, the vessel wall also undergoes shearing due to the flow of blood within the artery.

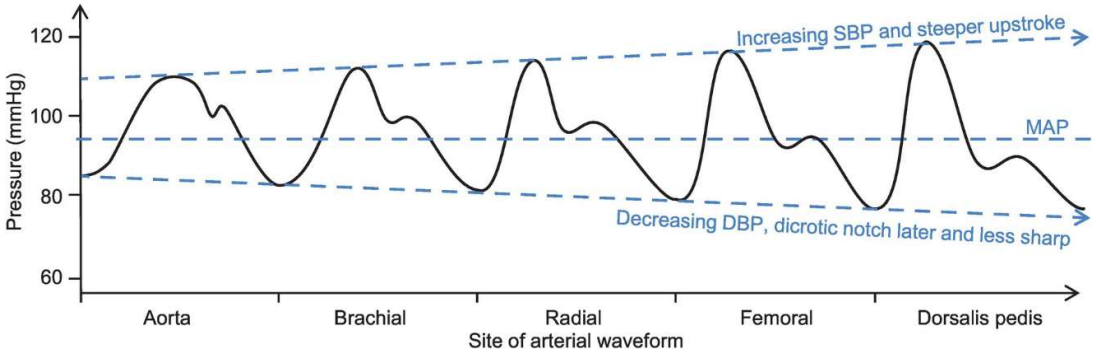

Figure 2.2: Blood pressure waveform within a vessel showing how the waveform changes as the blood travels away from the heart. Adapted from [21]

Blood vessel walls have a non-linear stress-strain curve with lower stiffness toe region with properties dominated mostly by elastin fibres. As strain increases, wavy collagen fibres lengthen and take on more of the load, providing a stiffer collagen dominated region. Selective digestion of elastin causes a decreased toe region, while selective digestion of collagen causes decreased stiffness (Figure 2.3).

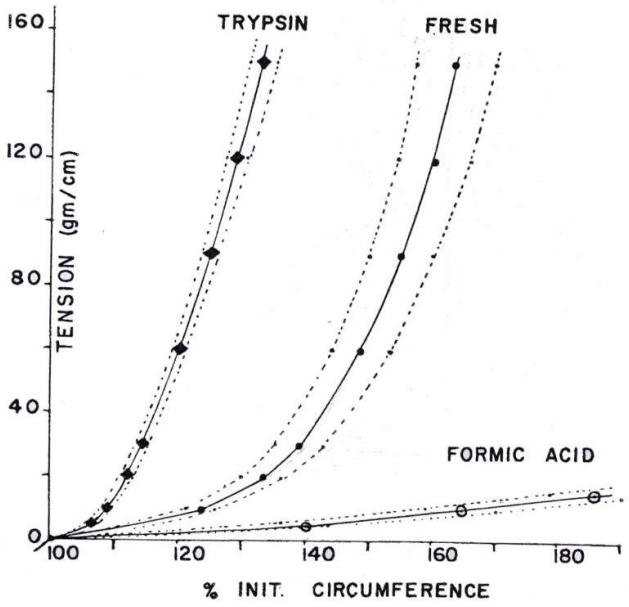

Figure 2.3: Tension – length diagram of human iliac arteries showing samples with collagen selectively digested with formic acid, or elastic selectively digested with Trypsin. Adapted from [22]

When within the body, the blood vessel exists in a loaded state. In mice aorta, vessels experience 40-50% circumferential strain and 10-70% longitudinal strain versus the unloaded condition, depending on location along the length of the vessel.[23] Vessels also undergo cyclic strain and the blood pulses through the vessels. This strain can change

depending on species location, and even the development of vascular disease. One human study showed that as the risk factors for atherosclerosis went up, strain in the carotid artery decreased from 5.1% to 3.1% cyclic strain.[24] Patients with documented atherosclerosis showed strains of 3.25% cyclic strain compared to 4.18% cyclic strain in healthy patients.[24]

Vascular disease can change the stiffness of the vessel and therefore the mechanical environment within the blood vessel. In humans atherosclerotic coronary arteries are stiffer than healthy arteries and bear more stress and less strain compared to the healthy ones.[25] While the overall artery might be stiffer, locally, plaque components such as lipid pools and thrombus are less stiff than the medial layer or fibrous cap of an atherosclerotic plaque.[26] Other vascular diseases, such as aneurysm can also change the mechanical environment within the vessel wall. In developed abdominal aortic aneurysms the tissue is stiffer and less distensible with a decreased elastin fraction,[27] while the tensile strength of the tissue decreases.[28] The mechanical properties of aneurysmal tissue may change as the aneurysm develops. Simulation of aneurysm development by elastin degradation has shown that tissue first becomes softer before eventually becoming stiffer.[29] Ultimately vascular disease can change the mechanical environment within arteries in complex ways.

2.1.2 Extracellular Matrix (ECM) Environment

The environment within the wall of an artery is also characterized by the arrangement of ECM. There are three main layers within an artery, the intima, the media, and the adventitia, as shown in Figure 2.4A. The intima consists of an internal elastic lamina on which there is a single layer of endothelial cells in rodents, or in larger mammals and humans, a thin layer of VSMC covered by a single layer of endothelial cells. The medial layer of a vessel is comprised of layers of elastin lamina between which there are glycosaminoglycans and circumferentially aligned collagen fibres. The circumferentially oriented collagen fibres keep the cells of the medial layer oriented circumferentially as well.[30,31] Because of these fibres oriented in the primary direction of strain, the media is the layer primarily responsible for the mechanical properties of the artery.[20] The adventitial layer is comprised of loosely arranged collagen fibres and capillaries.

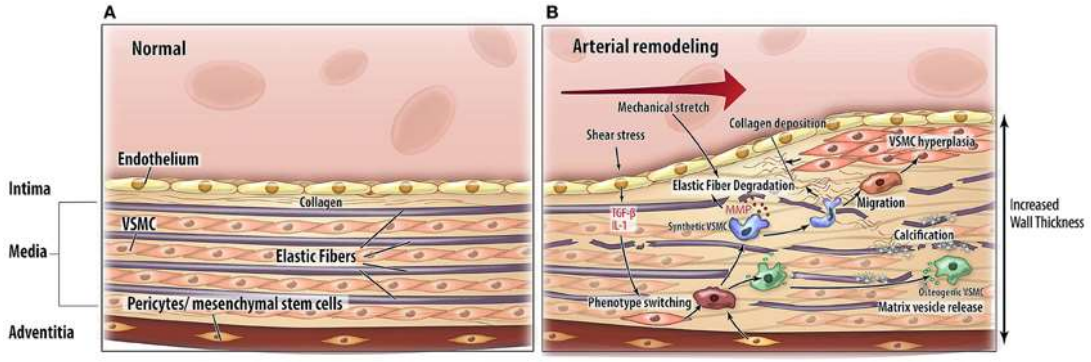

Figure 2.4: A representation of the layers of the arterial wall before (A) or after (B) the development of vascular ECM remodelling. Adapted from[32]

Vascular disease can cause changes in vascular ECM structure as can be seen in Figure 2.4B.[33,34]. For example, in mice, the development of atherosclerosis can cause collagen fiber angles to reorient to become less circumferential in direction.[33] Atherosclerotic plaques often have a paucity of collagen fibers within the lipid core, while fibrous plaque caps can show realignment of collagen fibers in the direction of principle strain.[34]

2.2 Cardiovascular Disease (CVD)

Cardiovascular disease is the leading cause of death in the world, with coronary heart disease and stroke being the leading CVD related diseases in the United States.[1] Atherosclerosis is a vascular disease characterized by the build-up of fatty or calcified plaques in the arterial wall. These plaques can often grow in size and occlude the blood flow within the vessel leading to a heart attack or the plaque can rupture and lead to a stroke.[35]

2.2.1 Stenting

A common option for treating vessel occlusion is stenting, with over three million stents implanted each year.[36] Stenting itself can alter the mechanical environment within the blood vessel. Specifically, inserting a stent into an artery can make the artery appear stiffer, and decrease cyclic strain amplitude, while increasing mean strain.[37,38] However, determining the strain applied by the stent locally is much more complex and varies depending on stent design.[6] Importantly, changes in stent design, and therefore the mechanical forces they apply, can change the location and severity of in-stent restenosis.[39]

Because of the effects of the mechanical environment of the vessel on restenosis many studies have been performed to model the mechanical effects of various stent designs. Many models have shown the importance of stent design on the strains within the vessel.[6,39-

[42] Additionally, the underlying geometry of the vessel can influence the mechanical environment, with vessels that narrow significantly over the length of the stent experiencing high stresses at the narrow end of the vessel.[43] This indicates that stent design can be critical in changing the mechanical environment within the blood vessel.

Stenting can also change the collagen fiber arrangement within a vessel. In transapical valve replacement, stent strut contact with the pulmonary artery caused collagen fibers near the stent to align parallel to the stent struts, while leaving fibers between struts unaffected.[44] Additionally, in previous experiments from our lab, application of a simulated stent strut has also shown realignment of collagen fibers parallel to the stent strut direction as shown in Figure 2.5.[45] These changes in collagen fiber orientation may change the directions of vascular cells, and consequently could influence the way in which these cells experience the strain environment.

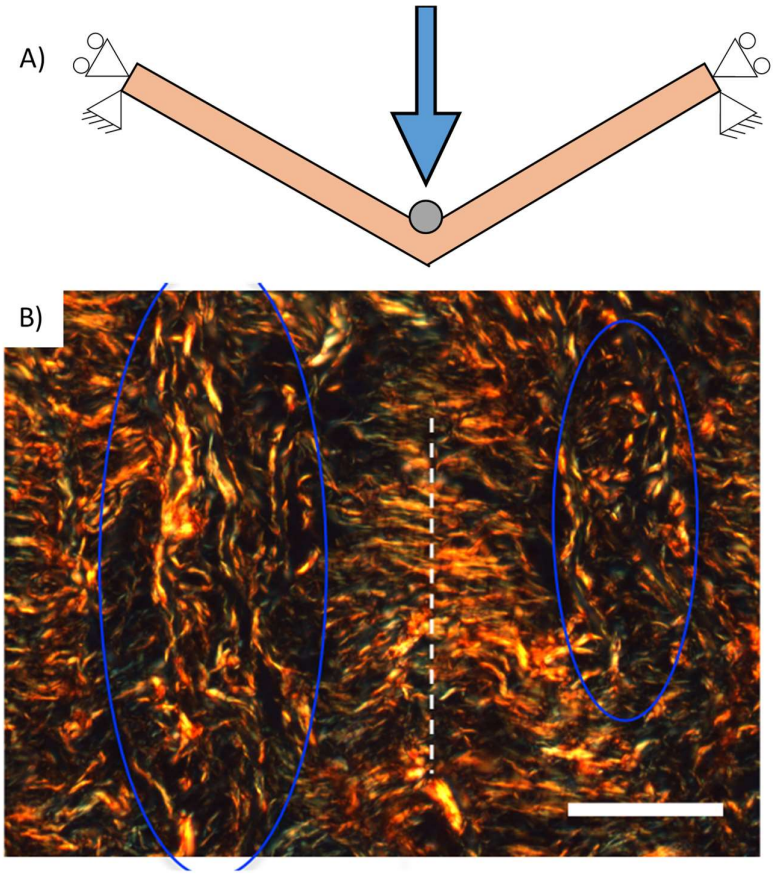

Figure 2.5: A diagram of stent indentation of arterial strips (A) and Picrosirius Red staining of collagen fibres showing regions of realigned collagen circled in blue near the stent strut (dotted white line). (B) Scale bar = 200 µm Adapted from [45]

2.2.2 In-Stent Restenosis

However, stenting also has complications including in-stent restenosis. Understanding how in-stent restenosis occurs and the factors involved will help to better inform stent design as well as treatments for in-stent restenosis. Ultimately, in-stent restenosis results from an over proliferation of cells within the lumen of the vessel. Restenotic areas of the vessel have been shown to have higher cellular content than the original atherosclerotic lesions.[46] A study in a porcine model showed that stenting resulted in an increased proliferation of cells, which peaked at day 7 after stent implantation.[47]

There are several factors that determine the severity of in-stent restenosis including stent design, damage imparted to the underlying tissue, mechanical properties of the stent. The designs that cause greater in-stent restenosis are often linked to increased strains within the vessel. One study suggested that stents that subjected arteries to higher stresses showed significantly more intimal thickening at stent struts[48] while another suggested the optimal stent structure has a minimum radial force for vascular support and maximum flexibility for vascular conformability.[49] In a comparative study, a stent with thicker struts and sharper corners showed increased damage to the underlying tissue which led to increased restenosis versus a Palmaz stent with rectangular struts and smooth corners.[50] One study has even suggested stents should not produce stress in the vessel wall greater than the end of the transitional domain of the vessel's stress-strain curve in order to produce the least amount of restenosis.[51]

Other studies have shown that properties that would change the mechanical environment in the vessel can change the extent of in-stent restenosis. In a healthy porcine model more rigid stents have been observed to induce greater intimal hyperplasia than flexible stents.[52] Another study showed that purposely mismatching the size of the stent to the artery caused increased restenosis.[53] Strut thickness has also been shown to influence the restenosis rate in vessels greater than 2.5 mm in diameter.[54] Stent strut number has also been shown to play a role in in-stent restenosis, with greater numbers of struts per cross section showing reduced restenosis as shown in Figure 2.6.[39] All these studies show the importance of mechanical cues in determining the severity of restenosis.

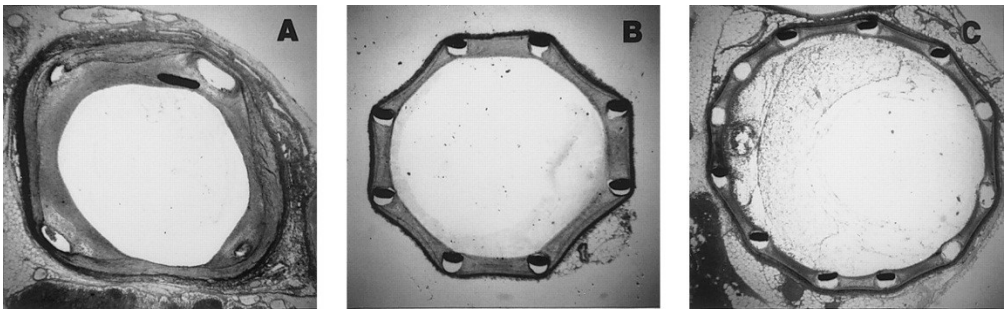

Figure 2.6: Images of in-stent restenosis showing how the number of stent struts can influence extent of intimal hyperplasia. Adapted from [39]

However, due to the prevalence of in-stent restenosis, drug eluting stents have increasingly been used. In 2014 only 18% of stents used were bare metal stents.[1] However, drug-eluting stents also have their own complications. Drug eluting stents have an increased risk of thrombosis due to a delayed healing of the endothelial layer of the vessel after stent implantation.[55] Ideally, there could be solutions to reduce in-stent restenosis that would not rely on eluting drugs that ultimately cause thrombosis. In order to develop these solutions, first we must understand the cellular mechanisms behind the development of in-stent restenosis.

2.3 The Origin of Neointimal Cells during Vascular Disease Progression

A hallmark of arterial pathology is the accumulation of neointimal cells, primarily vascular smooth muscle like cells (VSMC), leading to vessel remodelling and intimal medial thickening.[56] The exact origin of these neointimal cells is controversial. Historically, differentiated VSMC were considered the sole source. However, recent genetic lineage tracking experiments in arteriosclerotic vessels in mice following injury provide evidence for a stem cell origin of neointimal cells,[12,57 58 59] in addition to endothelial cells[57,60] and medial VSMC.[61-63] Figure 2.7 shows possible mechanisms for how VSMC, smooth muscle progenitor cells, MVSC, or MSC could contribute to neointimal formation. Evidence now suggests that resident vascular stem cells may become activated following injury, transition to VSMC-like cells and subsequently dictate, in part, the deleterious remodelling events that occur leading to vascular disease progression [57,64]

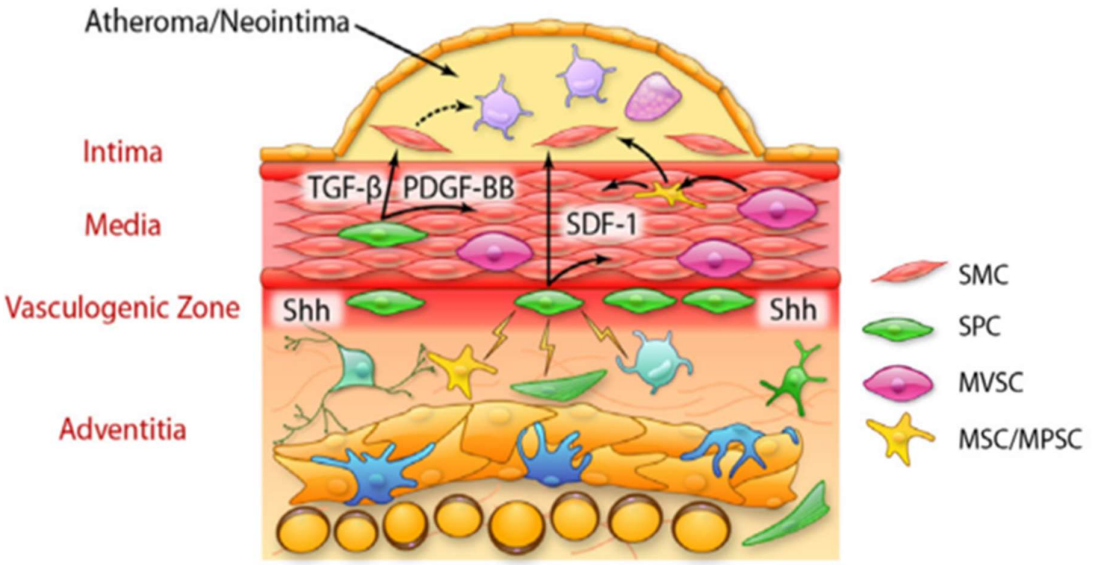

Figure 2.7: Diagram of suggested mechanisms for medial cell involvement in neointimal formation, including possible VSMC, smooth muscle cell progenitor (SPC), MVSC and MSC involvement. Adapted from [65]

2.3.1 Vascular Smooth Muscle Cells (VSMC)

VSMC are an essential component of arterial and venous blood vessels. They perform biosynthetic, proliferative and contractile roles within the vessel wall and are not considered to be terminally differentiated but rather capable of undergoing cellular re-programming and modulation of their phenotype in response to changing local environmental cues.[66] There is clear evidence that alterations in the differentiated state of the VSMC play a critical role in the pathogenesis of atherosclerosis and intimal hyperplasia, as well as in a variety of other major human diseases, including restenosis, hypertension, asthma, and vascular aneurysms.[67] There are several different theories about how these cell populations influence restenosis.[65] One longstanding theory suggests that contractile medial VSMC transition to synthetic VSMC and begin proliferation and extracellular matrix production on the intimal surface.[68,69] Others have shown that medial VSMCs can transdifferentiate into macrophage-like cells in advanced atherosclerotic lesions,[70] and that VSMCs can give rise to osteochondrogenic precursors and chondrocyte-like cells in calcified blood vessels in matrix Gla protein (MGP) deficient mice.[71] Several lineage tracing studies have confirmed VSMC as one of the cellular origins of neointimal cells.[61,72]A further recent lineage tracing study using confetti reporter mice implicated a small subpopulation of medial VSMC as one major source of neointimal cells during neointimal formation.[63] Specifically, Chappell *et al*. demonstrated extensive proliferation

of a small proportion of highly plastic VSMCs that results in the neointimal cell accumulation after injury and in atherosclerotic plaques.[63]

VSMC make up the majority of all cells within the arterial tunica media. In situ, they have an elongated structure and contractile proteins in order to contract blood vessel walls and regulate blood pressure. Traditionally, VSMC have been considered to be able to modulate between two distinct phenotypes, contractile and synthetic.[73] Cells *in vivo* typically have a contractile phenotype which exhibit an elongated shape, and expression of contractile proteins such as SM-MHC,[74-78] Calponin,[79-81] α-SMA,[82-84] SM22α,[79,85,86] h-Caldesmon,[87-89] Aortic carboxypeptidase-like protein (ACLP),[90,91] Desmin,[92,93] Metavinculin,[94] Telokin,[95] and Smoothelin.[96] However, none of these markers can be used to exclusively identify VSMC to the exclusion of other cell types, with the possible exception of SM-MHC.[73] VSMC have been shown to reversibly convert back and forth between contractile and synthetic phenotypes in response to change in serum concentration,[97] and a synthetic phenotype is typically considered to be described by a loss of contractile proteins, increase in proliferation, migration and extracellular matrix (ECM) synthesis.[98] However, other studies have indicated that increased proliferation may not be the best marker of synthetic phenotype.[67,99,100] Phenotype switching has also been associated with changes in cytoskeletal arrangement.[101] Typically, as VSMC are cultured, they go from a contractile phenotype to a synthetic phenotype. While VSMC comprise the largest percentage of cells within the media of artery, they are not an entirely homogeneous population.[102-105]

2.3.2 Medial Multipotent Vascular Stem Cells (MVSC)

Several studies have isolated and characterised resident vascular stem cells from vessels of various species (Table 2.1). Despite being characterised only relatively recently,[12] medial multipotent vascular stem cells (MVSC) have been implicated in vascular disease using animal models of vascular injury and human arteriosclerotic vessels.[12,57] Genetic lineage tracking studies have provided evidence for the presence of these resident medial vascular stem cells within the vessel wall that then migrate to the intima, proliferate and differentiate to neointimal VSMC-like cells following vascular injury.[12,57,59]

Table 2.1: MVSC Isolation and Markers

Cell Source	Isolation Method	Markers	Differentiation	Reference
Rat carotid	Explant	Sox10, Sox1, Snail, vimentin, nestin, Sox17, NFM, peripherin, Brn3a, Phox2b, S100β, CD29, CD 44	Schwann cells, peripheral neurons, VSMC, chondrocytes, osteoblasts, adipocytes	[12]
Human carotid	Explant	Sox10, Sox17, Pax-3/7, vimentin, NFM, S100β	Schwann cells, neuronal cells, VSMC, chondrocytes, adipocytes	[12]
Rat aorta	Explant	Sox10, Sox17, S100β	VSMC, osteogenic, adipogenic	[106]
Porcine aorta	Digestion from intact vessel	CD44, CD56 , CD90, CD73, vimentin, nestin, laminin, PDGFRα and β, NG2, α-SMA, Oct4	VSMC, osteogenic, adipogenic, chondrogenic, endothelial cells	[107,108]

MVSC are a small subpopulation of cells present within the medial wall of an artery and were first isolated and characterized from rat carotid arteries by explant culture.[12] The adventitia and endothelium were removed, sections of artery were placed on a surface coated with 1% Cellstart (Invitrogen), and cells were allowed to migrate out of the adventitial-facing side of the media.[12] MVSCs express several neural crest, endoderm and neural cell markers, as well as stem cell surface markers as shown in Figure 2.8.

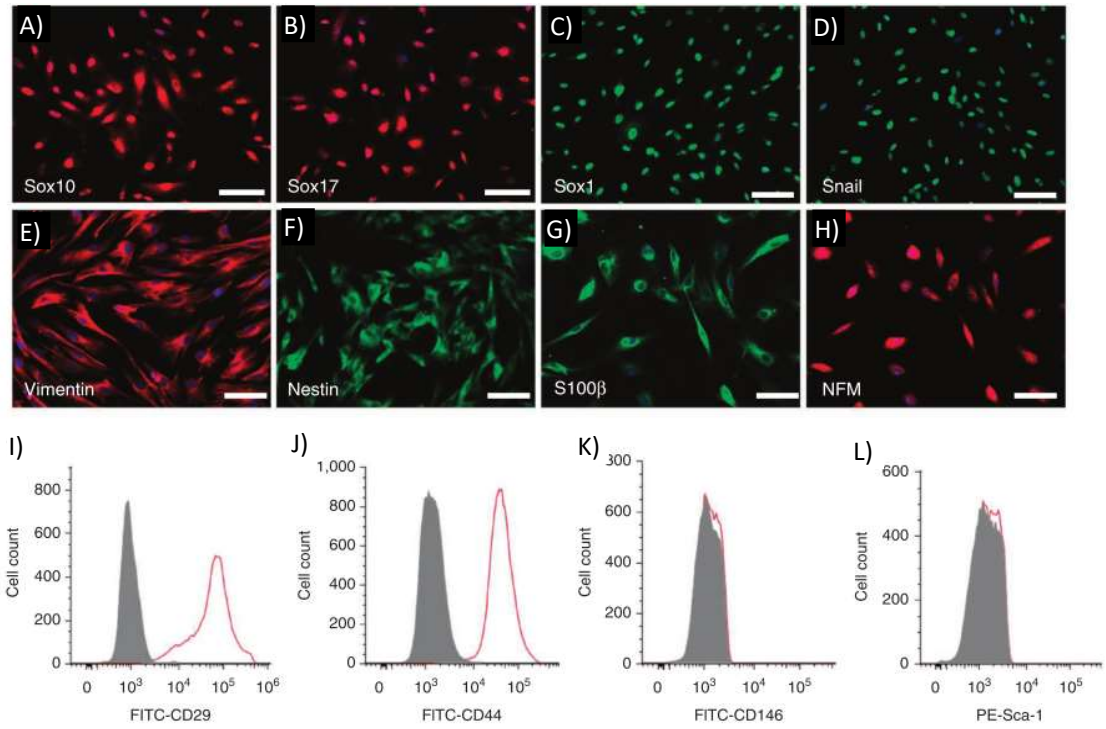

Figure 2.8: MVSC characterization showing cells stain positive for Sox10, Sox17, Sox1, Snail, Vimentin, Nestin, S100β, NFM, CD29 and CD44, while staining negative for CD146 and Sca-1. Adapted from [12] Scale bar = 100µm

What differentiates MVSC from the surrounding medial VSMC is their stemness, or ability to differentiate into multiple cell lineages. Critically, the MVSC phenotype is maintained when cells are grown in maintenance media containing Dulbecco's Modified Eagle's Medium (DMEM) supplemented with 2% Chick Embryo Extract (CEE), 1% Fetal Bovine Serum (FBS) and 20ng/ml Basic Fibroblast Growth Factor (bFGF).[12] Perhaps due to their location within the medial compartment, MVSC have a tendency towards myogenic differentiation if grown in DMEM medium supplemented with 10% FBS by increasing their expression of F-Actin stress fibres and the SMC differentiation markers, α-SMA, and Calponin 1.[12] Additionally, MVSC have the potential to differentiate into Schwann cells, peripheral neurons, chondrocytes and osteoblasts when chemically induced down these pathways. [12] MVSC are ubiquitous within the vessel wall as they have been isolated from the tunica media of several vessel types including jugular vein, aorta, abdominal artery, inferior vena cava, femoral artery and femoral vein, but not from the adventitia or endothelium despite being present within the adventitia.[12,109] Crucially, MVSC play a vital role in the development of the neointima since the majority of cells within rat and murine carotid artery lesions, following ligation-induced injury or endothelial denudation, stain

positive for MVSC markers.[12] Moreover, when MVSC are genetically marked using Sox10-Cre-LoxP in reporter mice and tracked, a significant proportion of neointimal cells are tracked as originating from a $Sox10^+$ MVSC population. [57]

Several groups have confirmed the presence of MVSC within rat aorta and validated their Sox10, Sox17, and S100β marker expression and multilineage differentiation capacity *in vitro*.[106,110] Their phenotype, growth and differentiation state is dictated by several factors. While there was little difference in Sox10 and Sox17 expression when cells were grown in maintenance or growth expansion media, cells grown in maintenance medium exhibited enhanced expression of MVSC markers, NFM, S100β and Ki67.[110] MVSC phenotype and growth was also controlled by endothelial factors, such as nitric oxide (NO), which decreased MVSC proliferation and promoted apoptosis and prevented myogenic differentiation by inhibiting the expression of SMC differentiation markers, Calponin 1 and α-SMA.[110]

Medial MVSC-like cells have also been successfully isolated from larger porcine aorta using an enzymatic dispersal approach[107]. Briefly, following enzymatic removal of the endothelial layer in intact ligated vessels, medial cells were further enzymatically dispersed using a 0.2% collagenase IA solution before plating cells in high glucose DMEM (hgDMEM) supplemented with 10% FBS for 3 days followed by serum depletion for 24 hours before returning to the hgDMEM media with 10% FBS.[107] These cells stained positive for CD44, CD56, CD90 and CD73 and negative for CD45 and CD34 and expressed Vimentin, Nestin, Laminin, Platelet-derived growth factor receptor α and β (PDGFRα and β), Neural/glial antigen 2 (NG2), α-SMA and Octamer-binding transcription factor 4 (Oct4) but negative for PECAM-1, SM-MHC and c-kit.[107] These cells also exhibited trilineage differentiation (osteogenic, chondrogenic, and adipogenic) capacity, formed capillary networks when co-cultured with human umbilical vein endothelial cells (HUVEC), [107] and underwent vasculogenic differentiation to endothelial cells in response to vascular endothelial growth factor (VEGF).[108] When grown in pericyte growth medium (PGM), less than 2% of cells expressed α-SMA in comparison to 100% of cells grown in hgDMEM and 10% FBS.[108]

2.3.3 Resident Adventitial Multipotent Vascular Stem Cells

Several studies have implicated adventitial $Sca\text{-}1^+$ cells (AdvSca1) in the aetiology of neointimal formation.[58,111-114] $AdvSca\text{-}1^+$ cells are known to play a role in developing

atherosclerotic lesions in vein grafts,[113] and are capable of migrating to the intima and contributing to neointimal formation in atherosclerotic plaques from ApoE deficient mice.[115 114] Single-cell gene sequencing confirmed that the majority of AdvSca-1$^+$ cells are local resident progenitor/precursor cells, since a very small proportion of AdvSCA-1+ displayed bone marrow cell markers.[111] In addition to adventitial Sca1$^+$ cells, adventitial pericytes may also have a role to play in vascular remodelling since pericyte-like MSC originating within the adventitial layer have been found to contribute to restenosis following arterial injury.[116]

2.3.4 Multiple Cell Origins of Neointimal Cells

It is clear from the aforementioned studies that multiple cell types contribute to neointimal formation and stenosis.[46] Each resident cell type may play a significant role in neointimal formation including VSMC, EC and MVSC.[57] Indeed, vascular lesions in humans exhibit evidence of multiple cell phenotypes including endothelial cell progenitor cells (CD34, AC133), dendritic cells (S100β) and neural crest derived cells (GFAP, NSE and NGFR) in addition to VSMC-like cells and macrophages.[46] In rodents, macrophage-like cells in plaques can be of both VSMC and non VSMC origin,[117] while the majority, but not all, of the neointima that forms following carotid ligation is derived from previously differentiated medial VSMC.[62] The presence of VSMC in neointimal tissue, as well as some bone marrow derived cells and endothelial cells (EC), with the proportion of each cell type widely varying between different specimens, has been confirmed by genetic lineage tracking analysis.[118] To further complicate matters, the origin of neointimal cells may also depend on the type of vascular injury.[119]

Collectively, these studies suggest that cells within vascular lesions may not derive solely from one cell source. Hence the contribution of each resident cell type must be examined in order to understand their collective role in vascular pathology. It is therefore important in this analysis to examine the relevant environmental factors and cues that impact on these different cell types. While there has been extensive interrogation of VSMC and how they respond to their micromechanical environment during vascular disease progression, less is known about how these same environmental cues influence resident vascular stem cell fate. Therefore, a greater understanding of how resident MVSC respond to altered strain environments and structural changes in extracellular matrix, typical of disease, will help to expand our knowledge of native progenitor cell response following vascular injury.

2.4 MVSC vs. VSMC Phenotype

While much has been done to characterize and track both MVSC and VSMC *in vivo,* the close proximity of the two cell types within the vessel wall has led to some studies comparing MVSC and VSMC populations in culture over time *in vitro*. The majority of freshly isolated rat aortic VSMC are positive for SM-MHC, but not Sox10 expression.[106] Similarly, enzymatic digestion of medial cells from the carotid artery produce a mixed population of cells; the majority of which are SM-MHC and Calponin-1 positive differentiated VSMC, yet there is a small population of smaller, SM-MHC and Calponin-1 negative cells.[12] After 3 days of culture in DMEM and 10% FBS medium, the latter cell type multiply and eventually dominate the culture.[12] Indeed, the fate of differentiated VSMC cells marked using SM-MHC-Cre-LoxP transgenic reporter mice and tracked *in vitro* has also been confirmed in culture following enzymatic digestion of murine medial cells.[57] In these studies, the cells in culture do not originate from a SM-MHC marked population.[57] Moreover, commercial rat, mouse and bovine VSMC cultured in medium supplemented with either 5% or 0.5% FBS exhibit both the VSMC markers SM-MHC, and MVSC markers Sox10 and Sox17 at high passages.[106] However, these cells cannot undergo osteogenic or adipogenic differentiation suggesting that these cells have lost their multipotent capacity.[106] Collectively, these data suggest that medial SM-MHC$^+$ VSMC and their progeny do not predominate when cultured *in vitro.*

Critically, the growth medium in which cells are grown and expanded *in vitro* may also dictate whether cells exhibit MVSC or VSMC phenotypic markers.[120] Isolated medial cells from rat aorta cultured in a high glucose DMEM with 20% FBS or a maintenance medium comprised of stem cell growth medium (SCGM) supplemented with 10% FBS, leukaemia inhibitory factor, and 2-mercaptoethanol exhibit differential expression of VSMC and MVSC markers.[120] Medial cells that adhered to tissue culture plastic after digestion exhibit lower expression of SMC differentiation markers (α-SMA, Calponin 1, SM22α and Smoothelin B) than non-adherent cells. Cells cultured in maintenance medium retained lower levels of SMC differentiation markers longer than those grown in the DMEM medium.[120] In addition, cells that were cultured in maintenance medium exhibit decreased MVSC marker expression over time.[120] Moreover, cells grown in maintenance medium containing PDGF-BB exhibited an increase in VSMC differentiation marker expression (α-SMA, SM22α, Calponin 1, Smoothelin), Collagen I, Collagen III, Matrix metalloproteinase (MMP) 2, MMP9, and Elastin[120] whereas, when cells had reduced MVSC marker

expression, there was a decrease in VSMC differentiation marker expression in response to PDGF-BB.[120] This suggests that MVSC have different reactions to the same signalling molecules depending on their differentiation state. The role of passage number is also important since lower passage undifferentiated cells contain greater endogenous reactive oxygen species (ROS) than higher passage differentiated MVSC[120].

While the effects of mechanical forces on VSMC phenotype in culture have been widely reported,[121,122] few studies have addressed the effects of biomechanical cues on MVSC fate, bar the role of microstructure on osteogenic differentiation of MVSC.[123] However, as MVSCs adopt a mesenchymal stem-like intermediate in the process of myogenic differentiation[12] it may be possible to extrapolate important insights from mechanobiological studies of MSCs in culture in addition to VSMC *in vitro*.

2.5 VSMC Response to Strain

VSMC have been shown to change phenotype in response to mechanical forces including mechanical strain.[124-128] Tensile strain has been one of the most extensively studied forces; both equiaxial and uniaxial tensile strain have been shown to change the phenotype as well as other properties of VSMC.[124-126] Both types of strain will be discussed separately in the following sections and are summarized in Figure 2.9 and Table 2.2.

Table 2.2: Vascular Smooth Muscle Cell Response to Cyclic Tensile Strain

Stimulus Type	Cell Type	Substrate	Reaction	Reference
Equiaxial Strain				
5%, 1Hz	RASMC	Laminin or Pronectin coated elastomer	Increased α-SMA expression	[129]
10%, 1.25Hz	RASMC	Gelatin coated elastomer	Increased expression of SM22α Increased expression of α-SMA Increased expression of Calponin	[130]
10%, 1 Hz	RASMC	Type I collagen, fibronectin or Celtak coated silicone	Decreased α-SMA Decreased Calponin Increased Vimentin	[131]
Physiological waveforms vs sinusoidal waveform	Human VSMC	Type I collagen coated silicone	Increased Desmin Decreased Tropomyosin Increased Calponin Increased SM22α	[132]

10%, 1 Hz	RASMC	Type I Collagen coated elastomer	Reduced cell number No change in apoptosis	[133]
10%, 1 Hz	HASMC	Type I Collagen coated elastomer	Reduced cell number	[134]
10%, 1 Hz	Rat VSMC	Elastomer membrane, coating not specified	Reduced cell number Increased apoptosis	[135]
1% to 6%, 1 Hz	HASMC, BASMC	Elastomer membrane, coating not specified	Increasing amplitude decreases proliferation and increases apoptosis	[37]
5%, 1.25 Hz	RASMC	Type I Collagen coated elastomer	Reduced cell number	[136]
15%, 1.25 Hz	RASMC	Type I Collagen coated elastomer	Increased cell number	[136]
0-7%, 1 Hz	BASMC	Type I Collagen coated elastomer	Increased cell number	[137]
10%, 1 Hz	RASMC	Pronectin coated elastomer	Increased MMP2	[138]
10%, 1 Hz	Human VSMC	Elastomer membrane, coating not specified	Increased Fibronectin Increased Collagen	[139]
20%, 1 Hz	VSMC	Elastomer membrane, coating not specified	Increased *collagen I* Increased *fibronectin*	[140]
10%, 1 Hz	Rat VSMC	Gelatin coated deformable membrane	Increased cell stiffness	[141]
7%, 15% or 20%, 1 Hz	MASMC	Collagen coated elastomer	Increased IL-6	[142]
Uniaxial Strain				
10%, 1 Hz	RASMC	Type I Collagen coated elastomer	Decreased Calponin Decreased SmoothelinB Alignment perpendicular to strain	[16]
10%, 1 Hz	BASMC	Type I Collagen coated elastomer	Increased cell number Alignment perpendicular to strain	[15]
10%, 1 Hz	HASMC	Type I Collagen coated silicone	Alignment perpendicular to strain	[13]
10%, 1 Hz	HASMC	Type I Collagen coated elastomer	Alignment perpendicular to strain	[14]

20%, 1 Hz	a7r5	Type I collagen coated elastomer	Alignment perpendicular to strain	[143]
7-24%, 1 Hz	BASMC	Type I collagen coated Silastic membrane	Alignment perpendicular to strain	[137]
8%, 0.1-1 Hz	Human coronary artery VSMC	Fibronectin coated PDMS	Increased speed of alignment with increased frequency	[144]
10%, 0.5-2 Hz	RASMC	Elastomer membrane, coating unspecified	Increased alignment with increased frequency	[145]
10%, 1 Hz	Bovine VSMC	Fibronectin coated elastic substrate	Alignment perpendicular to strain	[17]
10%, 1 Hz with micropatterned grooves parallel to strain	Bovine VSMC	Fibronectin coated elastic substrate	Alignment with grooves parallel to strain	[17]
5% Static	Human VSMC	Type I Collagen and chitosan coated silicone	Increased MMP2 Increased MMP9	[146]
5%, 1 Hz	Human VSMC	Type I Collagen and chitosan coated silicone	Decreased MMP2	[146]
25% or 50%	Human umbilical VSMC	Collagen gel	Alignment 15 degrees to strain direction	[147]
10%, 1 Hz	BASMC	Collagen gel ring	Alignment parallel to strain Increased myofilament bundles	[148]
7%, 1 Hz	RASMC	Collagen I sponge	Increased Elastin Increased contractile morphology	[149]
10%, 1 Hz	HASMC	Collagen:Fibrin construct	Increased α-SMA Increased SM22α	[150]
10%, 1 Hz	A10 VSMC	Polyurethane scaffold	Increased Calponin	[151]
10%, 1 Hz	Human coronary artery VSMC	Polyurethane scaffold	Decreased Calponin Decreased α-SMA	[152]
7%, 1 Hz	RASMC	PGA scaffold	Increased Collagen Increased Elastin	[153]
7%, 1 Hz	RASMC	Collagen I sponge	Decreased Osteopontin	[154]

2.5.1 Equiaxial Strain

VSMC response to various amplitudes and frequencies during equiaxial tensile strain experiments have been shown to affect VSMC phenotype, proliferation and apoptosis. The following sections will detail specifically the observations reported in the literature.

2.5.1.1 Effect on phenotype

Equiaxial strain has not been consistently studied at similar frequencies or amplitudes. 5%, 1Hz strain has been shown to increase contractile phenotype.[129] At 10% strain amplitude 1.25 Hz strain has been shown to induce a more contractile phenotype,[130] while 1Hz frequency has been shown to induce a more synthetic phenotype,[131] possibly indicating that frequency can change how strain affects VSMC phenotype. Interestingly, not just the amplitude of strain, but also the waveform, can influence contractile phenotype. Human VSMC exposed to strain profiles simulating physiological waveforms showed a more contractile phenotype than cells strained using a sinusoidal waveform.[132]

2.5.1.2 Effect on proliferation and apoptosis

Many studies have also shown that equiaxial tensile strain affects cell number. Multiple studies have shown a decreased cell number in response to 10%, 1Hz cyclic tensile strain.[37,133-135] Increasing strain amplitude has been shown to correlate with a decrease in cell number and increase in apoptosis.[37] However, other studies have shown an increase in cell number as a result of cyclic equiaxial strain,[136,137] and an increasing correlation between cell number and strain amplitude.[136] Because experiments show both increases and decreases and cell number in response to equiaxial cyclic tensile strain, there may be other factors which have not been considered which may determine whether cell number increases or decreases when VSMC are exposed to equiaxial strain.

2.5.1.3 Other Effects

Equiaxial tensile strain also has been shown to influence ECM production and the mechanical properties of VSMC. 10% and 20% cyclic tensile strain has been shown to increase production of fibronectin and collagen.[139,140] However, other studies have shown that 10% strain will increase levels of MMP2 which would degrade the collagen ECM.[138] Equiaxial tensile strain has also been shown to change VSMC mechanical properties,[141] increase IL-6 expression,[142] increase cell migration,[16,136] and affect cell cycle,[133,135,155,156] cell signalling pathways,[132,141,157-162] and cell signalling molecule secretion.[163,164]

Ultimately, mounting evidence in the literature demonstrates that cyclic equiaxial tensile strain can affect VSMC in a multitude of ways.

2.5.2 Uniaxial Strain

In addition to equiaxial strain, VSMC response to uniaxial tensile strain has also been extensively studied. The strain environment *in vivo* is closer to a uniaxial cyclic tensile strain environment, so this strain profile allows us greater insights into how VSMC act under physiological conditions. Uniaxial strain has been shown to cause changes in VSMC phenotype, proliferation, and alignment. Studies have looked at the effect of uniaxial tensile strain on VSMC grown in both 2D and 3D culture, and by combining each of these parameters, information can be obtained that can be used to perhaps model how different strain environments affect VSMC *in vivo.* The following sections will detail the observations reported in the literature.

2.5.2.1 2D Uniaxial Strain: Effect on Phenotype and Proliferation

Unlike results obtained in equiaxial experiments, 10%, 1 Hz uniaxial cyclic tensile strain has been shown to decrease contractile phenotype[16] and increase cell number.[15] This indicates that uniaxial strain may induce a different response in VSMC than equiaxial strain.

2.5.2.2 2D Uniaxial Strain: Effect on Cell Alignment

Uniaxial strain of 2D cultured VSMC has also been shown to induce VSMC alignment perpendicular to strain direction, indicating that VSMC exhibit strain avoidant behaviour. Several studies have indicated that 10% cyclic uniaxial 1 Hz tensile strain, will cause VSMC to align perpendicular to strain direction.[13-17] This response may be dependent on Nox4.[14] This strain-avoidant behaviour has also been demonstrated at 20% amplitude,[143] and in cells strained between 7-24% strain amplitude.[137]

Interestingly, studies have shown that strain-avoidant cell alignment can also be influenced by several factors including strain frequency and underlying microstructure. Increasing strain frequency has shown increased cell alignment in VSMC strained at 8% amplitude[144] and 10% amplitude.[145] Micropatterned grooves may override the natural strain-avoidant behaviour of VSMC, as cells have been shown to preferentially align parallel to micropattern direction even when strained parallel to groove direction.[17] This indicates that

we may be able to control VSMC response by modifying the strain and surface conditions in the VSMC microenvironment.

2.5.2.3 2D Uniaxial Strain: Other Effects

In addition to these changes, uniaxial cyclic tensile strain can induce a variety of other changes in VSMC. Contrary to what was seen under equiaxial strain, 5% cyclic Uniaxial strain has been shown to decrease production of MMP2.[146] Ultimately, VSMC are sensitive to cyclic tensile strain, but there are many factors such as amplitude, frequency and cell type that will determine the cellular response to tensile strain.

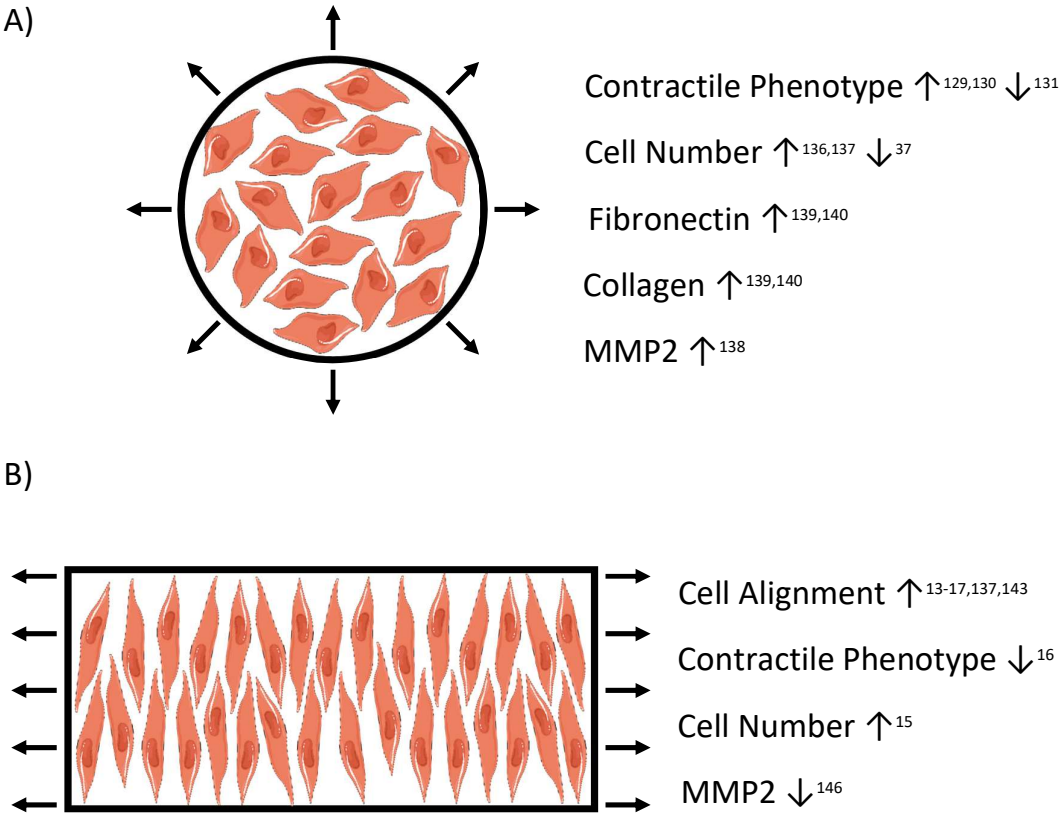

Figure 2.9: Examples of the application of equiaxial (A) and uniaxial (B) strain and associated changes in VSMC phenotype and ECM related protein expression

2.5.2.4 3D Uniaxial Strain: VSMC Response

Additionally, many uniaxial strain experiments on VSMC have cultured the cells in three dimensional constructs. 3D Collagen gel rings strained at 10%, 1 Hz for 4 weeks showed cells aligned parallel to strain.[148] Conversely, in 3D Collagen gel culture, human umbilical VSMC exposed to supraphysiological strains of 50% and 25% strain showed cellular

alignment at 15 degrees to perpendicular to strain direction.[147] This indicates that VSMC in 3D culture exposed to physiological strains may align parallel to strain while some degree of strain avoidance can still occur in response to high levels of uniaxial tensile strain.

Many experiments have shown that in 3D culture VSMC show an increase in contractile phenotype in response to strain including collagen gel rings strained at 10%, 1Hz; [148] Collagen I sponges strained at 7%, 1Hz;[149] Collagen:Fibrin constructs strained at 10%, 1Hz;[150] and polyurethane scaffolds strained at 10%, 1Hz.[151] However, VSMC origin may play a role in cellular response. While A10 VSMC in a polyurethane scaffold became more contractile in response to 10%,1 Hz cyclic uniaxial tensile strain,[151] human coronary artery VSMC in the same conditions showed a decrease in contractility under the same strain stimulus. [152]

Uniaxial tensile strain may also increase Elastin production in VSMC. 7%, 1 Hz cyclic tensile strain has induced increased Elastin production in VSMC cultured in both Collagen I sponges,[149] and poly(glycolic acid) (PGA) scaffolds.[153] 7%, 1 Hz strain has also decreased the expression of *osteopontin* in VSMC indicating a decreased likelihood of these cells depositing calcium.[154]

2.6 MSC Strain-Induced Vascular Differentiation

While resident vascular stem cells have not specifically been thoroughly investigated for their response to strain and ECM factors, other stem cell types have previously been examined. Therefore it may be possible to use the information obtained from these studies to predict how MVSC may respond in similar circumstances. One such comparable cell type are mesenchymal stem cells (MSC), which share the expression of some surface markers as well as multipotency potential with MVSC.[12] Therefore, understanding MSC to VSMC transition may provide insight into MVSC vascular differentiation. MSC have been shown to differentiate into many cell types including bone,[165,166] fat,[165] cartilage,[165] tendon,[166,167] nerve,[168,169] vascular smooth muscle,[170] cardiac tissue,[171,172] and skeletal muscle.[173] MSC are mechanosensitive cells[174] that are sensitive to ECM arrangement.[175,176] Various mechanical forces can induce differentiation into bone,[177,178] tendon,[167] cartilage,[179] cardiac,[171,172] and smooth muscle,[170] and skeletal muscle.[173] It may be possible to understand what factors encourage MVSC to differentiate down a vascular route by observing what stimuli cause vascular smooth muscle differentiation in MSC.

MSC have been shown to align perpendicular to strain direction in 10%, 1Hz uniaxial tensile strain.[180,181] Strain has been shown to induce a VSMC lineage in MSC when exposed to 10%, 1Hz uniaxial[180,182] or equiaxial cyclic tensile strain.[182] However, the uniaxial tensile strain only induced a transient increase in VSMC phenotype.[182] Despite MSC exposed to uniaxial strain showing a quicker response to strain than those exposed to equiaxial, they were unable to maintain those responses. Frequency of strain has also been shown to have an effect on smooth muscle differentiation in hMSC. Increasing frequency of cyclic uniaxial tensile strain has been shown to increase alignment and VSMC markers in MSC.[181] Overall, the literature suggests that cyclic tensile strain helps to induce vascular smooth muscle cell differentiation in MSC. Chemical factors can also be combined with cyclic tensile strain to induce vascular smooth muscle differentiation. 5%, 1 Hz uniaxial cyclic strain, TGF-β1 and a combination of the two have been shown to increase *calponin 1* expression in MSC.[183]

MSC have been shown to undergo vascular smooth muscle cell differentiation in response to chemical factors, strain, and substrate stiffness as summarized in Table 2.3. However, unlike MVSC, they do not spontaneously differentiate down a VSMC pathway when not cultured in a maintenance medium. One would expect MSC to be less likely to differentiate down a vascular pathway than MVSC because MSC are derived from bone marrow and are hematopoietic in nature, while MVSC are derived from the arterial wall. Nevertheless, MSC mechanosensitivity points to the likelihood that MVSC may also exhibit mechanosensitivity.

Table 2.3: MSC Vascular Smooth Muscle Differentiation

Stimulus Type	Cell Type	Reaction	Reference
Strain			
10% uniaxial, 1 Hz	mBMSC	Increased α-SMA Increased Calponin 1	180
10% equiaxial, 1 Hz	hMSC	Upregulation of α-SMA and SM22α by day 3	182
10% uniaxial, 1 Hz	hMSC	Transient increase of α-SMA and SM22α at day 1	182
10% uniaxial, 0.1 Hz to 1 Hz	hMSC	Increased frequency: Increased *α-sma* Increased *sm-mhc* Increased *calponin*	181
5% uniaxial, 1 Hz with microgrooves parallel to strain	hMSC	Increased *calponin 1*	184

3% or 10% uniaxial, 0.26 Hz with microgrooves parallel to strain	Rabbit MSC	Increased α-SMA Increased Caldesmon	[178]
10%, 1 Hz circumferential strain in 3D Collagen tubular constructs	HASMC	Increased *sm22α* Increased *α-sma*	[150]
5% uniaxial, 1 Hz with TGF-β1 5 ng/mL	hMSC	Increased *calponin*	[183]
ECM			
Polyacrylamide gel 8-17 kPa stiffness	hMSC	Increased MyoD1 expression	[169]
Collagen coated glass slides vs. polyacrylamide gel 1 kPa stiffness	hMSC	Increased alpha actin Increased calponin	[185]
Laminin	hMSC	Increased αSMA Increased calponin	[186]

2.7 Other Cardiovascular Stem Cell Response to Strain

While other vascular stem cells do exist and have been previously reviewed,[187] these cells also lack studies on cellular response to mechanical stimuli. However, a few other types of stem cells have been studied that may provide insight into the potential behaviour of MVSC in response to cyclic tensile strain. It has been found that when stimulated with 10%, 1 Hz uniaxial cyclic tensile strain, human foetal cardiomyocyte progenitor cells (CMPC) did not exhibit strain avoidant behavior.[188] Interestingly, once CMPC were induced to differentiate towards cardiomyocytes, this same strain profile caused alignment perpendicular to the strain direction.[188] This result may mean that if we can consider MVSC to be a VSMC progenitor, MVSC may align less strongly than VSMC in response to strain. Interestingly, the study also hints that cell density may influence strain avoidance results, as the authors noted that some undifferentiated CMPC reorientation was observed in areas of high cell density.[188] Interestingly, French *et al.* also report that rat cardiac progenitor cells (CPC) reorient perpendicular to strain direction when exposed to 5%, 10% or 15% 1 Hz uniaxial cyclic tensile strain, with alignment most pronounced on FN and Collagen I coated surfaces.[189] French *et al.* also observed cell division increased on FN coated samples in both unstrained CPC and CPC exposed to 5% strain. At higher strain levels, strain appeared to override this effect.[189] Despite not being of resident vascular origin, embryonic stem cells (ESC) subjected to uniaxial cyclic strains also show strain avoidance when exposed to 1 Hz uniaxial cyclic strain at amplitudes between 2% and 12%.[190] As strain amplitude was increased, ESC showed increased production of α-SMA and SM-MHC as well as an

increased cell number. Shimizu *et al.* also investigated the effects of PDGF-BB and found that 10 ng/ml PDGF-BB also increased α-SMA and SM-MHC in ESC similar to levels found at 8% strain amplitude.[190] These studies on a range of stem cells indicate that strain avoidant reorientation is likely to occur with MVSC. However, it may be the case that structural cues may be able to override these strain-based cues.

Given the mechanosensitivity of other similar cell types, it seems likely that MVSC may also be mechanosensitive. The critical role of MVSC in neointima formation[12] shows that understanding the behaviour of MVSC in response to their mechanical environment is critical to help understand vascular disease.

From this review of the literature, we can begin to predict how we would expect MVSC to react to various mechanical and ECM parameters. The most easily predicted response would be that to uniaxial tensile strain. Both VSMC and MSC react to uniaxial cyclic tensile strain by aligning perpendicular to the direction of strain and VSMC indicate that alignment may increase with increasing frequency. However, uniaxial cyclic tensile strain appears to decrease contractile phenotype in VSMC and increase contractile phenotype in MSC, so MVSC reaction could depend on whether or not they have more in common with VSMC or MSC. Equiaxial cyclic tensile strain appears to have much more variable effects. In MSC, it appears to increase VSMC phenotype, however, amongst VSMC experiments, equiaxial strain has been shown to either increase or decrease the contractile phenotype of the cells depending on parameters of the mechanical stimulus given. We might also expect that the ECM would affect the differentiation of MVSC. In VSMC, laminin and elastin were shown to increase the contractile phenotype of those cells, while collagen and fibronectin would be expected to produce a more synthetic phenotype.

2.8 VSMC Microstructure Response

Cells within the vascular wall, however, are only one part of the vascular environment. The cells are embedded within the extracellular matrix of the vessel. Because of the ECM *in vivo,* in order to understand how vascular cells behave in vivo, we first must understand how they respond to the ECM components present. ECM additionally provides a microstructure that can also determine how cells behave. In this section we look into how ECM components and microstructure can influence VSMC phenotype, proliferation and ECM remodelling.

2.8.1 Effect of ECM in 2D Culture

Several studies have shown that changing the ECM proteins VSMC are in contact with can influence their phenotype. Several studies have shown that Laminin (LN) induces a more contractile VSMC phenotype than Fibronectin (FN),[191-193] Collagen I,[192] Arginine-Glycine-Aspartate peptide (RGD) coated gels.[193] Plastic, α-Elastin were also shown to induce a more contractile phenotype that Collagen I and FN.[192] ECM coating can also influence VSMC phenotype in reaction to tensile strain: VSMC grown on LN show a greater contractile response than VSMC grown on Pronectin when exposed to 5% strain at 1 Hz.[129]

ECM coating has also been shown to have an influence on VSMC proliferation and cell cycle. VSMC grown on Collagen I and FN showed greater cell number than cells cultured on LN, plastic or α-Elastin.[192] VSMC have also shown greater cell numbers when grown on denatured Collagen gels than on native Collagen gels.[194] While cell number has been shown to increase with increasing cell stiffness,[195] other studies have shown that this increase with stiffness only occurs on Collagen and FN, while LN shows decreasing cell number as stiffness increases.[196] This indicates that ECM may play a role in how cells sense the stiffness of their surrounding environment.

2.8.2 Effect of ECM in 3D culture

Additionally, 3D ECM structure can influence VSMC behaviour. 3D VSMC culture in Collagen has shown increased cell proliferation, [197] increased expression of Collagen,[197,198] and decreased contractile markers.[197] Addition of Elastin to 3D VSMC culture scaffolds increased cell number as well as increasing Collagen I and contractile marker expression.[199] 3D culture can also change VSMC reaction to chemical factors. VSMC cultured in a Collagen lattice showed decreased TGF-β1 induced Collagen synthesis, but cells in a Collagen matrix showed greater incorporation of this new Collagen into the surrounding matrix. [200] These studies show that VSMC alignment can be influenced by the dimensionality of the surrounding culture environment. Table 2.4 summarizes how ECM proteins affect VSMC phenotype.

2.8.3 VSMC on Aligned Substrates

The surrounding structure has been shown to play a role in VSMC alignment. While this structure would be provided by the ECM *in vivo,* where collagen fibres align predominantly circumferentially in a vessel, these studies have mainly been performed on engineered

surfaces. Aligned structures can have effects on various properties of VSMC including cell alignment, differentiation, and proliferation.

VSMC have been shown to align parallel to structural cues including microgrooved collagen substrates,[201,202] micropatterned PDMS,[17,203,204] microprinted fibronectin or laminin lines,[205] biodegradable microchannels,[206] and aligned electrospun[207] and melt-spun fibres[208], see Figure 2.10. This alignment is affected by the width of micropatterns. When microgroove size is decreased, alignment of VSMC in the direction of the grooves increases.[209,210]

This alignment can also affect other properties of the VSMC. VSMC grown on a microgrooved collagen surface had increased expression of α-SMA and Calponin 1 versus an unstructured collagen surface.[201] Likewise, VSMC on melt-spun fibres showed increased α-SMA,[208] and VSMC on discontinuous microchannels showed SM-MHC after reaching confluence.[206] On the other hand, VSMC on microprinted fibronectin or laminin lines showed no change in contractile markers, although they did show an increase in contractile force.[205] Additionally, VSMC grown on a microgrooved surfaces had decreased proliferation.[201,203] All of this points to VSMC alignment causing VSMC to take on a more contractile phenotype.

Table 2.4: Vascular Smooth Muscle Cell Response to the Different Extracellular Matrix Proteins and Their Morphology

Stimulus Type	Cell Type	Reaction	Reference
2D ECM			
Fibronectin vs Laminin	RASMC	Decreased α-SMA Decreased SM22α Decreased Vimentin	191
Collagen I, Fibronectin vs. Laminin, plastic or α-Elastin	Rabbit aortic VSMC	Increased Vimentin Increased cell number	192
Laminin vs Fibronectin and RGD-gels	Human coronary artery VSMC	Decreased *α-sma* and *calponin* after 14-17h seeding period	193
Laminin vs Pronectin with 5% equiaxial cyclic tensile strain, 1 Hz	RASMC	Increased α-SMA	129
Denatured collagen gel vs native collagen gel	RASMC	Increased cell number	194
Increasing substrate stiffness	HASMC	Increased cell number with increased stiffness	195
Collagen I and FN on changing substrate stiffness	RASMC	Increased cell number with increased stiffness	196

Laminin on changing substrate stiffness	RASMC	Decreased cell number with increased stiffness	[196]
3D ECM			
3D Collagen vs. 2D	HASMC	Lower percentage of cells in S phase More cells in G0/G1 phase Increased *collagen I* Decreased *α-sma*	[197]
3D Collagen vs. 2D	Porcine aortic VSMC	Decreased Collagen	[198]
Elastin/Collagen 3D scaffold vs. Collagen 3D scaffold	HASMC	Increased cell number Increased Collagen I Increased α-SMA Increased Calponin Increased SM-MHC	[199]
3D Collagen vs. 2D	Porcine aortic VSMC	Decreased TGF-β1 induced Collagen synthesis Increased integration of synthesized collagen into surrounding matrix	[200]

2.8.4 VSMC Response to Aligned Structure and Strain

A previous study of VSMC, as well as endothelial cells and fibroblasts, demonstrated the influence of cell type on how nanotopography influences cell alignment, with fibroblasts showing greater sensitivity to small scale topography.[211] However, when exposed to strain, VSMC both in the thickest 70 μm microgrooves, where cells could fully elongate across the width of the microgroove, and the thinnest 15 μm microgrooves showed more strain avoidant realignment than in the middle microgroove width of 40 μm.[17] This indicates that there is a sweet spot of microgroove width in which cells will remain the most aligned, even when exposed to uniaxial tensile strain.

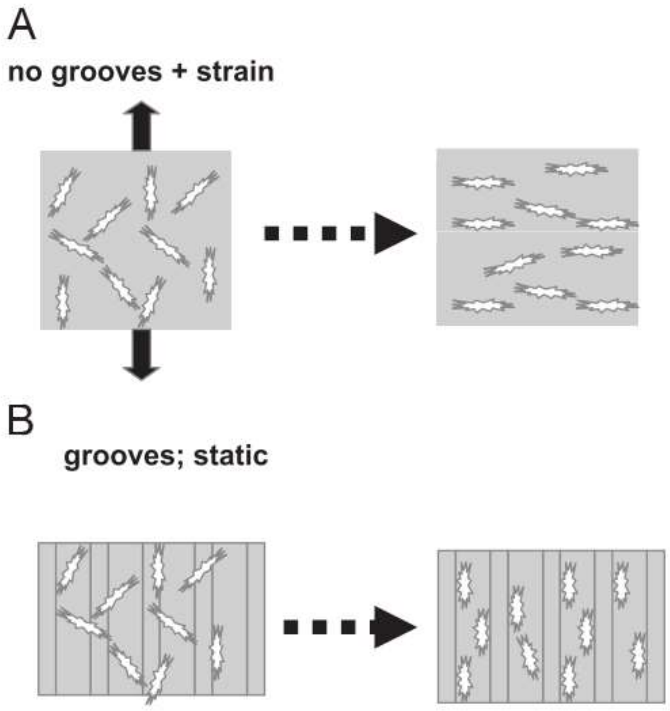

Figure 2.10: Diagram showing both the strain (A) and structure (B) response for VSMC with cells aligning perpendicular to strain direction, and parallel to microgroove direction. Adapted from [17]

Ultimately, it is clear that extracellular matrix environment is important in VSMC proliferation, phenotype and alignment. If MVSC act similarly to VSMC, we would expect a more contractile VSMC phenotype on Laminin, and a more synthetic and proliferative phenotype on Collagen and Fibronectin. We would also expect alignment and an increased contractile phenotype in response to an aligned microstructure, and that the dimensions of this microstructure would influence whether or not the structure or strain dominated MVSC behaviour. However, since VSMC are not stem cells, they may not be the best model for understanding MVSC behaviour.

2.9 Cardiovascular Stem Cell Microstructure Response

In order to understand how MVSC might behave in response to extracellular matrix or microstructure cues, we can look to other stem cell types. Several types of stem cells have been shown to differentiate down a smooth muscle lineage, including MSC and neural crest stem cells (NCSC).

2.9.1 ECM Induced Differentiation

Smooth muscle differentiation of MSC has also been shown to be dependent on the stiffness of the substrate on which they are grown.[168] MSC grown on polyacrylamide gels of 8-17

kPa stiffness showed MyoD1 expression, while those at a lower stiffness expressed neurogenic markers, and those at higher stiffness expressed osteogenic markers. [169] On stiff Collagen coated glass slides, hMSC express greater levels of VSMC markers than on relatively soft Collagen coated polyacrylamide gels.[185] Growing MSC on a Laminin coating increases expression of VSMC markers.[186] This increased contractile phenotype in the presence of Laminin is similar to the phenomenon observed in VSMC, indicating that Laminin may be important in maintaining a contractile VSMC phenotype.

2.9.2 Stem Cells on Aligned Substrates

MSC vascular smooth muscle differentiation can be induced through micropatterning. Microgrooves increase expression of α-SMA and Calponin 1 of MSC on both soft and stiff PDMS.[212] MVSC response to aligned substrates has also been previously investigated. MVSC also align with the direction of PDMS microgrooves.[123] Additionally, differences in cell responses to topography and strain may have to do with differences in cell size as shown in Figure 2.11. In static conditions, having smaller microgrooves results in increased alignment of MVSC.[123]

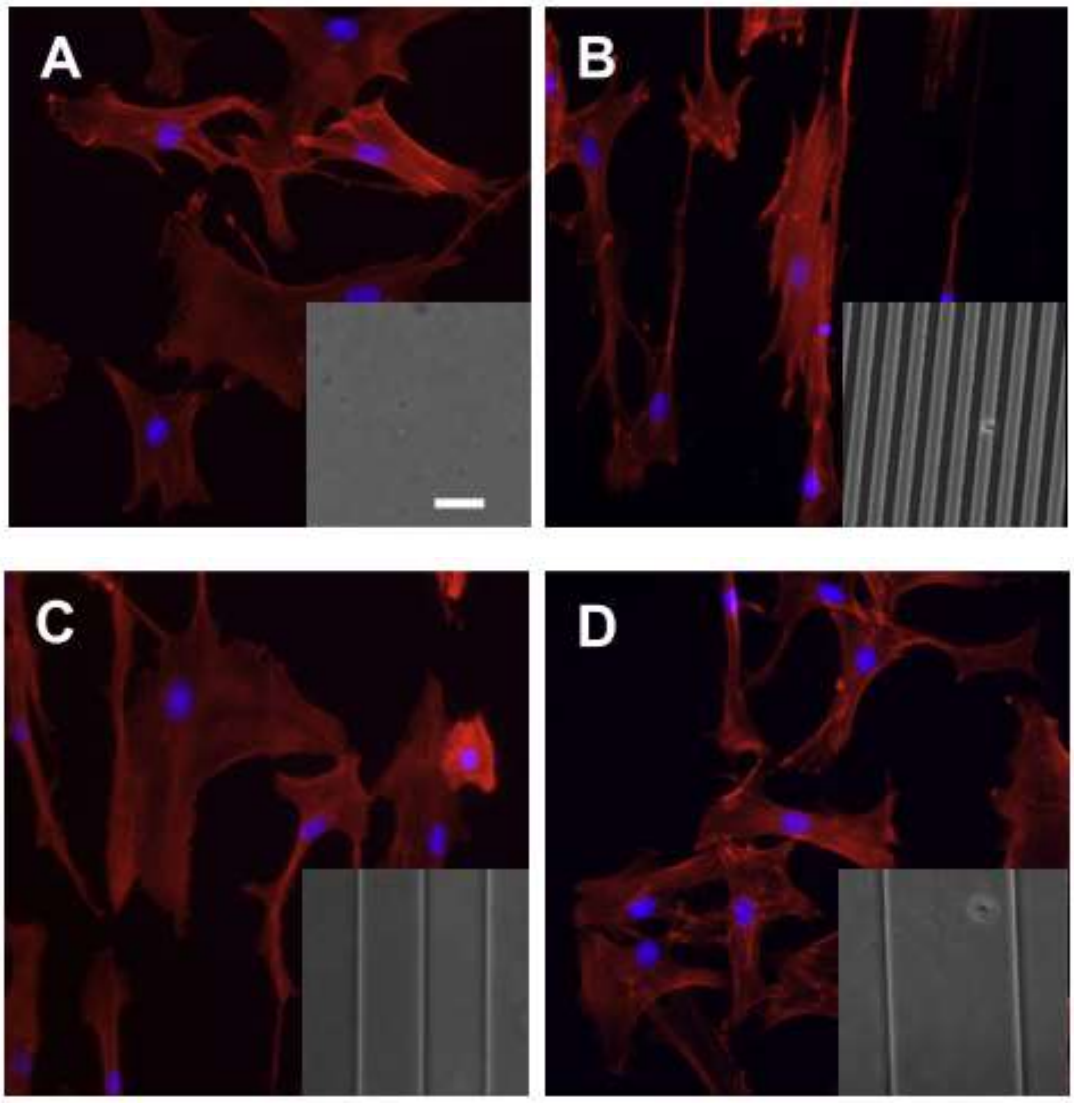

Figure 2.11: MVSC grown on an unpatterned surface (A) and 10µm (B), 50µm (C), and 100µm (D) microgrooves. Adapted from[123]

2.9.3 Stem Cells with Combined Aligned Structure and Strain

Because the vascular environment is also one that experiences tensile strain, understanding how these stem cells behave on microstructures in the presence of strain would be necessary to understanding how MVSC would behave in an *in vivo* environment. In another study, Li et al. produced a neural crest stem cell (NCSC) line and used micropatterned membranes to induced NCSC alignment.[213] Interestingly, Li et al. report that the underlying structure prevented strain-avoidant realignment of NCSC when they were exposed to 5% strain. Li et al. also found strain to induce contractile marker expression, specifically, Calponin 1 within 2 days and SM-MHC within 5 days as well as increasing cell number after 1 day.[213]

When NCSC were strained perpendicular to micropattern direction, they still increased cell proliferation, but they no longer increased Calponin 1 expression.[214]

Tensile strain, in combination with cues from the environmental geometry, has also been shown to effect vascular smooth muscle differentiation of MSC. MSC forced to align parallel to the direction of cyclic uniaxial tensile strain using micropatterned grooves showed an increase in VSMC markers at both 5%, 1Hz strain[184] and 3% and 10%, 0.26 Hz strain.[178] MSC subjected to strain in 3D tubular constructs increased VSMC gene expression. [150]

2.10 Summary

Given the mechanosensitivity of other similar cell types, it seems likely that MVSC may also be mechanosensitive. The critical role of MVSC in neointima formation[12] shows that understanding the behaviour of MVSC in response to their mechanical environment is critical to help better understand vascular disease. Armed with the knowledge of the optimum environment to encourage MVSC to repopulate the contractile VSMC population, as opposed to causing intimal hyperplasia, will be crucial to future vascular device design. Vascular devices could be designed to send the correct signals to induce recovery without contributing to vascular pathologies.

From this review of the literature, we can begin to predict how we would expect MVSC to react to various mechanical and ECM parameters. The most easily predicted response would be that to uniaxial tensile strain. Both VSMC and MSC react to uniaxial cyclic tensile strain by aligning perpendicular to the direction of strain and for VSMC alignment may increase with increasing frequency. However, uniaxial cyclic tensile strain appears to decrease contractile phenotype in VSMC and increase contractile phenotype in MSC, so MVSC reaction could depend on whether or not they have more in common with VSMC or MSC. Equiaxial cyclic tensile strain appears to have much more variable effects. In MSC, it appears to increase VSMC phenotype, however, amongst VSMC experiments, equiaxial strain has been shown to either increase or decrease the contractile phenotype of the cells depending on parameters of the mechanical stimulus given. We might also expect that the ECM would affect the differentiation of MVSC. Microstructural cues have been shown to cause alignment of VSMC in the direction of those micro features. ECM fibres should likewise cause MVSC alignment. Ultimately, this may be a way to control MVSC alignment.

In order to understand how MVSC behave in an environment with changing mechanical and ECM properties, experiments must be performed in order to understand how MVSC respond to mechanical strains and the underlying ECM microstructure. This thesis intends to answer these questions, first comparing the reactions of MVSC and VSMC to tensile strain and ECM microstructure, and then investigating how MVSC respond to a simulated stent wire indentation. Specifically, the proliferation, differentiation and alignment changes of both MVSC and VSMC will be examined after cells are exposed to equiaxial and uniaxial tensile strain. Additionally, native collagen structure will be used to demonstrate how cell alignment relative to the direction of uniaxial tensile strain affects cell proliferation and differentiation. This thesis will examine how MVSC respond to a simulated stenting loading environment, in order to elucidate what role they might play in in-stent restenosis.

Chapter 3 Multipotent Vascular Stem Cells and Vascular Smooth Muscle Cells Differ in their Response to Equiaxial Tensile Strain

3.1 Introduction

Given the potential role MVSC might play in vascular disease and intimal hyperplasia, it is important that we understand how these cells might react to the mechanical forces they experience within the vessel. Despite the known role of a changing mechanical environment on vascular disease, no previous research has been done to establish the mechanosensitivity of MVSC. Additionally, since MVSC *in vitro* are thought to differentiate towards a VSMC phenotype, seeing how MVSC differentiation towards a VSMC phenotype would affect this response could further explore how these cells respond to a loading environment.

TGF-β1 is the most commonly used factor to induce vascular smooth muscle differentiation and several studies have shown that TGF-β1 increases myogenic markers in MSC.[215-218] Specifically, stimulating with TGF-β1 has been shown to upregulate α-SMA in human MSC (hMSC) at 1 ng/ml,[216,218] 5 ng/ml,[217]and 10 ng/ml.[215] Crucially, 5 ng/ml has also been shown to upregulate Calponin 1 and Myocardin.[217] In addition, TGF-β1 has been shown to upregulate SM22α at concentrations greater than 0.1 ng/ml[217] and upregulate Calponin at concentrations greater than 1ng/ml.[218]

This chapter describes a preliminary investigation into the mechanosensitivity of MVSC, and whether MVSC and VSMC respond differently to strain. It further explores if induction of a VSMC phenotype in MVSC with TGF-β1 would alter that strain response.

3.2 Methods

3.2.1 Cell Culture

RASMC were obtained from Lonza and cultured in XPAN with or without the addition of 10ng/ml of recombinant human TGF-β1 (Sigma). MVSC were isolated as previously described by Kennedy et al.[106] Briefly, cells were explanted from rat aorta tissue from which the adventitia had been removed. MVSC were cultured in maintenance medium (MM1+) (hgDMEM with Glutamax (Thermo-Scientific) with 2% chick embryo extract (MP Biomedical), 1% FBS (ATCC), 1% N2 (Invitrogen), 2% B27 (Invitrogen), 100 nM retinoic acid (Sigma-Aldrich), 50 nM 2-mercaptoethanol (Sigma-Aldrich), and 1% penicillin and streptomycin (Thermo-Scientific)) or XPAN with 10ng/ml TGF-β1.

3.2.2 Tensile strain

Cells were strained on the Flexcell® FX-5000™ Tension System which had been previously calibrated as shown in Appendix II. Cells were seeded at 10^5 cells per well in 6 well, pronectin coated Bioflex™ plates with three wells per experiment. Cells were allowed to adhere for 48 hours in their respective culture medium, then serum starved in DMEM with 0.2% FBS for 24 hours. At this point the strain regime was started. After serum starvation, day 0 cells were harvested. Other cells were strained in XPAN medium. Cells were strained at 1Hz and 2-8% strain amplitude or left unstrained for 24 hours as a control.

3.2.3 Gene Expression

Cells were lysed and scraped in Buffer RLT (Qiagen) and mRNA was isolated using QiaShredders (Qiagen) followed by the RNeasy Micro Kit (Qiagen). Messenger RNA was then reverse transcribed into cDNA using the High Capacity cDNA Reverse Transcription Kit (ThermoFisher Scientific). Real-Time qPCR was performed using SYBR Select Master Mix (Bio-Sciences Ltd) and the PrimeTime qPCR primers (IDT) in Table 3.2 on an Applied Biosystems® 7500 Fast Real-Time PCR System. PCR results were analysed using the ΔΔCt method using TBP as the reference gene. Primers used are listed in Table 3.1.

Table 3.1: Rat Gene Primers

Gene	***Primer***
TBP	*Rn.PT.39a.22214837*
MYH11	*Rn.PT.58.37122318*
CNN1	*Rn.PT.58.7442518*

3.2.4 Immunocytochemistry (ICC)

To assess cell phenotype, cells were seeded on glass slides at a density of 5200 cells/cm^2 and cells were allowed to adhere for 2 days. Cells were fixed in 10% formalin for 10 minutes and then rinsed twice with PBS. Cells were blocked and permeabilized in 5% BSA and 0.2% Triton X-100 for 30 minutes at room temperature. Primary antibody was used in PBS with 0.5% BSA and 0.2% Triton X-100 overnight at 4°C at a concentration of 1:50 for Myosin11 (ab53219), and 1:200 for Calponin (ab46794) and SM22α (ab14106). Cells were incubated in secondary antibody (ab150073) 1:1000 in PBS with 0.5% BSA and 0.2% Triton X-100 for 1 hour at room temperature. Cells were then incubated in DAPI 1:1000 in PBS for 30 minutes at room temperature. Cells were rinsed in PBS between each

incubation step. Cells were imaged using an Olympus IX83 epifluorescent inverted microscope using CellSens software. The antibodies used are listed in Table 3.2.

Table 3.2: Antibodies

Protein	***Antibody***	***Concentration***
SM-MHC	Sigma M7786	1:50
Calponin 1	Sigma C2687	1:50
α-SMA	Sigma A5228	1:50

3.2.5 Statistics

For cell counts statistical significance was determined using an ordinary one way ANOVA with post hoc Holm-Sidak's multiple comparisons test. The significance of percentage of calponin positive cells was evaluated using a Kruskal-Wallis test. For qPCR experiments, the significance was determined between the ΔΔCt values using a two way ANOVA with post-hoc Tukey's test.

3.3 Results

This preliminary study investigated the differences in strain response between RASMC and rMVSC with and without TGF-β1 to induce a contractile phenotype. First, cell phenotype was characterized through the use of ICC. Long term culture of rMVSC in medium

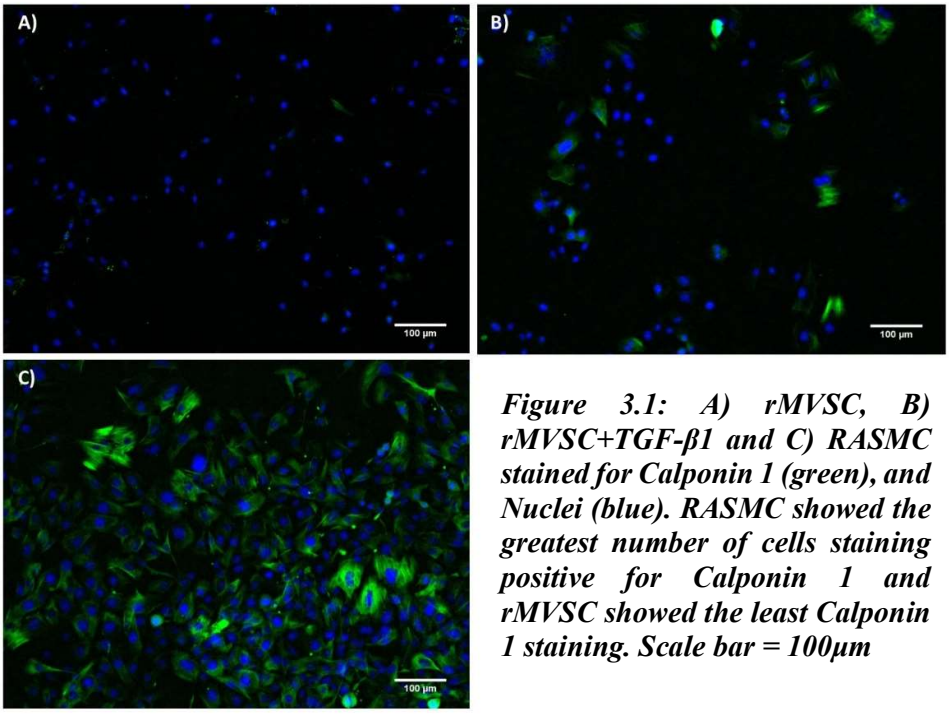

Figure 3.1: A) rMVSC, B) rMVSC+TGF-β1 and C) RASMC stained for Calponin 1 (green), and Nuclei (blue). RASMC showed the greatest number of cells staining positive for Calponin 1 and rMVSC showed the least Calponin 1 staining. Scale bar = 100µm

containing TGF-β1 increased the number of cells expressing Calponin, from 1.7% to 61%, however, this was still lower than the 95% of RASMC expressing Calponin 1 (Figures 3.1, 3.2). No cell population stained positive for Myosin 11.

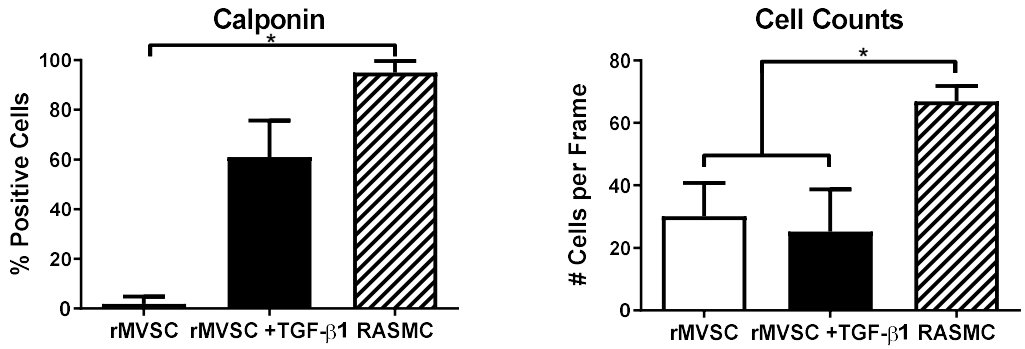

Figure 3.2: Calponin 1 protein expression in rat vascular cells. RASMC showed the greatest number of cells expressing Calponin 1, while rMVSC showed almost no cells expressing Calponin1. rMVSC both with and without TGF-β1 show lower cell numbers over the same area as RASMC possibly indicating lower cell proliferation. *p<0.05, **p<0.01, ***p<0.001, ****p<0.0001 n = 3

After 24 hours of 2-8% strain amplitude, all cell populations were assessed for the expression of the contractile genes MYH11 and CNN1. In all cell populations, there was a similar small decrease in CNN1 versus the control (Figure 3.3). Only the cells treated with TGF-β1 showed a decrease that was significant. rMVSC showed a significant increase in MYH11 in response to strain, while RASMC with TGF-β1 showed a significant decrease in MYH11 in response to strain. Although these cells showed different directions of MYH11 change, these populations started out at vastly different levels of CNN1 and MYH11 expression. Treatment of rMVSC with TGF-β1 raised CNN1 expression to the 20 fold more of RASMC, but not as high as the 80 fold more of RASMC with TGF-β1. However, treating rMVSC with TGF-β1 barely raised MYH11 expression 3 fold whereas RASMC had 150 fold more MYH11 and RASMC treated with TGF-β1 expressed 570 fold more MYH11 (Figure 3.4).

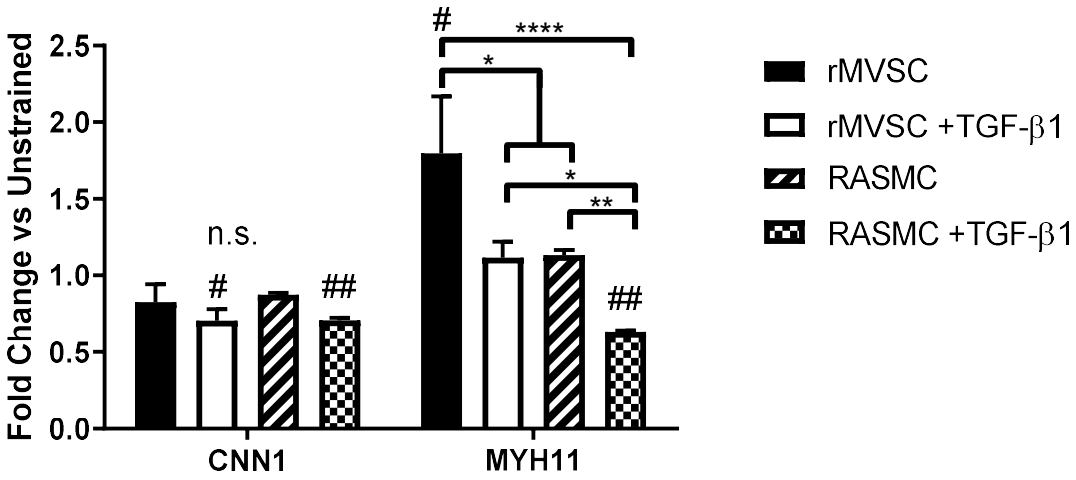

***Figure 3.3**: Gene expression in rat cells exposed to 24 hours of 2-8% amplitude strain. All populations showed a decrease in CNN1 in response to strain, though only significantly in populations cultured in TGF-β1. rMVSC showed an increase in MYH11 expression in response to strain while RASMC + TGF-β1 showed a decrease in MYH11 expression in response to strain. # represent significance between strained and unstrained *p<0.05, **p<0.01, ***p<0.001, ****p<0.0001 n = 3*

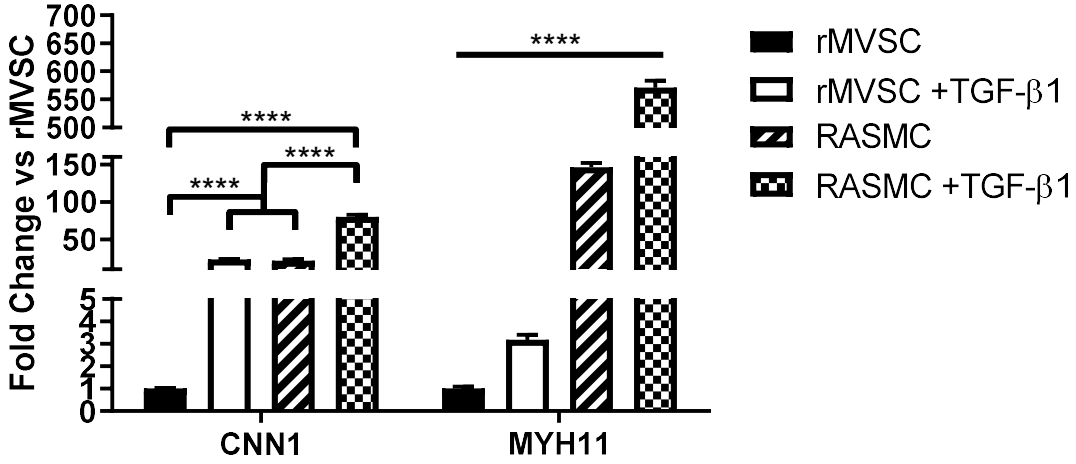

***Figure 3.4**: Comparative gene expression between unstrained rat cell populations. Culture in TGF-β1 increased expression of CNN1, and MYH11 *p<0.05, **p<0.01, ***p<0.001, ****p<0.0001 n = 3*

3.4 Discussion

The different contractile VSMC gene expression in response to strain between rMVSC and RASMC confirms the idea that MVSC and VSMC react differently in response to strain. Rat MVSC increased MYH11 expression in response to 24 hours of strain, while RASMC had no change and RASMC grown in the presence of TGF-β1 decreased expression. Therefore, MVSC and contractile VSMC have differing reactions to the same mechanical stimuli. While strain might encourage MVSC to differentiate into a VSMC phenotype and replace any damage due to strain, this same strain may cause contractile VSMC to lose their contractile function.

TGF-β1 induced increased contractile smooth muscle cell gene and protein expression in both rMVSC and RASMC. However, when it came to MVSC gene expression, only CNN1 approached the levels of even the synthetic VSMC, while MYH11 expression was still nowhere near that of VSMC. This indicates that MVSC may never fully differentiate into contractile VSMC or that additional stimuli might be required in order to fully reach contractile VSMC differentiation.

These strain experiments were performed on the Flexcell system. However, as shown in Appendix II, the Flexcell device does not maintain a consistent strain profile over time. This means that if cells are cultured long term on the Flexcell device they may not be experiencing a consistent level of strain. Additionally, the Flexcell device provides equiaxial strain. Uniaxial strain would be more comparable to the internal strain environment of a blood vessel, which while not entirely uniaxial, is anisotropic, with the circumferential being the dominant loading direction. This uniaxial tensile strain can be applied using the Bose BioDynamic System. This system was used in the subsequent uniaxial tensile strain studies These preliminary studies indicate that MVSC and VSMC do have different responses to cyclic tensile strain, and these two populations of cells require further study to elucidate these differences.

.

Chapter 4 Resident Multipotent Vascular Stem Cells Exhibit Amplitude Dependent Strain Avoidance Similar to that of Vascular Smooth Muscle Cells

4.1 Introduction

While Chapter 3 established that MVSC and VSMC had different responses to the application of equiaxial strain, the strain in a vessel *in vivo* is primarily in the circumferential direction, making uniaxial strain a closer representation of the strain cells would experience in the vascular media. Although strain levels within the vessel can change due to vascular disease, or vascular interventions, only a handful of papers have investigated the effect of uniaxial strain amplitude on cells (including vascular[219] and esophageal[220] smooth muscle cells, endothelial cells[221], fibroblasts and osteoblasts), and most studies on uniaxial tensile strain focus only on one amplitude.[222] Preliminary studies with VSMC exposed to equiaxial strain (Appendix I) show that strain amplitude affects the contractile phenotype of the cells.

Despite the fact that MVSC may potentially play a role in vascular disease, and vascular tissue is a mechanically responsive tissue, no studies to-date have investigated the effects of uniaxial strain on MVSC. This study investigates the response of MVSC to uniaxial cyclic tensile strain and compares it to that of VSMC. Additionally, effects of strain amplitude on both cell types was also investigated. Comparing these two cell types can help us to understand the role that each cell type may play in response to vascular interventions such as stenting and vascular bypass grafts. Also, understanding the role of these cells in intimal hyperplasia, in particular, could help to develop treatments or devices that mediate the proliferative response of these cells. Therefore, it is of critical importance to understand the effects of cyclic tensile strain amplitude on both MVSC and VSMC.

4.2 Methods

4.2.1 Cell Isolation and Culture

Rat SMC (RASMC) were obtained by enzymatic digestion of the aorta of three adult Sprague Dawley rats. Rat aortas were dissected and the adventitial layer was removed. Aorta were manually cut into pieces no larger than $1mm^3$ and digested in a sterile solution of 0.7mg/mL Collagenase type 1A (Sigma-Aldrich) and 0.35mg/mL Elastase type III

(Sigma-Aldrich) in PBS at 37ºC for 2 hours with agitation. RASMC were cultured in high glucose DMEM with Glutamax (Bio-Sciences) with 10% FBS (Gibco) and 2% Penicillin/Streptomycin (Bio-Sciences). RASMC were used from p6 to p8.

Rat MVSC (rMVSC) were isolated by explant as previously described[223] and were cultured in high glucose DMEM with Glutamax (Bio-sciences), with 1% Penicillin/Streptomycin(Bio-Sciences), 1% N-2 supplement (Gibco), 2% B-27 supplement (Gibco), 20ng/mL bFGF (Corning), 2% chicken embryo extract (ATCC), 100 nM retinoic acid(Sigma-Aldrich), 50 nM 2-mercaptoethanol (Gibco). rMVSC were used from p18 to p20.

4.2.2 PDMS

Sylgard 184 polydimethylsiloxane (PDMS) elastomer was used in a 10:1 ratio of base to curing agent.[224] PDMS was poured to 1mm thick and then placed under a vacuum for 20 minutes to remove bubbles. Silicone was cured at 60ºC for 16 hours. Strips were cut to 5mm wide, and 20mm long for static conditions, or 30mm long for strips loaded into the Bose strain device, which had a strain region of 20mm long. PDMS surface was treated with 70% sulfuric acid for 5 minutes to make surface more hydrophilic. PDMS strips were then sterilized for one hour in 100% ethanol and rinsed in sterile PBS. Strips were coated in 10µg/ml pronectin (Sigma-Aldrich) in phosphate buffered saline (PBS) (Sigma-Aldrich) for 1 hour and then pronectin solution was removed and strips were allowed to dry before cells were seeded at $5.5x10^3$ cells/cm^2 which allowed the cells to remain subconfluent before the application of strain. Cells were allowed to adhere for 1 hour before dishes were flooded with medium. Cells were grown for three days on the strips before the start of strain application.

4.2.3 Application of Strain

Strips were loaded into clamps within a BioDynamic 5200 (TA Instruments) with two strips placed side-by-side in each bioreactor chamber (Figure 4.1). Bose chambers were filled with 10% FBS medium supplemented with 2µl/mL Primocin. PDMS strips were given a 0.1N preload. Samples were strained uniaxially for 24 or 72 hours using displacement controlled strain, at 1Hz frequency and a mean strain of 5% strain at three strain amplitudes of 2%, 6% or 10%, resulting in strains of 4-6%, 2-8% and 0-10% strain to represent strain amplitudes experienced in stiffened (4-6%), healthy (2-8%) or degenerative (0-10%) vascular tissue.[37]

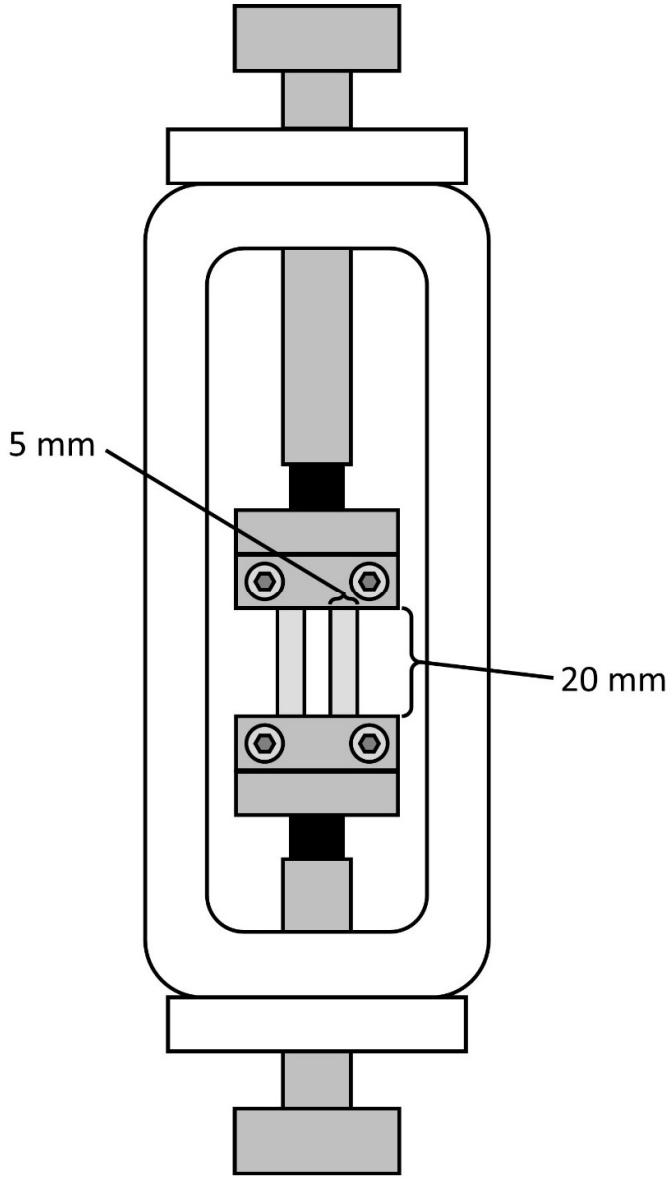

Figure 4.1: Bose Biodynamic chamber setup. Two 30mm by 5 mm PDMS strips are clamped on either end, leaving a 2cm by 0.5cm sample area. Chambers are oriented vertically in the Bose Biodynamic strain device, and strain is applied by moving the bottom by the specified amplitude.

4.2.4 Immunostaining

PDMS strips were fixed in 10% formalin for 20 minutes at room temperature and stored at 4ºC until they were stained. Strips were blocked and permeabilized in a solution of 5% BSA and 0.2% Triton-X 100 in PBS at room temperature for 40 minutes with agitation. Strips were then rinsed twice in PBS. Primary antibody solution was prepared in 0.5% BSA and 0.2% Triton-X 100 in PBS, with the antibodies at the concentration shown in Table

4.1. Strips were incubated in primary antibody overnight at 4ºC. Strips were rinsed three times in PBS. Secondary antibody solution was prepared 0.5% BSA and 0.2% Triton-X 100 in PBS with 1:1000 secondary antibody, 1:500 rhodamine Phalloidin, and 1:1000 DAPI. Strips were incubated in secondary antibody solution in the dark at room temperature for 1 hour. Strips were rinsed three times in PBS and stored at 4ºC protected from light before imaging.

Table 4.1: List of Immunostaining Antibodies and Concentrations

Primary Antibodies	***Concentration***	***Product Code***
Ki67	1:200	Abcam ab15580
Calponin 1	1:100	Sigma C2687
SM-MHC	1:100	Sigma M7786
αSMA	1:100	Sigma A5228

4.2.5 Imaging and Image Analysis

All images were taken on a Leica SP8 scanning confocal microscope at 20x. For samples on PDMS, 10 random fields were taken for each sample with the nuclei used for the focal point. Images were taken at a resolution of 1024x1024 pixels and a scan speed of 200 Hz. DAPI-stained nuclei were thresholded using ImageJ. Then the *Fill Holes* and *Watershed* features of ImageJ were used to correct any holes caused by thresholding, and to separate touching nuclei. This thresholded image was then analysed in ImageJ using *Analyze Particles*, excluding any particles < 20μm^2 and on the edges, producing nuclear area measurements and fitted ellipses for each nucleus. These ellipses provided a major and minor axis length as well as an orientation (Figure 4.2). Nuclear circularity was determined by dividing the length of the minor axis by the major axis. Actin alignment was determined using the MatFiber MatLab program (Figure 4.3).[225] Ki67 nuclei were determined by masking Ki67 with thresholded nuclei and then counting positive nuclei using ImageJ particle analysis. Immunostaining intensity measures were determined by creating a mask for the cell area using the Trainable Weka Segmenter tool within MatLab to segment out the cell area using the f-actin stain. Within the masked area, the stain intensity was determined, then normalized to a secondary antibody only control.

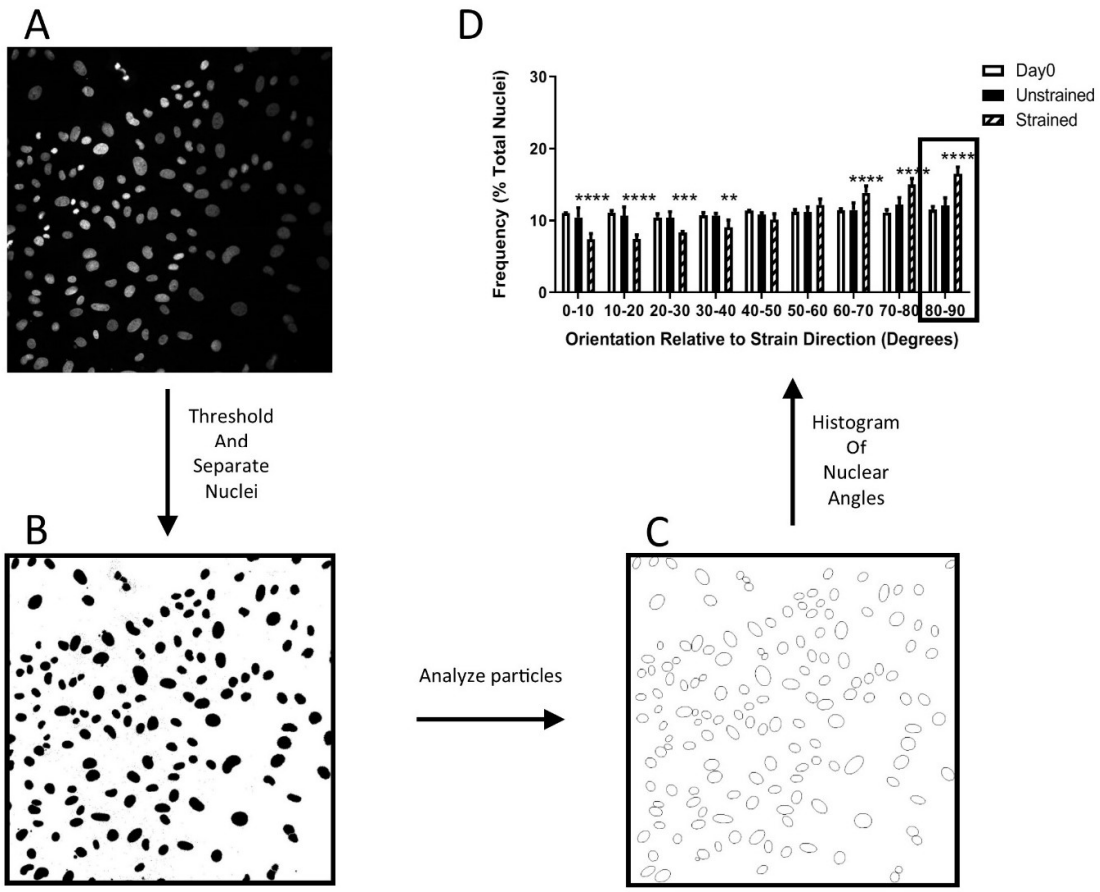

Figure 4.2: Nuclear alignment analysis. Image of DAPI-stained nuclei (A) is thresholded using ImageJ. Then the* Fill Holes *and* Watershed *features are used to correct any holes caused by thresholding, and to separate touching nuclei (B). This thresholded image was then analysed in ImageJ using* Analyze Particles*, excluding any particles < 20μm^2 and on the edges, producing fitted ellipses for each nuclei (C). These ellipses provide a major and minor axis length as well as an orientation. The nuclear orientations were then represented as a frequency histogram (D) from 0-90^o relative to strain direction.

4.2.6 Statistics

Statistics were performed using GraphPad Prism version 8.1.1. Significance was determined using 2-way ANOVA with a Tukey's post-hoc test or a Sidak's post-hoc test. Each measurement was based on $n \geq 3$ independent samples.

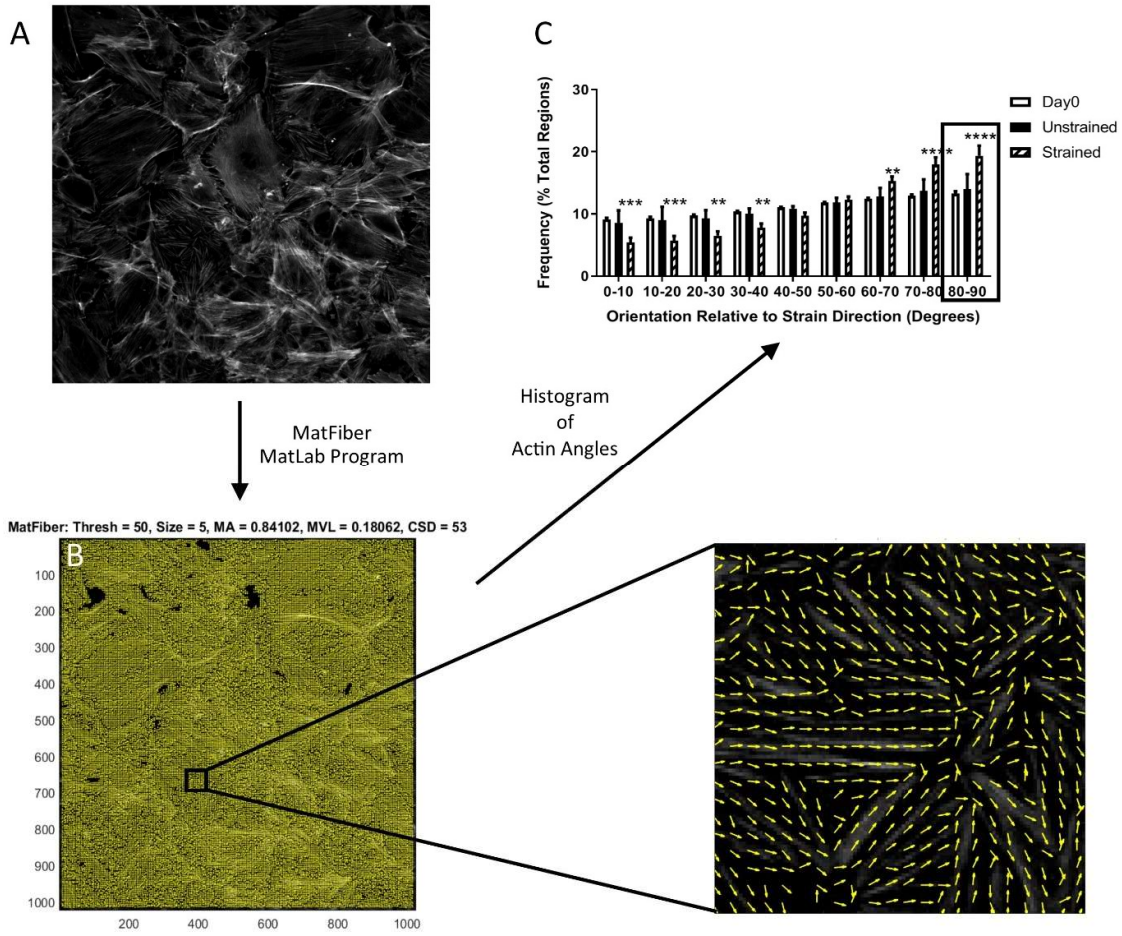

***Figure 4.3**: Actin alignment analysis. Image of Phalloidin-stained f-actin (A) is analysed using the MatFiber MatLab program.[225] This provides an orientation vector for each region (B) which is then plotted as a frequency histogram (C) from 0-90º relative to strain direction.*

4.3 Results

Rat MVSC and RASMC were exposed to three different strain levels of 1Hz, cyclic uniaxial tensile strain centred around 5% strain: 4-6%, 2-8%, and 0-10% strain for 24 or 48 hours (Figure 4.4, Figure 4.5). Cell alignment was determined by looking at the distribution of the alignment of nuclei.

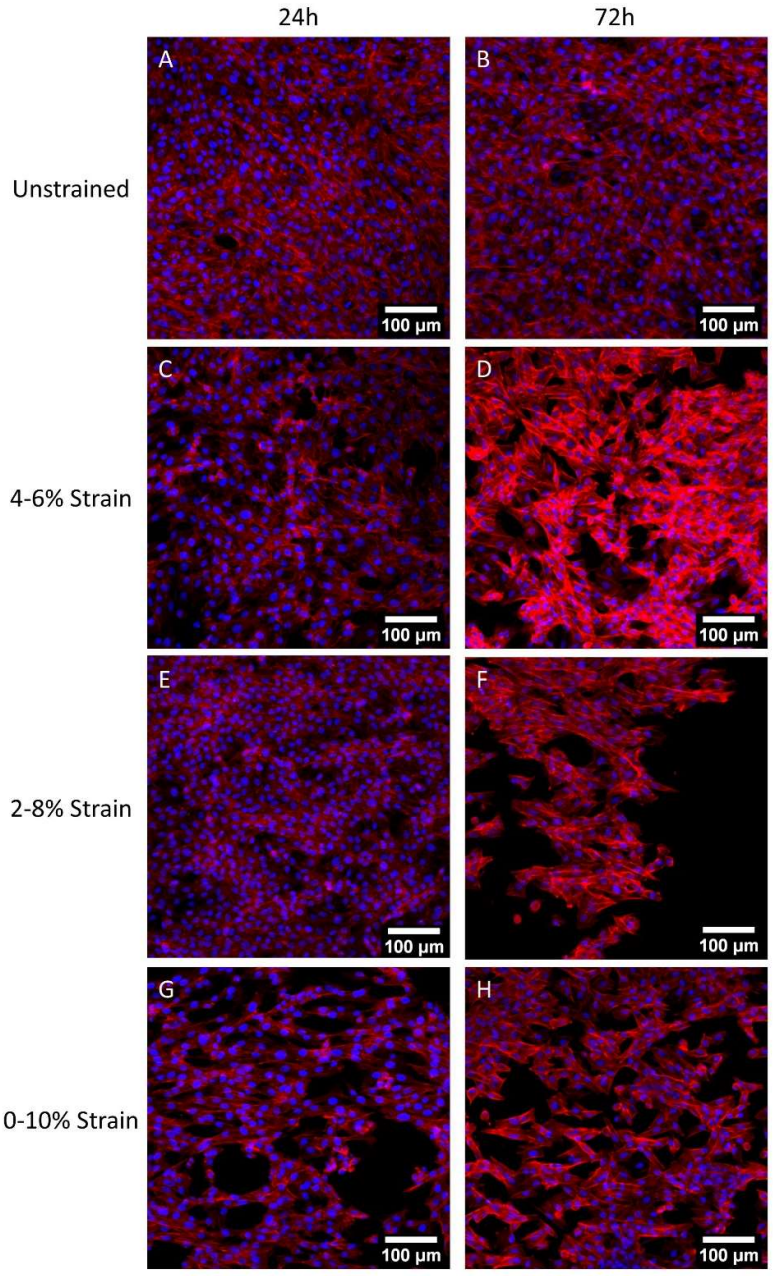

Figure 4.4: Representative images of rMVSC after 24 (A, C, E, G) or 72 hours (B, D, F, H) of no strain (A, B), or 4-6% (C, D), 2-8% (E, F), or 0-10% (G, H) 1 Hz cyclic tensile strain. Blue – DAPI nuclei, Red – Phalloidin f-actin. Scale bar = 100µm

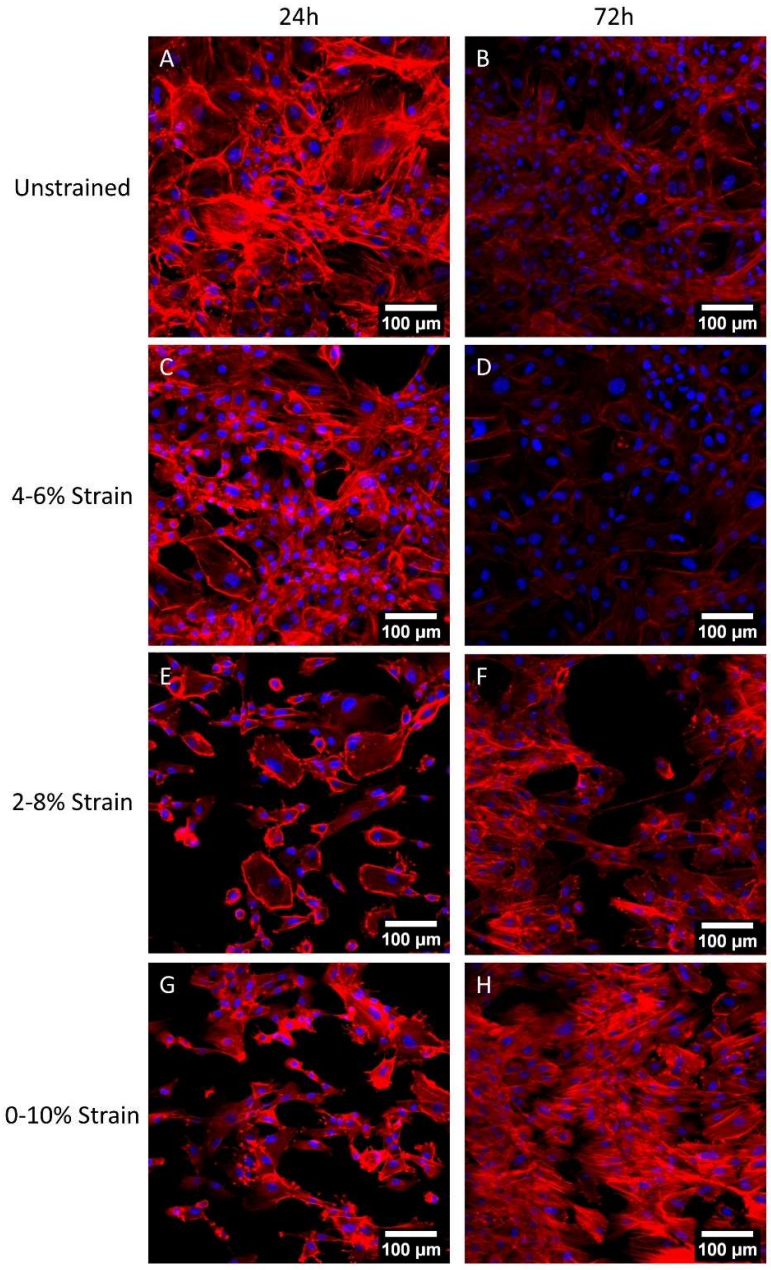

Figure 4.5: Representative images of RASMC after 24 (A, C, E, G) or 72 hours (B, D, F, H) of no strain (A, B), or 4-6% (C, D), 2-8% (E, F), or 0-10% (G, H) 1 Hz cyclic tensile strain. Blue – DAPI nuclei, Red – Phalloidin f-actin.

Rat MVSC had significant nuclear alignment perpendicular to the strain direction at 2-8% strain and 0-10% strain at both 24 hours (Figure 4.6A) and 72 hours (Figure 4.6B). At 24 hours 4-6% strain had significantly less alignment than both other strain levels (Figure 4.6A), while 4-6% strain had significantly less alignment than 0-10% strain at 72 hours (Figure 4.6B). Similarly, RASMC had significant nuclear alignment perpendicular to strain direction at 2-8% strain and 0-10% strain at both 24 hours (Figure 4.6C) and 72 hours

(Figure 4.6D). At both time points, all RASMC strain amplitudes had significantly different degrees of alignment from all other strain amplitudes (Figure 4.6C, D). When rMVSC and RASMC were compared, for the 2-8% and 0-10% strain amplitudes after 24 hours of strain, rMVSC had greater nuclear alignment perpendicular to strain direction than RASMC (Figure 4.6E). Conversely, at 72 hours of strain, RASMC exposed to 0-10% strain amplitude had greater alignment perpendicular to the strain direction than rMVSC (Figure 4.6F).

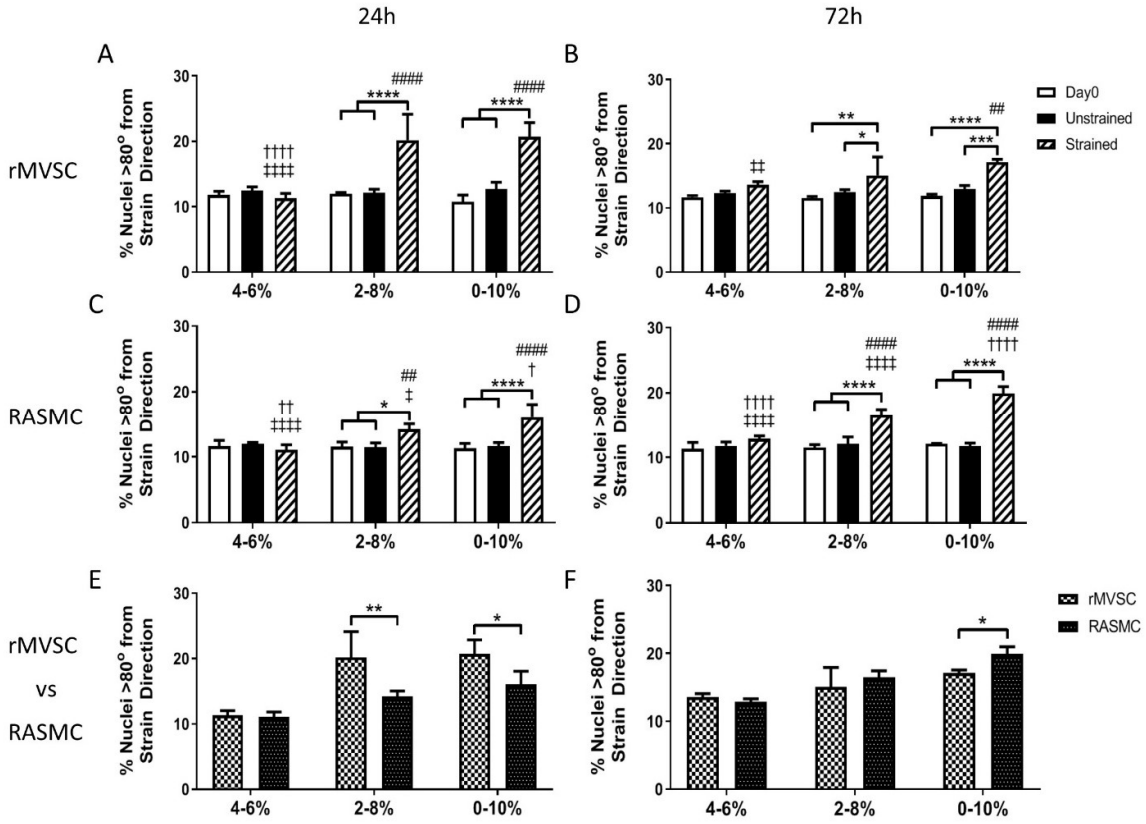

Figure 4.6: Percentage of nuclei oriented greater than 80 degrees away from strain direction for rMVSC (A,B,E,F) or RASMC (C,D,E,F) exposed to 1Hz uniaxial cyclic tensile strain at 4-6% strain, 2-8% strain, 0-10% for 24 hours (A,C,E) or 72 hours (B,D,F). In all cases except for 4-6% strain at 24 hours, rMVSC show significant alignment perpendicular to strain direction. In all cases except for 4-6% strain conditions RASMC show significant alignment perpendicular to strain direction. At 2-8% and 0-10% strain, at 24 hours, rMVSC showed greater alignment than RASMC. At 72 hours, 0-10% strain RASMC showed greater alignment than rMVSC. *p<0.05, **p<0.01, ***p<0.001, ****p<0.0001 # - Significantly different than 4-6% strained † - Significantly different from 2-8% strained ‡ - Significantly different than 0-10% strained. Repeated symbols signify level of significance. n ≥ 3

Additionally, cell alignment was also determined by measuring the alignment of the f-actin cytoskeleton. Rat MVSC had significantly greater f-actin reorganization parallel to the strain direction as compared to unstrained controls after 24 hours of 2-8% strain (Figure 4.7A) and after 0-10% strain at 72 hours (Figure 4.7B). Additionally at 24 hours, alignment of cells at 4-6% strain was significantly different than both other strain levels (Figure 4.7A), while at 72 hours f-actin alignment of cells at 0-10% strain was significantly different than both other strain levels (Figure 4.7B). RASMC had significant f-actin alignment perpendicular to strain direction at 0-10% strain at 24 hours (Figure 4.7C) and at 2-8% strain and 0-10% strain at 72 hours (Figure 4.7D). At 24 hours, 0-10% strain had significantly greater f-actin alignment than both other strain levels (Figure 4.7C), while at 72 hours, all strain levels had significantly different alignment from each other (Figure 4.7D). When comparing strained rMVSC and RASMC actin cytoskeletal alignment, at 24 hours rMVSC had greater f-actin alignment perpendicular to strain direction at 2-8% strain (Figure 4.7E). However, at 72 hours, RASMC had greater actin alignment than rMVSC at strain amplitudes of 2-8% and 0-10% strain amplitude (Figure 4.7F).

To determine actin fibre dispersion, the mean vector length (MVL) was determined for all measured directional unit vectors of actin alignment. A value of 1 indicates that all fibres were aligned in the same direction, while a value of 0 indicates a completely random fibre direction. At 24 hours rMVSC had a strain induced increase in MVL at 2-8% strain, and there was a significant difference in MVL between 4-6% strain and 2-8% strain (Figure 4.8A). By 72 hours, rMVSC MVL increased at 0-10% strain, and 0-10% strain had an increased MVL versus other strain levels (Figure 4.8B). RASMC had a significant increase of mean vector length due to strain at 0-10% strain amplitude at both time points (Figure 4.8C, D). At 24 hours 0-10% strain had a significantly higher MVL than 4-6% strain (Figure 4.8C), while at 72 hours 0-10% strain had a significantly higher MVL than both 4-6% and 2-8% strain (Figure 4.8D).

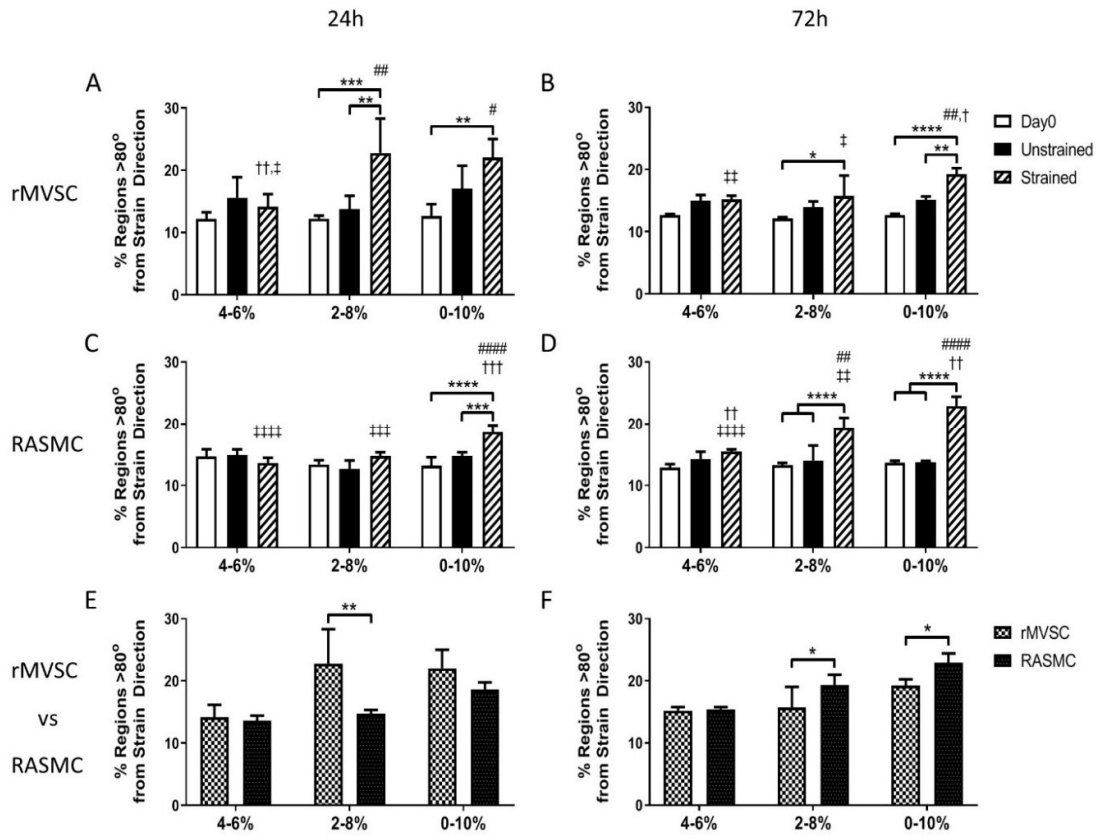

Figure 4.7: Percentage of f-actin regions oriented greater than 80 degrees away from strain direction for rMVSC (A,B,E,F) or RASMC (C,D,E,F) exposed to 1Hz uniaxial cyclic tensile strain at 4-6% strain, 2-8% strain, 0-10% for 24 hours (A,C,E) or 72 hours (B,D,F). rMVSC show significant alignment perpendicular to strain direction at 24 hours at 2-8% strain and both time points of 0-10% strain. In all cases except for 4-6% strain at 24 hours, RASMC show significant alignment perpendicular to strain direction. At 2-8% and 0-10% strain, at 24 hours, rMVSC showed greater alignment than RASMC. At 72 hours, 2-8% and 0-10% strain RASMC showed greater alignment than rMVSC. *p<0.05, **p<0.01, ***p<0.001, ****p<0.0001 # - Significantly different than 4-6% strained † - Significantly different from 2-8% strained ‡ - Significantly different than 0-10% strained. Repeated symbols signify level of significance. n ≥ 3

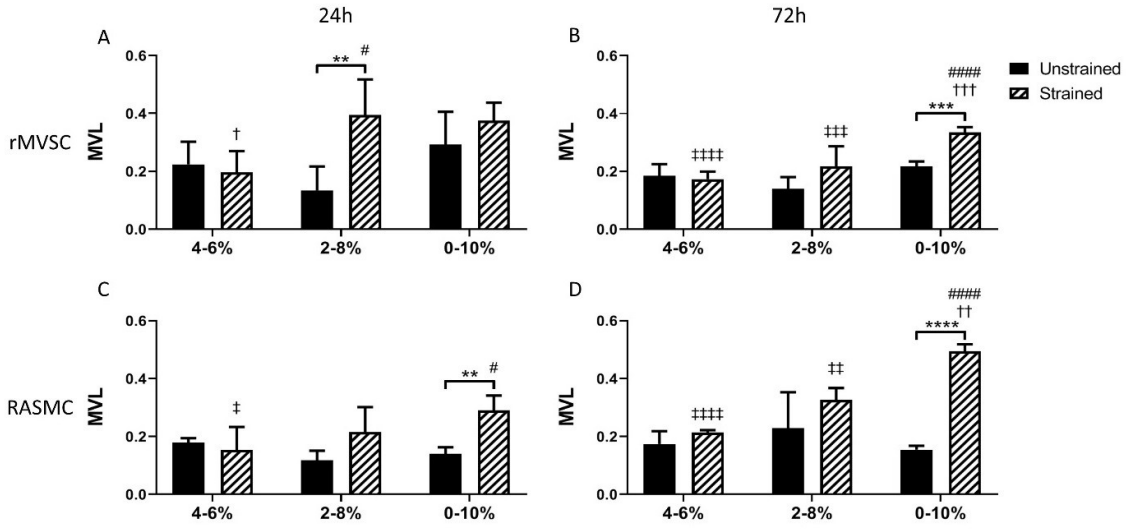

Figure 4.8: Mean vector length (MVL) for f-actin fibre distribution for rMVSC (A,B) and RASMC (C,D) at 24 hours (A,C) and 72 hours (B,D) for strain levels of 4-6%, 2-8%, 0-10%. A MVL near 1 indicates less dispersion of actin fibres, while an MVL near 0 indicates a random distribution of fibres. At 24 hours rMVSC at 2-8% strain show increased MVL after 24 hours of strain and 2-8% strain has a significantly higher MVL than 4-6% strain. At 72 hours rMVSC show increased MVL at 0-10% strain compared to unstrained control as well as 4-6% and 0-10% strain. RASMC showed increased MVL at 0-10% strain amplitude at both time points. At 24 hours 0-10% strain showed significantly higher MVL than 4-6% strain, while at 72 hours 0-10% strain showed significantly higher MVL than both 4-6% and 2-8% strain. *p<0.05, **p<0.01, ***p<0.001, ****p<0.0001 # - Significantly different than 4-6% strained † - Significantly different from 2-8% strained ‡ - Significantly different than 0-10% strained. Repeated symbols signify level of significance. n ≥ 3

In addition to alignment, both cell types were assessed for the effect of strain amplitude on overall change in cell number. For rMVSC and RASMC, strain decreased cell number at 0-10% strain after 24 hours strain (Figure 4.9A, C). At 72 hours, rMVSC decreased in cell number at all strain levels (Figure 4.9E). Then, whether or not this decrease in cell number was due to a decrease in cell proliferation was investigated. This was done by measuring the percentage of cells that stained positive for the nuclear cell division marker Ki67. While most conditions had no significant differences in Ki67 expression due to strain, for rMVSC the number of cells expressing Ki67 increased after 72 hours of 2-8% strain (Figure 4.9F).

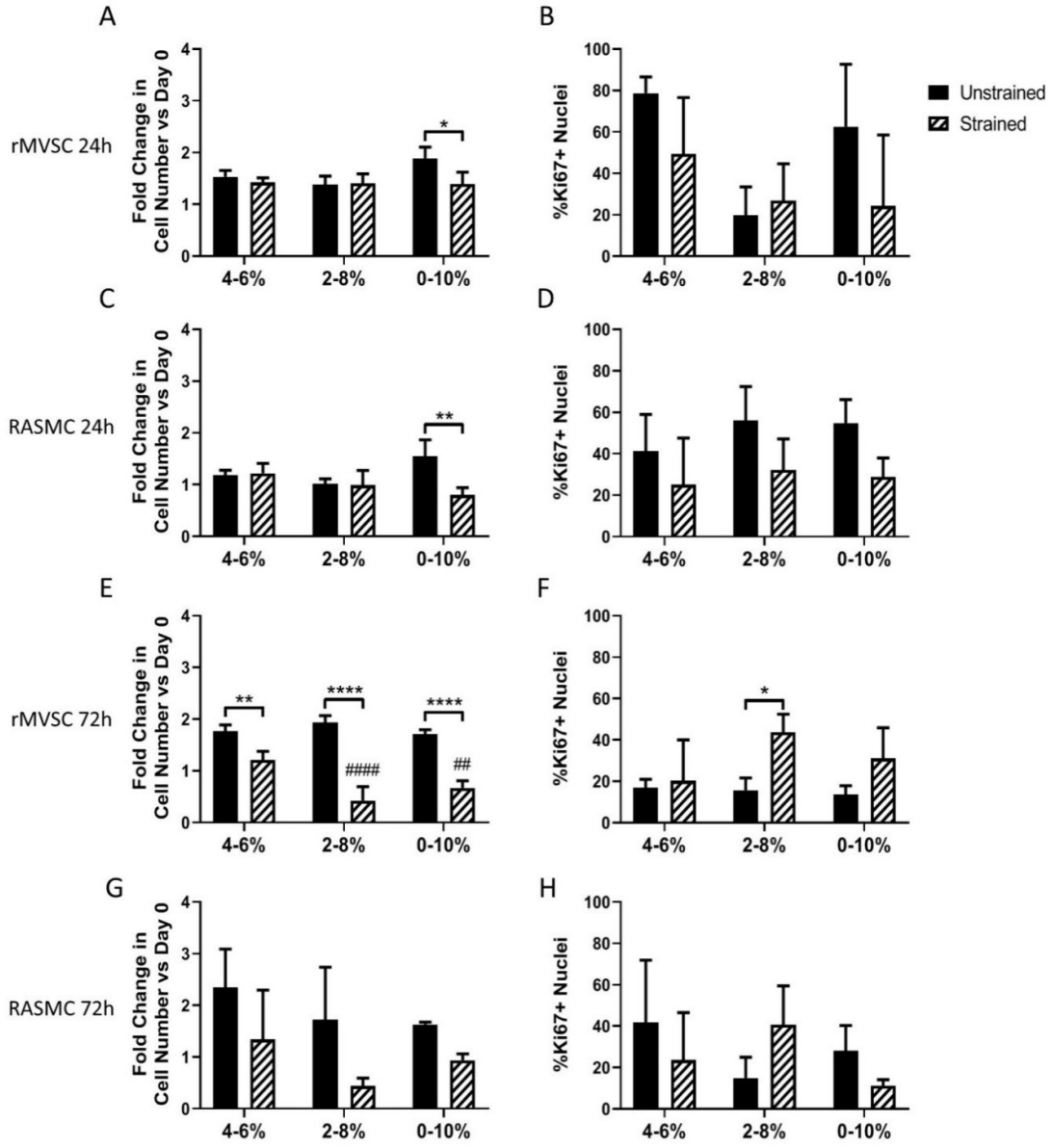

Figure 4.9: Fold change in number of nuclei versus day 0 (A,C,E,G) and percentage of Ki67 positive nuclei (B,D,F,H) for rMVSC (A,B,E,F) and RASMC (C,D,G,H) at 24 hours (A,B,C,D) and 72 hours. Both rMVSC and RASMC show a strain-induced decrease in cell number at 0-10% strain at 24 hours. At 72 hours, rMVSC show a decrease in cell number at all strain levels, with 4-6% strain showing a significant difference with the two other strain amplitudes. Ki67 expression shows a strain induced increase in rMVSC at 2-8% strain. *p<0.05, **p<0.01, ***p<0.001, ****p<0.0001 # - Significantly different than 4-6% strained † - Significantly different from 2-8% strained ‡ - Significantly different than 0-10% strained. Repeated symbols signify level of significance. n ≥ 3

In addition to measuring nuclear alignment, nuclear circularity and nuclear area were also measured. Strain significantly decreased rMVSC nuclear circularity at all time points and strain amplitudes (Figure 4.10A, B). RASMC exhibited a strain induced decrease in nuclear

circularity only at 24 hours of 0-10% strain (Figure 4.10C). Nuclear area changed due to strain in RASMC. RASMC increased in nuclear area after 72 hours of 4-6% strain, while they decreased in nuclear area after 24 hours of 2-8% strain. No significant differences in nuclear area occurred due to different strain amplitudes. In most cases, RASMC had significantly larger nuclei than rMVSC (Figure 4.11). Contractile markers αSMA, Calponin 1 and SM-MHC were also assessed after 72 hours of cyclic tensile strain. None of these three markers had a significant change in response to strain (Figure 4.12). Representative images for these stains can be found in Appendix III.

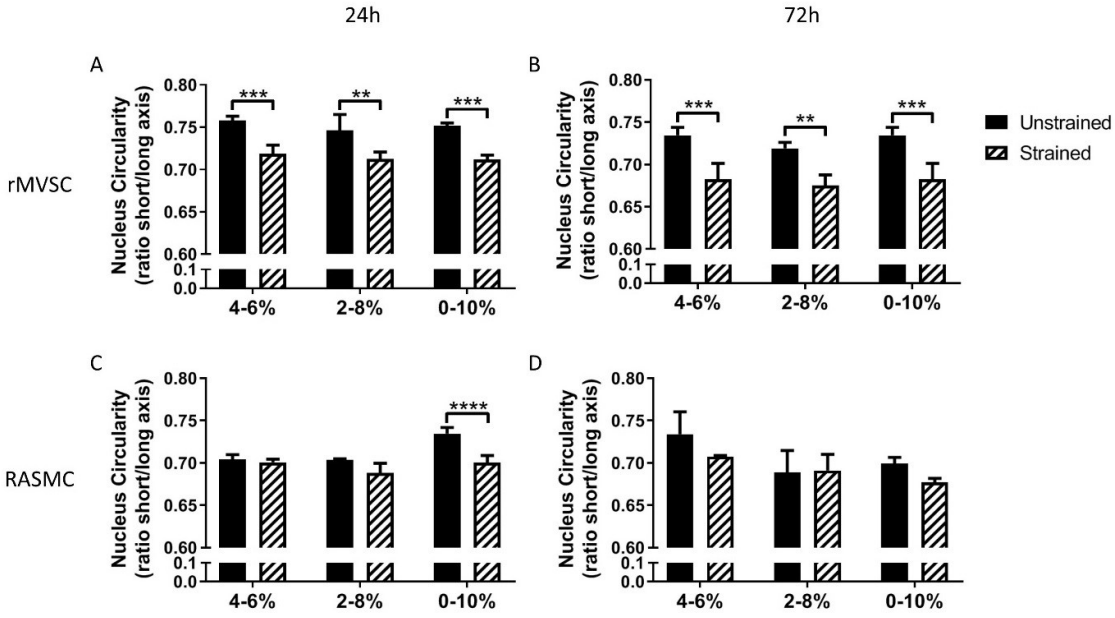

Figure 4.10: Circularity, or ratio of minor to major axis of nuclei for rMVSC (A,B) and RASMC (C,D) at 24 hours (A,C) and 72 hours (B,D for strain levels of 4-6%, 2-8%, and 0-10%(E,F). Under all conditions and time points, rMVSC showed a decrease in nuclear circularity due to strain. RASMC showed a strain induced decrease in nuclear circularity after 24 hours of 0-10% strain. *p<0.05, **p<0.01, ***p<0.001, ****p<0.0001 n ≥ 3

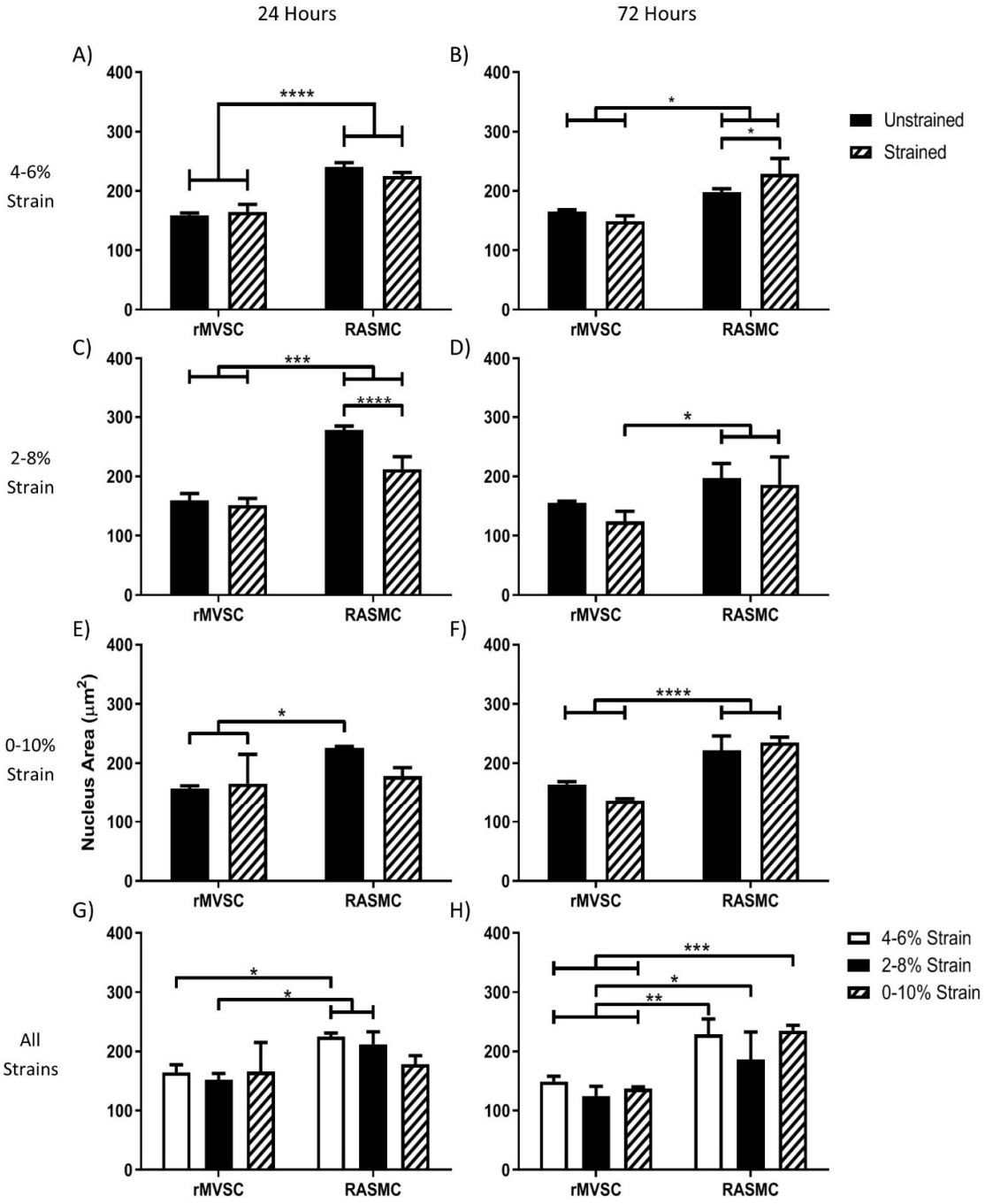

Figure 4.11: Average nuclear area for rMVSC and RASMC at 24 hours (A,C,E,G) and 72 hours (B,D,F,H) for strain levels of 4-6%(A,B), 2-8%(C,D), 0-10%(E,F), and a comparison between strained samples at all levels(G,H). RASMC showed increased nuclear area after 72 hours of 4-6% strain and decreased nuclear area after 24 hours of 2-8% strain. RASMC usually had significantly larger nuclei than rMVSC. *p<0.05, **p<0.01, ***p<0.001, ****p<0.0001 n ≥ 3

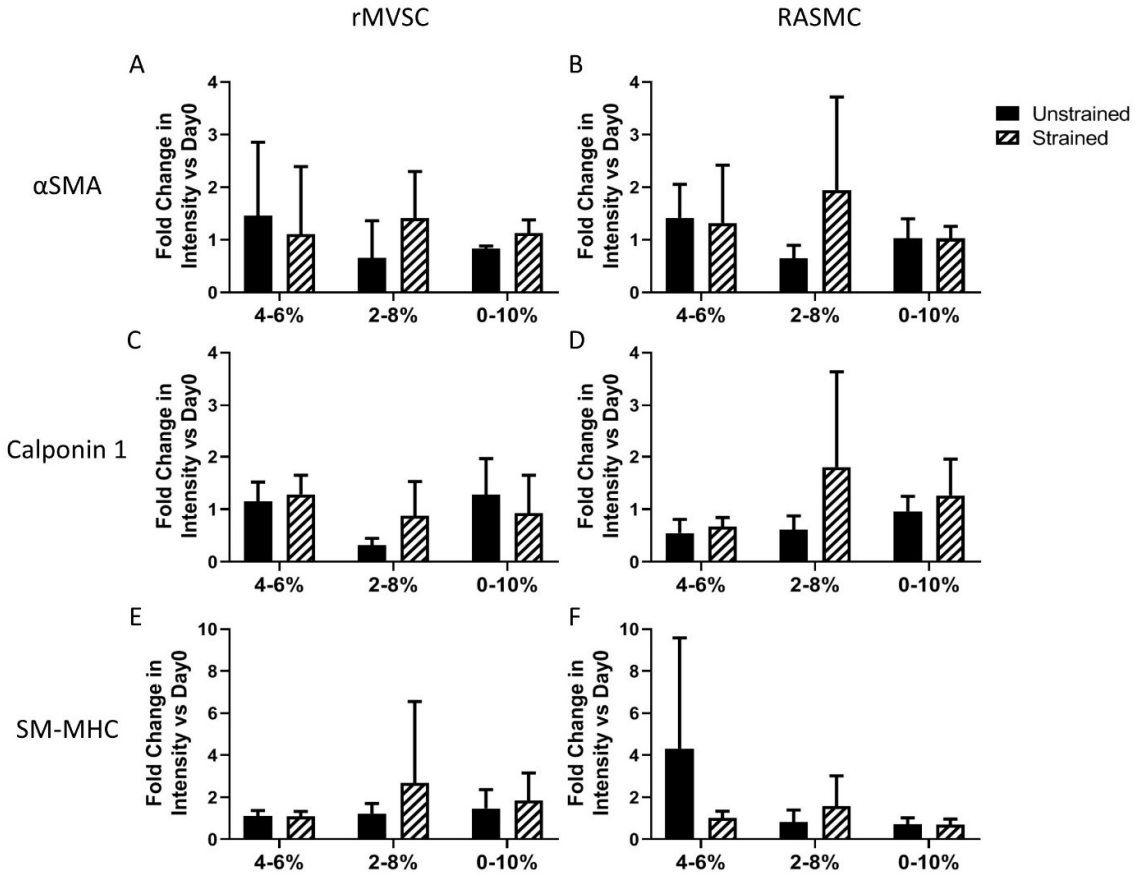

Figure 4.12: Fold change of contractile marker stain intensity vs day 0 for rMVSC (A,C,E) and RASMC(B,D,F) at 72 hours for strain levels of 4-6%, 2-8%, 0-10% for αSMA (A,B), Calponin 1 (C,D), and SM-MHC (E,F). No contractile markers showed a significant difference between strained and unstrained conditions.

4.4 Discussion

As the first study to look at the response of MVSC to any mechanical stimuli, we have determined that MVSC are, in fact, mechanosensitive cells that will exhibit strain avoidant behaviour when exposed to cyclic uniaxial tensile strain. MVSC are also responsive to the amplitude of cyclic tensile strain applied. On an unstructured elastic surface, they behave similarly to VSMC, however they exhibit a few important differences including differences in the extent of strain avoidance and in how cellular structures respond to tensile strain.

4.4.1 Alignment

These experiments show that both RASMC and rMVSC are responsive to strain amplitude of uniaxial tensile strain. They also confirm that both rMVSC and RASMC exhibit strain avoidant behaviours which has been observed previously in VSMC,[13-17] however the degree to which they exhibit this behaviour is dependent on the strain amplitude and cell type.

rMVSC show nuclear alignment perpendicular to strain directions at all strain levels by 72 hours, however significant actin realignment perpendicular to strain levels is only observed in the 0-10% strain, demonstrating that MVSC have a significant realignment of nuclei even when this realignment has not happened in the actin cytoskeleton. On the other hand, RASMC only show significant strain avoidant realignment in the nuclei at the 2-8% and 0-10% strain levels at 72 hours, while showing significant actin realignment in all strain levels. This indicates that VSMC have a greater strain-avoidant actin alignment response than nuclear alignment response. This behaviour is also evident in the actin dispersion analysis as measured by the mean vector length of actin fibres. MVSC show a significant increase in MVL at 0-10% strain only at 72 hours while VSMC show a significant increase in MVL for the 0-10% strain level as early as 24 hours. Much like our experiments, previous studies have shown VSMC alignment perpendicular to strain in response to 0-10% cyclic tensile strain after 24 hours.[13-17] However these studies did not investigate any lower strain amplitudes, or longer time points. Unlike our studies, most of these studies used a lower cell density and looked at overall alignment of the cells[13-15,17] as opposed to looking at the alignment of the subcellular structures involved in mechanotransduction, while only one determined alignment using nuclear alignment.[16]

The less robust actin response observed in the MVSC may be due to the presence of less well developed actin cytoskeletal contractile apparatus compared to the more differentiated

VSMC. As evidence of this theory, cardiac progenitor cells (CPC) show little actin cytoskeletal development and show decreased reorientation perpendicular to strain because of this.[188] However, following differentiation a developed actin cytoskeletal can be observed, and CPC have also been shown to display a strain-avoidant response.[188] While MVSC do show development of f-actin stress fibres, as less differentiated cells, they may have a less well-developed structure, and this may explain why MVSC are less aligned than VSMC by 72 hours of strain. Other studies have suggested that it may not be the level of strain on the overall cell body, but the specific level of compressive force on the actin stress fibres that determines the strain reorientation response of the cell's actin cytoskeleton.[226] Therefore, any differences observed between MVSC and VSMC reorientation may be due to differences in cytoskeletal organization between the two cell types.

This difference in actin cytoskeletal response between the two cell types may indicate a difference in how these cells sense strain. The actin cytoskeleton is an important mechanotransducer that allows cells to sense strain from the surrounding environment and is critical in the strain-avoidant realignment of cells. Strain avoidant realignment of cells has been shown to be dependent on Rho/ROCK signalling, and thus actin remodeling,[227] as well as being dependent on myosin II which is important in the ability of actin stress fibres to maintain tension within the fibres of the actin cytoskeleton.[228] Therefore, any significant differences between how the actin cytoskeleton responds to tensile strain could affect how the two cell types respond to strain, stiffness or other mechanical cues.

This study clearly shows that VSMC and MVSC both show the same behaviour of increasing strain-avoidant alignment with increasing strain or increasing strain rate. Despite this there are some differences between the two cell types that are worth noting. Firstly, RASMC show significant differences between all strain levels which indicates that VSMC may be able to more specifically sense varying strain levels. Interestingly this result has also been demonstrated for other cell types including vascular smooth muscle cells,[219] endothelial cells,[221] osteoblasts and fibroblasts.[222] Importantly, the evidence in this chapter confirms that this pattern is also true for MVSC, which may not have been evident given that cardiac progenitor cells have been shown not to respond to tensile strain before differentiation,[188] while oesophageal smooth muscle cells have been shown to align parallel to strain at a low strain amplitude, while aligning perpendicular to strain direction at a higher strain amplitude.[220]

Ultimately it may be strain rate as opposed to strain amplitude influencing the strain avoidance response. Strain rate can be increased either by increasing strain amplitude while frequency remains constant, or increasing frequency while amplitude remains constant. Other studies have shown that changing frequency of strain on VSMC changes alignment. Some studies have shown that increasing frequency, and thus increasing strain rate increases strain avoidance, [144,229] which would be consistent with the results we observed with increasing amplitude increasing alignment perpendicular to strain. However, another study has shown increasing frequency decreased cell alignment perpendicular to strain, [145] which could indicate that frequency may in fact be distinct from strain amplitude, instead of being linked by strain rate.

Ultimately, both MVSC and VSMC demonstrate similar strain avoidant behaviour, however the earlier reorientation of MVSC may indicate a critical role in early response to changes in cyclic tensile strain. Both cell types are sensitive to strain amplitude, with RASMC showing a stronger distinction between strain levels, thus indicating that the precise strain level may be more important for RASMC.

4.4.2 Cell number/Proliferation

Both cell types had a strain-induced decrease in cell number for the highest 0-10% strain amplitude at 24 hours, however by 72 hours only MVSC significantly decreased in cell number when subjected to strain. This decrease in cell number due to strain is similar to what was previously observed in cells exposed to equiaxial strain on VSMC.[37,133-135] However, other studies of VSMC exposed to equiaxial and uniaxial strain showed a strain-induced increase in cell number.[15,136,137] Therefore, it is unclear how tensile strain affects VSMC cell number. Similarly, studies on amplitude of VSMC equiaxial strain of various strain amplitudes showed either a decrease in cell number as amplitude was increased, [37] or that cell number increased as strain amplitude increased.[136] However, in this study, for uniaxial tensile strain, amplitude did not correlate positively or negatively with cell number. This may be due to the strain-avoidant realignment as cells exposed to equiaxial strain cannot realign to avoid sensing strain.

However, the decrease in cell number observed at the highest strain levels cannot be explained by a reduction in cell proliferation. In our experiments, proliferation was not significantly affected at most strain levels. However, the percentage of proliferating MVSC significantly increased at 72 hours 2-8% strain. This implies that reduced cell number is

due to cell death rather than a decrease in cell proliferation. While VSMC have shown strain-induced apoptosis,[37] there are also other potential mechanisms for VSMC death, for example autophagy, which has been demonstrated in VSMC involved in atherosclerosis.[230]

4.4.3 Nuclear Shape/Size

Another difference observed between MVSC and VSMC is the sensitivity of nuclear shape to tensile strain. Rat MVSC had a strain-induced decrease in nuclear circularity at every strain amplitude and time point, while RASMC only showed a strain-induced decrease in nuclear circularity at the highest strain level at the 24-hour timeline. It is possible that this difference could be due to differences in nuclear stiffness between stem cells and differentiated cells. A previous study showed that cell nuclei stiffen as stem cells differentiate [231]

This change in nuclear shape might be indicative of a way in which rMVSC are sensing strain. The nucleus has been identified as a mechanotransducer, either due to being influenced by cytoskeletal mechanotransduction,[232,233] or due to its own internal mechanotransduction mechanisms.[234] Therefore, any differences in the deformation of the nucleus, may indicate that the different cell types are experiencing strain in a different way.

While there were no strain induced differences in nuclear area, there were significant differences in nuclear size between rMVSC and RASMC, with rMVSC having significantly smaller nuclei than RASMC. In the studies where MVSC were first isolated, it was observed that these cells were significantly smaller than the VSMC isolated from the same tissue.[12] Therefore, it would logically follow that these smaller cells would have proportionally smaller nuclei. This is a clear indicator that this MVSC population is phenotypically different to VSMC and may play a different role within the vasculature.

4.4.4 Contractile Markers

This study did not show a significant change in any VSMC contractile markers in either cell type in response to strain. While a decrease in Calponin 1 has previously been demonstrated in VSMC exposed to 24 hours of 0-10% cyclic tensile strain, [16] this study only looked at changes at the 72 hour time point, so may have missed a time sensitive strain response. A previous study demonstrated that MSC exposed to cyclic uniaxial tensile strain transiently increased contractile markers at 24 hours before returning to baseline levels as cells reoriented perpendicular to strain.[182] However, when MSC were constrained by microgrooves to remain parallel to strain direction, they showed an increased contractile

phenotype, but this change was not observed in cells oriented perpendicular to strain direction.[184] This could indicate that as MVSC and VSMC reorient perpendicular to strain, they are losing their phenotypic response to cyclic tensile strain. Further work is necessary to better understand how MVSC respond to strain when forced to fully experience cyclic tensile strain by constraining cells parallel to strain direction.

4.4.5 Concluding Remarks

This research has raised a number of questions for further investigation. Firstly, if the decrease in cell number is not based on a decrease in cell proliferation, then there must be an increase in cell death. Understanding the mechanisms of this cell death could help to understand how to control vascular cell death in response to tensile strain.

Additionally, understanding the differences in MVSC and VSMC mechanotransduction could aid in targeting the different cell types in vascular disease. Further studies need to be performed to elucidate the mechanisms involved in the differences between these two cell types and their nuclear and f-actin responses to strain.

Elucidating the differences in cellular response between different strain levels is helpful in fitting cell behaviour to a mechanobiological model. Previous models have coupled finite element modelling of vascular tissue with agent-based modelling of vascular cell response in order to understand vascular tissue response to varying mechanical stimuli.[235] Having experimental data for specific strain levels can help to calibrate such models for cellular response at different strain levels. Ultimately, this knowledge could help inform the design of next generation vascular devices, and help the development of multiscale computational models, which can be used to better understand the interaction of vascular cells and their complex mechanical environment.

While these experiments can provide insight into how strain alone can influence MVSC and VSMC, these cells *in vivo* are imbedded within an aligned collagen, elastin and glycosaminoglycan matrix which causes them to remain aligned parallel to the direction of strain. Therefore, future experiments should investigate the response of MVSC to strain on surfaces where they can no longer align perpendicular to the strain direction.

Ultimately, this study has shown that MVSC respond to uniaxial tensile strain by strain avoiding and turning parallel to the direction of strain, similar to what is observed in VSMC. However, MVSC align more quickly than VSMC, which may indicate a role in

early strain response. Differences in actin cytoskeletal and nuclear deformation response suggest differences in how responsive these cells are to different strains. These insights are critical in investigating how MVSC and VSMC contribute to vascular disease, as well as helping to engineer better vascular interventions and devices to help treat these diseases.

Chapter 5 Multipotent Vascular Stem Cell Strain-Induced Proliferation is Dictated by Orientation of ECM Fibres

5.1 Introduction

While Chapter 4 has demonstrated that both MVSC and VSMC have the ability to strain avoid, *in vivo* VSMC are constrained by collagen fibres and align with these fibres and parallel to the dominant direction of strain.[30,31] Therefore, while they cannot undergo strain avoidant reorientation in a healthy *in vivo* environment, they may have the opportunity to reorient in an environment where collagen fibres can remodel, such as certain vascular diseases where collagen fibre orientation is known to change.[33,34]

Despite MVSC being considered by some to play a critical role in vascular disease, this is the first study to investigate the role of native fiber structure on MVSC, and how fiber structure influences the reaction of MVSC to strain. In order to elucidate the role of MVSC in the development of vascular disease, it is vital to understand how these cells behave in a mechanical environment that simulates the *in vivo* environment. Also, in order to determine how a changing collagen environment impacts vascular cell's response to tensile strain, the uniaxial tensile strain response of MVSC and VSMC was studied in the presence of native collagen structure, with fibers arranged either primarily in the direction of strain, or perpendicular to the direction of strain. Ultimately, this helps to understand the interplay between collagen structure alignment and tensile strain on vascular cell response and vascular disease progression.

5.2 Materials and Methods

5.2.1 Cell Isolation and Culture

RASMC were obtained by enzymatic digestion of the aorta of three Sprague Dawley rats. Rat aortas were dissected from adult rats, and the adventitial layer was removed. Aorta were manually cut into pieces no larger than $1mm^3$ and digested in a sterile solution of 0.7mg/mL Collagenase type 1A (Sigma-Aldrich) and 0.35mg/mL Elastase type III (Sigma-Aldrich) in PBS at 37ºC for 2 hours with agitation. RASMC were cultured in high glucose DMEM with Glutamax (Bio-Sciences) with 10% FBS (Gibco) and 2% Penicillin/Streptomycin (Bio-Sciences). Rat MVSC were isolated by explant as previously described[106] and were cultured in stem cell media containing high glucose DMEM with Glutamax (Bio-sciences), with 1% Penicillin/Streptomycin(Bio-Sciences), 1% N-2

supplement (Gibco), 2% B-27 supplement (Gibco), 20ng/mL bFGF (Corning), 2% chicken embryo extract (ATCC), 100 nM retinoic acid(Sigma-Aldrich), 50 nM 2-mercaptoethanol (Gibco). RASMC were used from p6 to p8. Rat MVSC were used from p18 to p20.

5.2.2 Decellularized Tissue

Porcine carotid arteries were dissected fresh and cryopreserved by freezing at a rate of -1°C per minute in tissue freezing medium (TFM) composed of 0.1M sucrose (Sigma-Aldrich) and 12.75% DMSO (VWR) in RPMI 1640 medium (Gibco). These arteries were then decellularized using a protocol based on a previous decellularization technique from the lab.[236] Briefly, they were perfused with 0.1 NaOH for 15 hours and then rinsed in saline for 65 hours. Vessels were then incubated in DNase solution for 19 hours. Decellularized vessels were then returned to TFM and frozen until ready for use. Vessels were cut into 5mm x 10mm strips for static samples or 5mm x 15mm strips for strained samples, which had a strain region of 10mm length. Strips were cut either circumferentially on the vessel for fibres parallel to strain direction, or axially on the vessel, for fibres perpendicular to strain direction, as shown in Figure 5.1A. Before cell seeding, strips were sterilized in 100% ethanol for at least 1 hour, then rinsed twice in sterile deionized water and twice in sterile PBS. Strips were then pinned flat as shown in Figure 5.1B, and seeded with $1.33x10^4$ cells/cm^2 which allowed cells to remain subconfluent before the application of strain, thus preventing cells that were not adhered directly to the decellularized vessel. Cells were allowed to adhere for 1 hour before strips were unpinned and transferred to culture for a further 3 days prior to initiating the application of strain.

5.2.3 Application of Strain

Strips were loaded into clamps within a Bose BioDynamic 5200 with two strips placed in each bioreactor chamber as shown in Figure 5.1C. Bose chambers were filled with high glucose DMEM with Glutamax (Bio-sciences) supplemented with 10% FBS and 2µl/mL Primocin. A preload of 0.05N was applied to all strips. Samples were strained uniaxially using displacement controlled strain, from 0-10% strain at 1Hz for 24 or 72 hours.

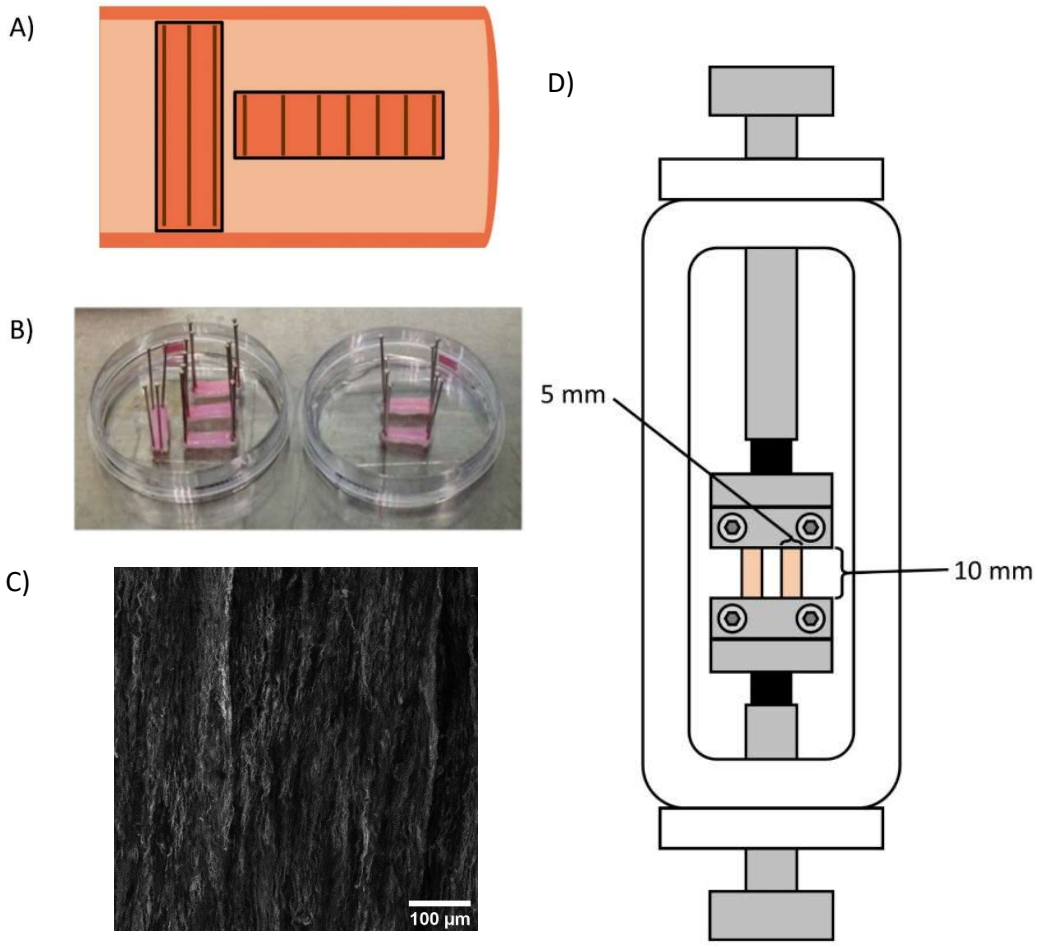

Figure 5.1: A) Diagram showing how strips were cut from decellularized porcine carotid arteries in order to obtain strips with fibres oriented parallel or perpendicular to strain direction. B) Strips pinned for cell seeding. C) Decellularized tissue showing collagen aligned circumferentially. D) Setup of bioreactor chambers.

5.2.4 Staining Protocol

Strips were fixed for more than 24 hours at 4ºC. Strips were blocked and permeabilized in a solution of 5% BSA and 0.2% Triton-X 100 in PBS at room temperature for 40 minutes with agitation. Strips were then rinsed twice in PBS. Primary antibody solution was prepared (0.5% BSA, 0.2% Triton-X 100, PBS) and antibodies were used in accordance with the concentration information shown in Table 5.1. Strips were incubated in primary antibody overnight at 4ºC with agitation. Strips were rinsed three times in PBS. Secondary antibody solution was prepared (0.5% BSA, 0.2% Triton-X 100, PBS) at a concentration of 1:1000, with 1:500 rhodamine Phalloidin, and 1:1000 DAPI. Strips were incubated in

the secondary antibody solution in the dark for 48 hours at 4ºC with agitation. Strips were rinsed three times in PBS and stored at 4ºC protected from light before imaging.

Table 5.1: List of Immunostaining Antibodies and Concentrations

Primary Antibodies	Concentration	Product Code
Ki67	1:200	Abcam ab15580
Calponin 1	1:100	Sigma C2687

5.2.5 Imaging Protocol

All images were taken on a Leica SP8 scanning confocal microscope at 20x. For each sample, a continuous area of at least 24 images was scanned with a z-stack taken at intervals of 10µm. The images were taken as 1024x1024 pixel images with a scan speed of 400 Hz.

5.2.6 Image analysis

Nuclear analysis was performed with ImageJ particle analysis to get nuclear number, nuclear orientation, major and minor axis, and nuclear area as previously described in Chapter 4. Actin alignment was determined using the MatFiber Matlab program.[225] Ki67 nuclei were determined by masking Ki67 with nuclear area, and then counting positive nuclei using ImageJ particle analysis as previously described in Chapter 4. Immunostaining intensity measures were determined as previously described, in Chapter 4 then normalized to a secondary antibody only control.

5.2.7 Statistics

Statistics were performed using GraphPad Prism 8.2.0. Significance was determined using 2-way ANOVA with a Tukey's post-hoc test or a Sidak's post-hoc test as determined by the statistics software. When comparing across both parallel and perpendicular strain for both cell types a 3-way ANOVA was used with a Tukey's post-hoc test. Each experiment had $n \geq 3$ samples.

5.3 Results

For rMVSC seeded on decellularized tissue strips application of 10%, 1Hz uniaxial tensile strain for ten days resulted in cells aligned with the direction of collagen fibers regardless of whether or not the cells were oriented parallel or perpendicular to the direction of strain. (Figure 5.2).

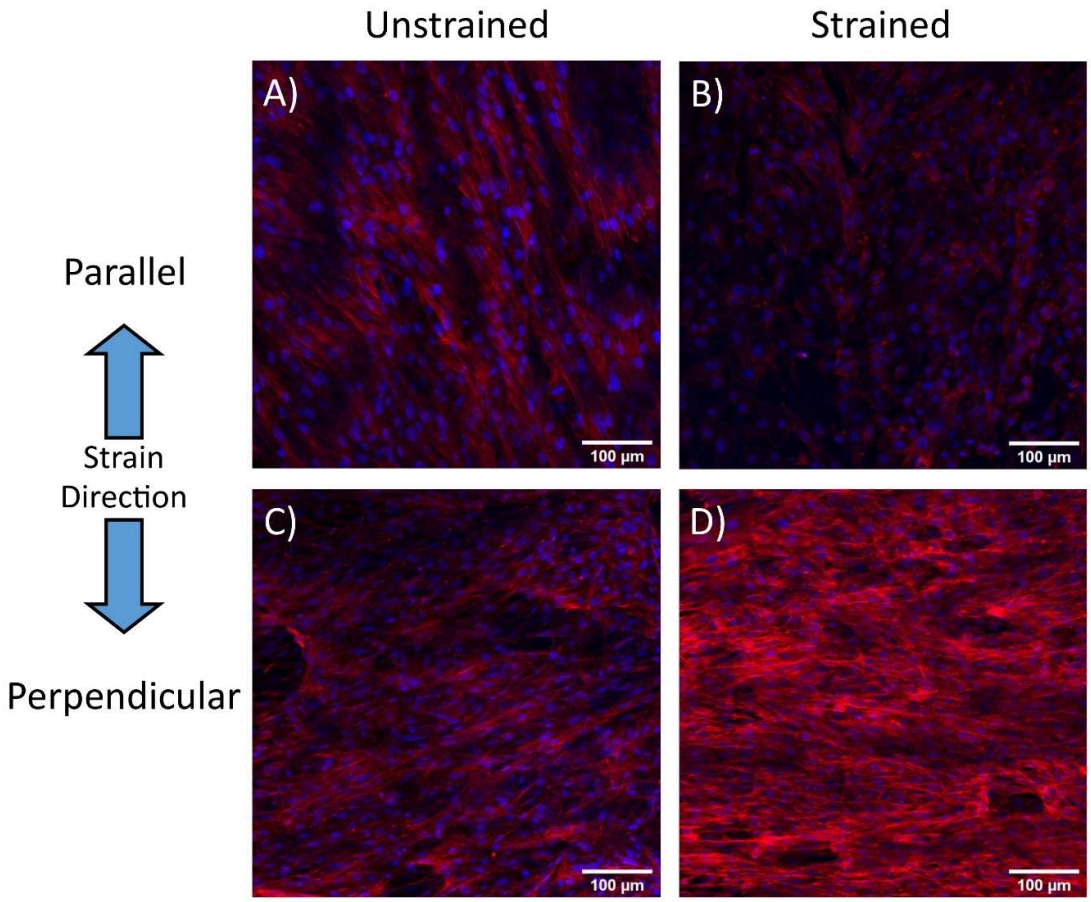

Figure 5.2: Representative images of rMVSC on decellularized porcine carotid artery samples left unstrained (A, C), or strained parallel (B) or perpendicular (D) to the direction of collagen fibres. Blue – Nuclei Red – F-actin

The cellular orientation was determined both by the direction of the major axis of the nuclear ellipse (Figure 5.3A,C) and also by the orientation of f-actin cytoskeletal fibres (Figure 5.3B,D) which showed a distribution of cells aligned primarily in the direction of fibre alignment.

RASMC remained aligned with the direction of the underlying collagen, with the exception of samples that were strained parallel to fibre direction (Figure 5.4). Analysis of nuclear and f-actin alignment showed alignment in the direction of collagen fibres, except for cells strained parallel to fibre direction which had a decreased percentage of cells aligned in the direction of strain (Figure 5.5).

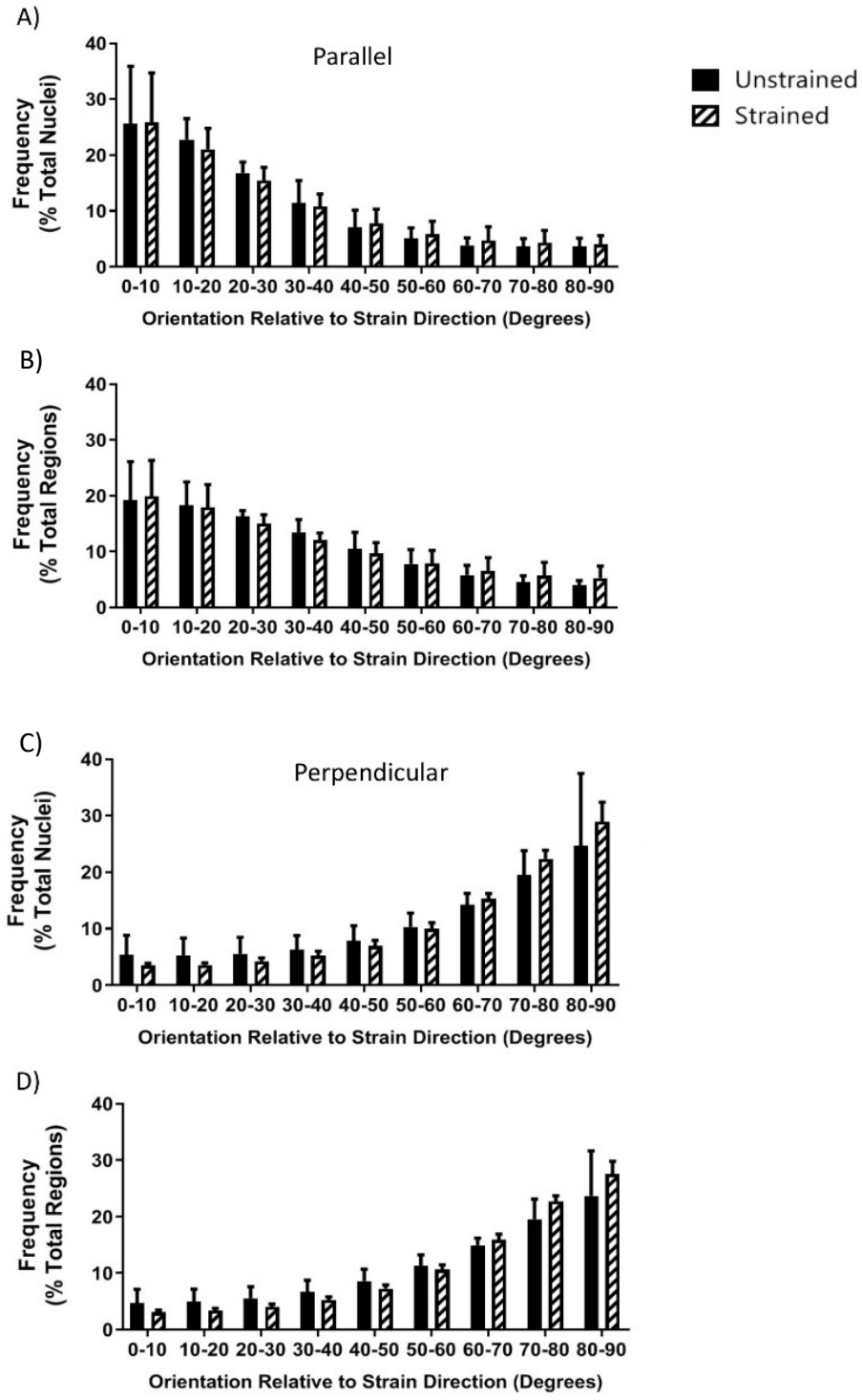

Figure 5.3: The alignment distribution of rMVSC nuclei (A, C) and f-actin (B, D) on decellularized porcine carotid artery samples left unstrained, or strained parallel (A, B) or perpendicular (C, D) to the direction of collagen fibres. $n \geq 3$

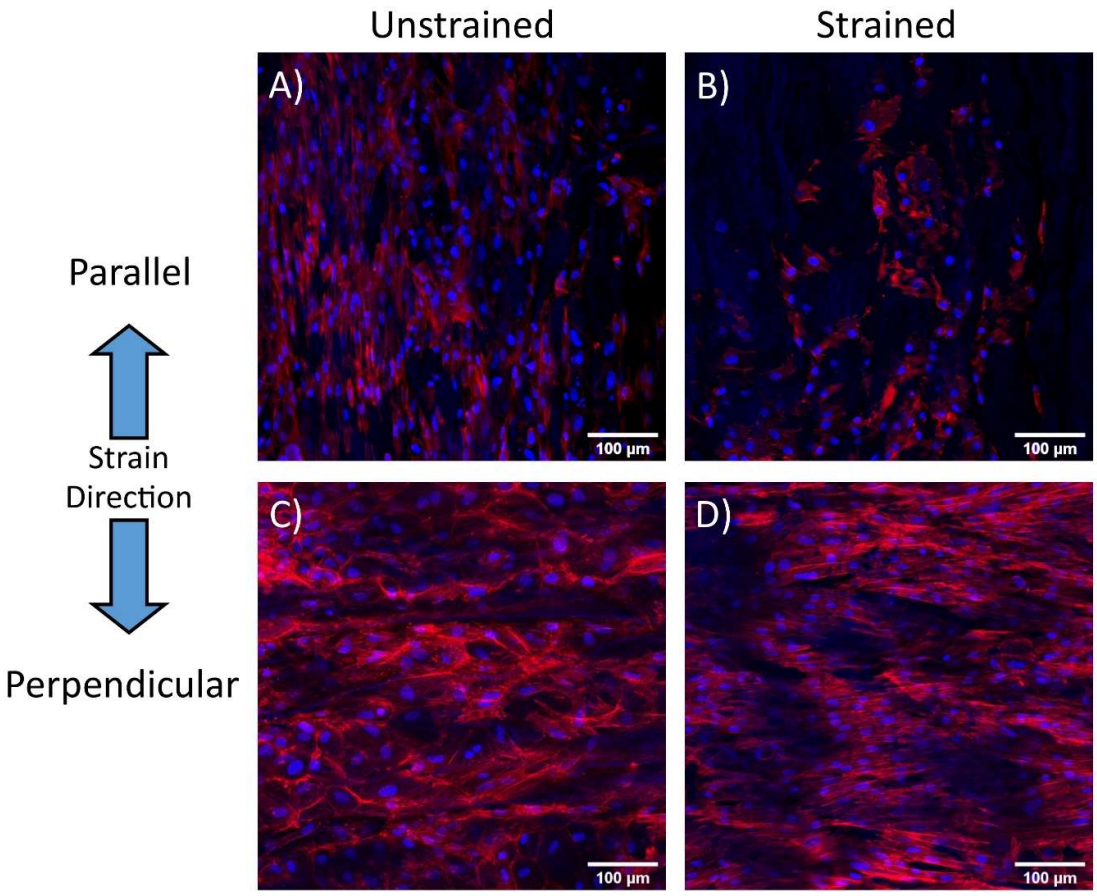

Figure 5.4: Representative images of RASMC on decellularized porcine carotid artery samples left unstrained (A, C), or strained parallel (B) or perpendicular (D) to the direction of collagen fibres.Blue –Nuclei, Red – F-actin

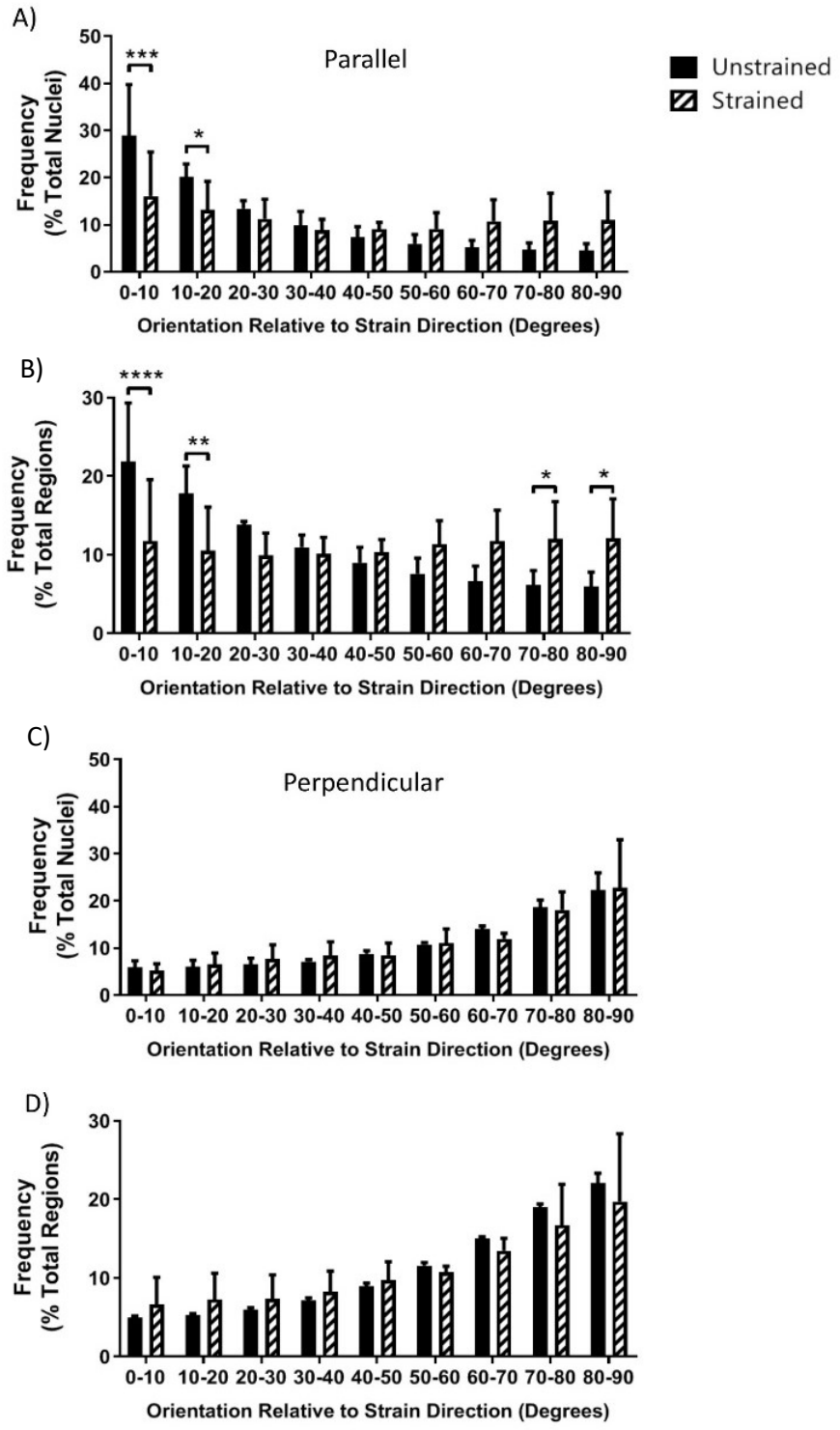

Figure 5.5: The alignment distribution of RASMC nuclei (A, B) and f-actin (C, D) on decellularized porcine carotid artery samples left unstrained, or strained parallel (A, C) or perpendicular (B, D) to the direction of collagen fibres. *p<0.05, **p<0.01, ***p<0.001 n ≥ 3

In order to determine how strain influenced the overall number of cells, cell nuclei were counted to determine cell number. For rMVSC, there was no significant change in cell number between cells that were left unstrained, or cells that were strained either parallel or perpendicular to fiber direction (Figure 5.6A). RASMC that were strained parallel to fiber direction did show a decrease in cell number (Figure 5.6A). Cells were also assessed for proliferation by counting the number of Ki67 positive nuclei which would indicate an actively dividing cell. Rat MVSC which were exposed to strain parallel to fiber direction showed an increased percentage of Ki67 positive nuclei compared to cells that were strained perpendicular to fiber direction (Figure 5.6B). RASMC did not exhibit any significant differences in Ki67 expression between strained and unstrained cells, regardless of strain direction (Figure 5.6B).

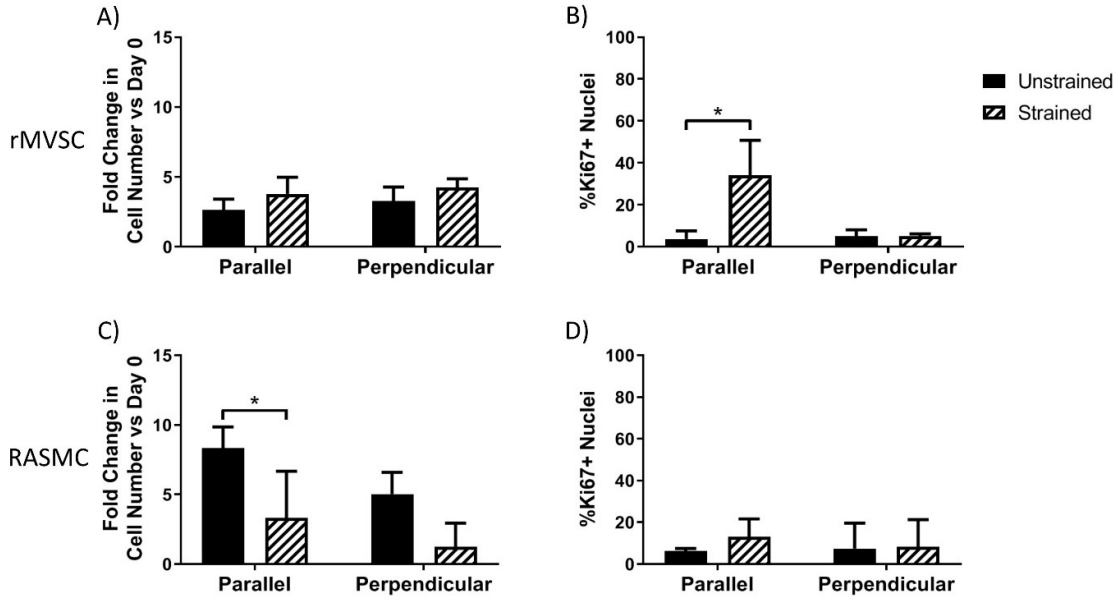

Figure 5.6: Fold change in cell number (A, C) and percentage of Ki67 positive cells (B, D) for both rMVSC (A, B) and RASMC (C, D) strained parallel or perpendicular to collagen alignment direction. * $p < 0.05$ $n \geq 3$

When RASMC samples were investigated on a sample-by-sample basis, the cells exhibited one of two different behaviors. Of the four samples tested, two of the samples had cell nuclei which remained aligned parallel to fiber direction, while two samples had cells which exhibited strain avoidant realignment perpendicular to strain and fiber direction (Figure 5.7, 5.8A, B). The cells that did remain aligned parallel to strain direction showed a greatly decreased cell number compared to the samples in which the cells reoriented perpendicular to strain direction (Figure 5.8D).

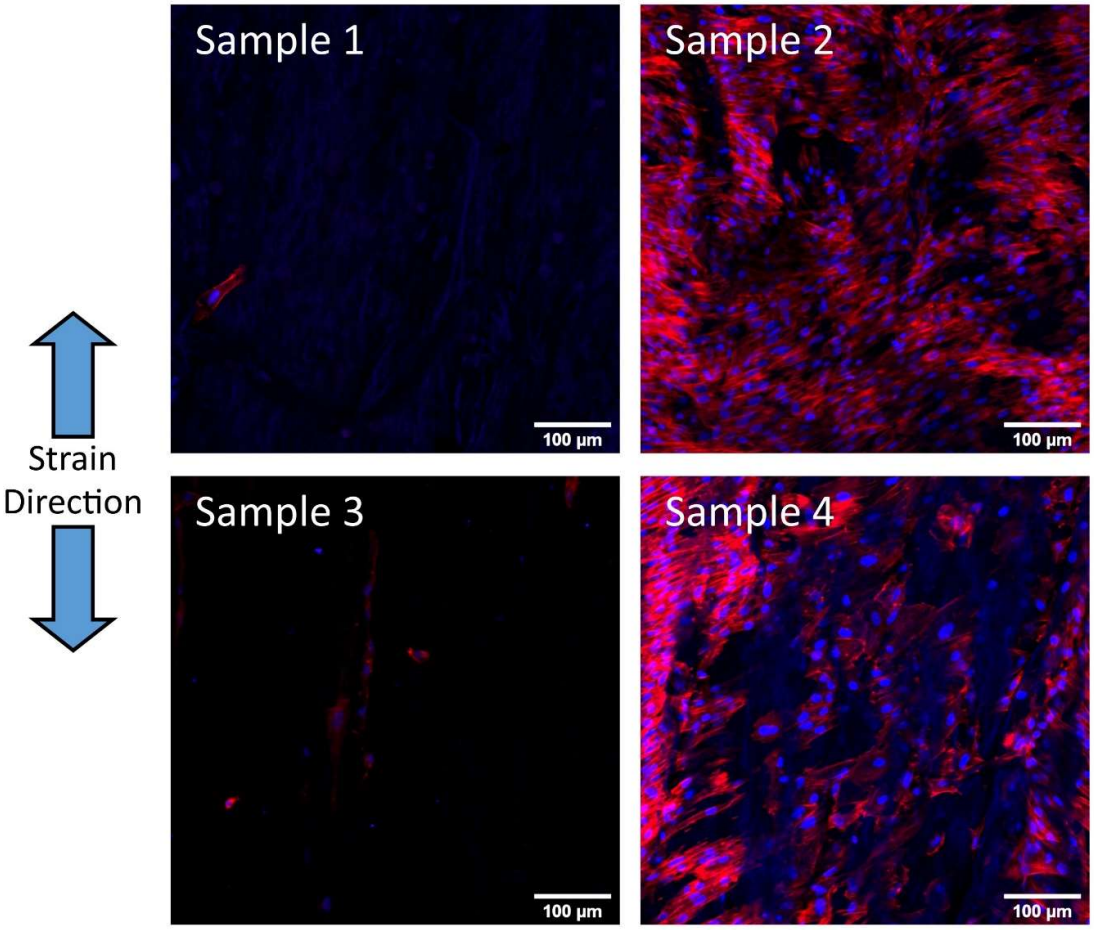

Figure 5.7: Representative images of VSMC strained parallel to fibre direction showing decreased number of cells when cells remained aligned with fibres (Sample 1,3) compared to cells that reoriented perpendicular to fibres (Sample 2,4)

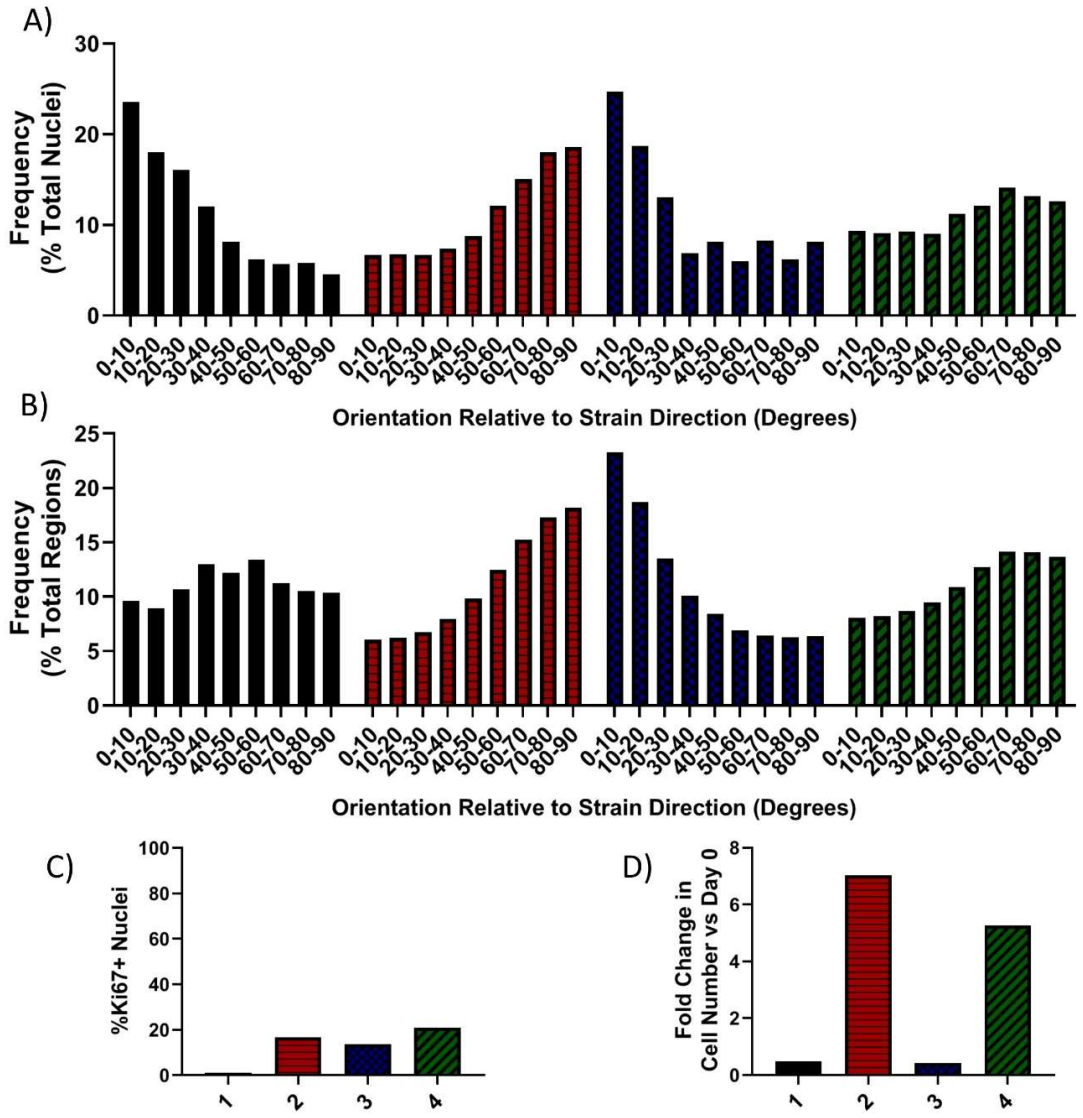

Figure 5.8: The alignment distribution of RASMC nuclei (A) and f-actin (B) on decellularized porcine carotid artery samples when strained parallel to the direction of collagen fibres for each individual sample. Percent of Ki67+ nuclei (C) and fold change in cell number (D) broken out by sample. Samples in which the cells remained parallel to strain direction (1 & 3) showed lower fold change in cell number.

Cell nuclei were also assessed on their size and shape. RASMC decreased in size when exposed to strain perpendicular to fiber direction, while rMVSC showed no significant changes in nuclear size (Figure 5.9A). Neither rMVSC nor RASMC showed significant changes in nucleus circularity in response to strain (Figure 5.9B).

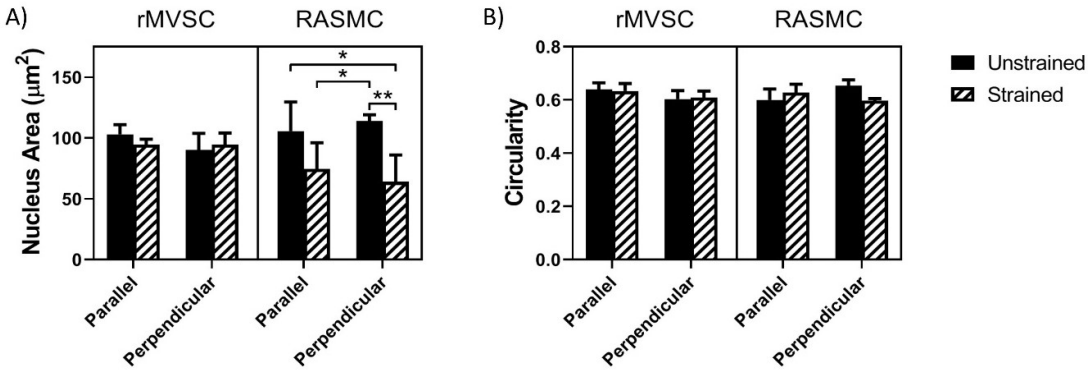

Figure 5.9: Nuclear area (A) and circularity of the nucleus, measured by the short axis divided by the long axis of the nuclear ellipse (B) for rMVSC and RASMC strained at 10%, 1Hz cyclic uniaxial tensile strain, or left unstrained for 10 days. *p<0.05 **p<0.01 n ≥ 3

Rat MVSC and RASMC were assessed for Calponin 1 protein expression in order to determine if either cell was adopting a contractile VSMC phenotype. None of the cell types showed a significant change in Calponin 1 expression when strained either perpendicular or parallel to fiber direction (Figure 5.10). Representative images for these stains are provided in Appendix III.

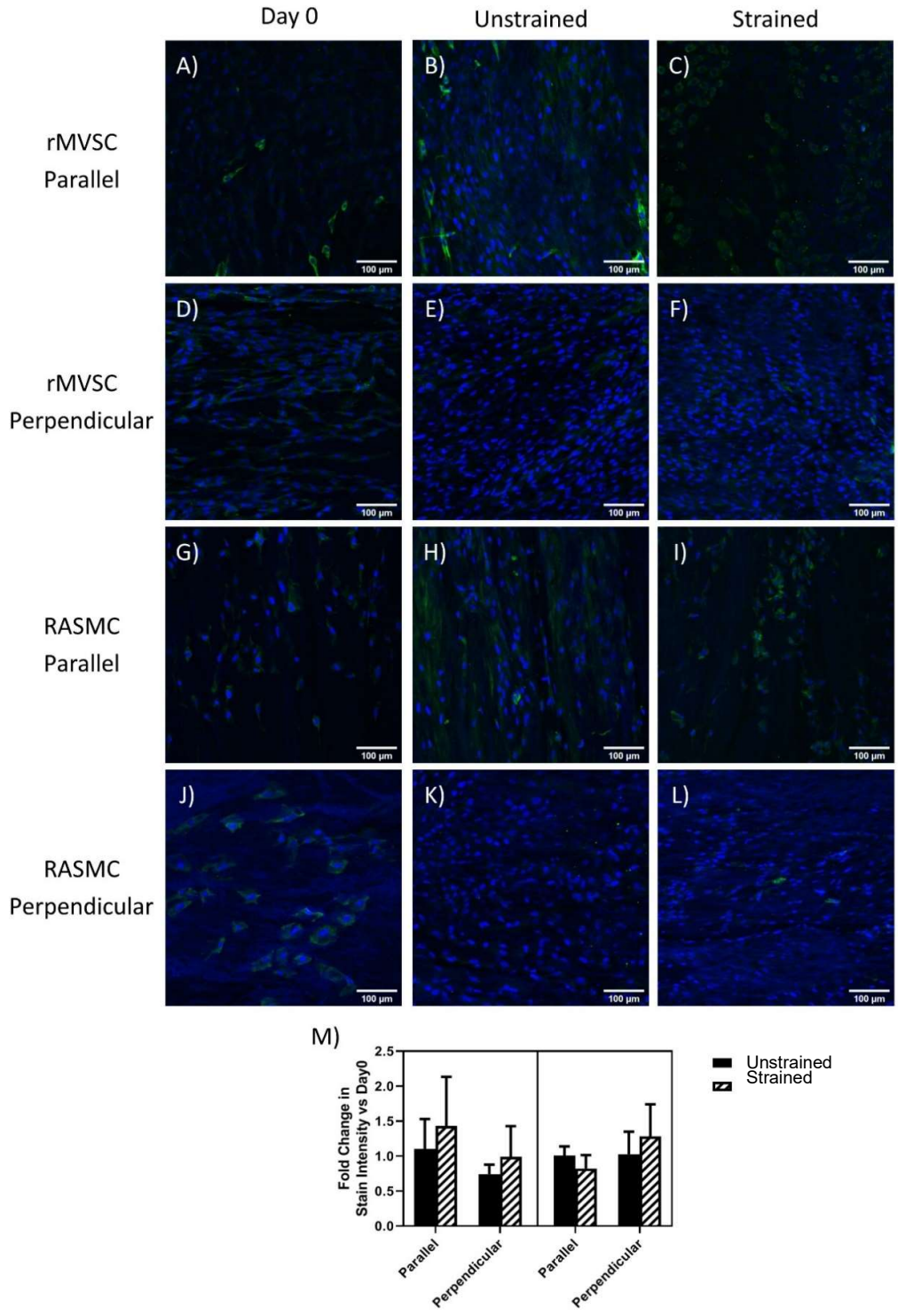

Figure 5.10: Representative images of rMVSC (A-F) and RASMC (G-L) stained for nuclei (blue) and Calponin 1 (green) before strain (A, D, G, J) after 10 days without strain (B, E, H, K) or 10 days of 10%, 1Hz uniaxial tensile strain parallel (C, I) or perpendicular (F, L) to fibre direction. Stain intensity analysis (M) showed no significant differences between conditions. Scale bar = 100 µm

5.4 Discussion

This research is the first to investigate the effects of both structure and tensile strain on MVSC, a cell type that has been shown to play a role in intimal hyperplasia. By comparing MVSC and VSMC, we begin to elucidate the role of each cell type in the progression of vascular disease.

5.4.1 Alignment

The aligned structure of the medial layer of the decellularized artery induced both nuclear and cytoskeletal alignment in the direction of fiber alignment in both MVSC and VSMC. VSMC have previously been shown to align parallel to structural cues including microgrooved collagen substrates,[201,202] micropatterned PDMS, [17,203] and aligned electrospun[207] and melt-spun fibers. [208] MVSC also align with the direction of PDMS microgrooves.[123] The native collagen structure used in these experiments causes cell alignment in a similar manner to engineered patterned surfaces despite having a less controlled topography. The collagen fibres in our decellularized substrate act in a similar manner to these synthetically patterned substrates. In these samples, the fibres ranged from approximately 0.5 to 4μm in diameter. Therefore, these decellularized vessels can be used to prime vascular cells to align in a circumferential direction, just like the VSMC in a native artery.

When exposed to strain, MVSC remained constrained by structure, while VSMC only remained constrained by structure in some instances and showed strain avoidant realignment in others. This is a distinct difference between how these two cell types behave when exposed to native collagen structure and uniaxial tensile strain. A previous study of VSMC, as well as endothelial cells and fibroblasts, demonstrated how nanotopography influenced cell alignment in these cells in different ways, with fibroblasts showing greater sensitivity to small scale topography and VSMC showing quite a varied response depending on the scale of the topographical features.[211] Differences in cell responses to topography and strain may have to do with differences in cell size. In static circumstances in the previously published study, having smaller microgrooves resulted in increased alignment of both VSMC[209,210] and MVSC.[123] However, when exposed to strain, VSMC both in the thickest 70 μm microgrooves and the thinnest 15 μm microgrooves showed more strain avoidant realignment than in the middle microgroove width of 40 μm.[17] This indicates that there is a sweet spot of microgroove width in which cells will remain the most aligned, even when subjected to uniaxial tensile strain.

This may answer the question as to why VSMC are constrained by the fibers in some instances and not in others. One possible explanation is that the spacing between the fibers is on the threshold of the distance that would constrain VSMC. VSMC are larger than MVSC,[12] which could indicate that the ideal fiber spacing for each cell type in order to maintain cell alignment would be a different size. Therefore, natural variations in the collagen fiber pattern between different arteries may have been just above or just below the size threshold necessary to constrain VSMC to remain aligned with the direction of strain. Another explanation could be caused by the variation in VSMC themselves. VSMC are a heterogeneous population,[105] therefore it is possible that variations in starting cell size, as opposed to variations in collagen fiber arrangement, determined the differences in how the cells interacted with the surrounding structure.

5.4.2 Proliferation/Apoptosis

When exposed to strain parallel to the direction of cell alignment, the number of dividing, Ki67+ MVSC increased. Conversely when VSMC remained aligned in the direction of strain, cell number decreased. This shows a major difference between how these two cell types may respond to high levels of strain. Previous studies on unstructured substrates have shown either an increase,[15] or a decrease, as was seen in Chapter 4, in VSMC number in response to 10%, 1 Hz uniaxial cyclic tensile strain. However, in these experiments, cells were free to reorient and strain avoid. When an elastic substrate is strained parallel to cell alignment, the cell itself deforms to a greater degree.[237] Cell alignment makes a large difference in proliferation for MVSC and in cell number for RASMC. This indicates that cells that are actually aligned in the direction of strain are sensing the full extent of the strain. For MVSC, cells aligned in the direction of strain, and therefore sensing the strain, increase in proliferation, but do not significantly increase in cell number. Because of this it is likely that MVSC death is also increasing when the cells sense strain. In contrast, RASMC aligned in the direction of strain decrease in cell number. Because there is no detectable decrease in proliferation, there is likely a similar increase in cell death caused by apoptosis,[37] although there are other mechanisms that have been shown to cause cell death in VSMC.[230] This shows how cell alignment relative to strain ultimately determines whether or not the cells will react to the applied strain.

5.4.3 Conclusions

Chapter 4 determined that MVSC and VSMC on non-structured surfaces show very similar alignment changes and cell number changes in response to strain. With structure we begin to see clear differences in these two cell populations. MVSC that cannot reorient to strain avoid proliferate when exposed to uniaxial tensile strain. On the other hand, VSMC that remain oriented parallel to the direction of strain show reduced proliferation and/or increased apoptosis. This would indicate that when VSMC are exposed to damaging levels of cyclic strain they would die off, and the small population of MVSC exposed to that same strain would begin proliferating to replace those dead VSMC. However, MVSC, which are stimulated to divide by cyclic tensile strain, could then over proliferate causing intimal thickening and even stenosis. This indicates a significant role for MVSC in vascular disease. It is also important that both cell types need to be taken into account when designing vascular interventions that modulate the mechanical environment within a blood vessel. The presence of two cell types with opposite proliferation responses to tensile strain may indicate that both cell types may play a role in intimal hyperplasia under differing conditions. Lineage tracing studies have implicated MVSC[12,57,59] or VSMC[61-63] in intimal hyperplasia, and the differences may come down to variations in the exact mechanical environment between the studies. This suggests that the differences between aligned MVSC and VSMC should be investigated at different strain amplitudes in order to see if there is a strain condition under which VSMC proliferation dominates.

This research highlights the importance of cell orientation in terms of controlling vascular cell growth. When designing tissue engineered vessels or vascular interventions that change the mechanical environment in the blood vessel, it is essential to understand not only the strain applied to the underlying substrate, but how this strain translates to the strain sensed by the cells. Sensed strain is dependent upon cellular alignment. This indicates the importance of including cell orientation as a component of any multi-scale model which aims to determine cellular responses to changes in mechanical forces in the vascular environment. Additionally, changing the parameters within these models can be used to investigate whether or not cells that behave more like MVSC or cells that behave more like VSMC are responsible for the behavior of vascular cells observed in diseased states. Ultimately, this study shows how critical both cell types and structural cues are to determining the strain response of vascular tissue.

Chapter 6 MVSC Exposed to Cyclic Stent Strut Indentation Mimic In-Stent Restenosis

6.1 Introduction

In the previous chapters MVSC mechanosensitivity was determined. As shown in Chapter 4, MVSC are sensitive to strain amplitude, while Chapter 5 demonstrated that ECM fibre microstructure and cell orientation were critical in demonstrating differences between MVSC and VSMC mechanoresponse. These experiments have shown important differences in how MVSC and VSMC respond to a tensile strain environment. While these have established MVSC mechanosensitivity, it is also important to establish how MVSC react in a loading environment that is known to cause a diseased state in vascular cells, in order to establish if MVSC may play a key role in the development of this vascular disease.

In this chapter we aim to simulate how MVSC would respond to a stenting environment in order to better understand the role of these cells in in-stent restenosis. In order to do this we designed and implemented a bioreactor system that simulated the loading of a single stent strut. This was used to load strips of decellularized porcine carotid artery that had been recellularized with MVSC, in order to isolate the response of that cell type. This allowed us to demonstrate the influence of MVSC on in-stent restenosis.

6.2 Methods

6.2.1 Cell Isolation and Culture

Rat MVSC (rMVSC) were isolated by explant as previously described[106] and were cultured in high glucose DMEM with Glutamax (Bio-sciences), with 1% Penicillin/Streptomycin(Bio-Sciences), 1% N-2 supplement (Gibco), 2% B-27 supplement (Gibco), 20ng/mL bFGF (Corning), 2% chicken embryo extract (ATCC), 100 nM retinoic acid(Sigma-Aldrich), 50 nM 2-mercaptoethanol (Gibco). Rat MVSC were used at p19.

6.2.2 Cell Seeding

Porcine carotid arteries were dissected fresh and cryopreserved by freezing at a rate of -1^{o}C per minute in tissue freezing medium (TFM) composed of 0.1M sucrose (Sigma-Aldrich) and 12.75% DMSO (VWR) in RPMI 1640 medium (Gibco). These arteries were then decellularized as previously described in Chapter 5. Briefly, they were perfused with 0.1 NaOH for 15 hours and then rinsed in saline for 65 hours. Vessels were then incubated in

DNase solution for 19 hours. Decellularized vessels were then returned to TFM and frozen until ready for use. Vessels were cut into 5mm x 10mm strips for static samples or 5mm x 15mm strips for strained samples, which had a strain region of 10mm length. Strips were cut circumferentially on the vessel, and the intima was removed. Before cell seeding, strips were sterilized in 100% ethanol for at least 1 hour, then rinsed two times in sterile deionized water and two times in sterile PBS. Strips were then pinned flat, and seeded with $1.33x10^4$ cells/cm^2 which allowed cells to remain subconfluent before the application of strain, thus preventing cells that were not adhered directly to the decellularized vessel. Cells were allowed to adhere for 1 hour before strips were unpinned and transferred to culture for a further 3 days prior to initiating the application of strain.

6.2.3 Application of Indentation

Two indentation devices were melt-extrusion 3D printed in PLA. The static applied a static 10% elongation of the tissue (Figure 6.1). The dynamic stenting device fit into a Bose Biodynamic 5000 system that could be indented to an arbitrary level (Figure 6.2). Full technical drawings can be found in Appendix IV. Strips were loaded into sterile rigs with two strips placed side by side. Bose chambers or tubes were filled with 10% FBS medium supplemented with 2µl/mL Primocin. In the bioreactor, the wire indenter was moved so that it was just resting on the surface of the strips. The wire was then indented 2.3mm into the tissue strips at 1Hz for 10 days in order to apply a 10% elongation of the tissue (Figure 6.1D).

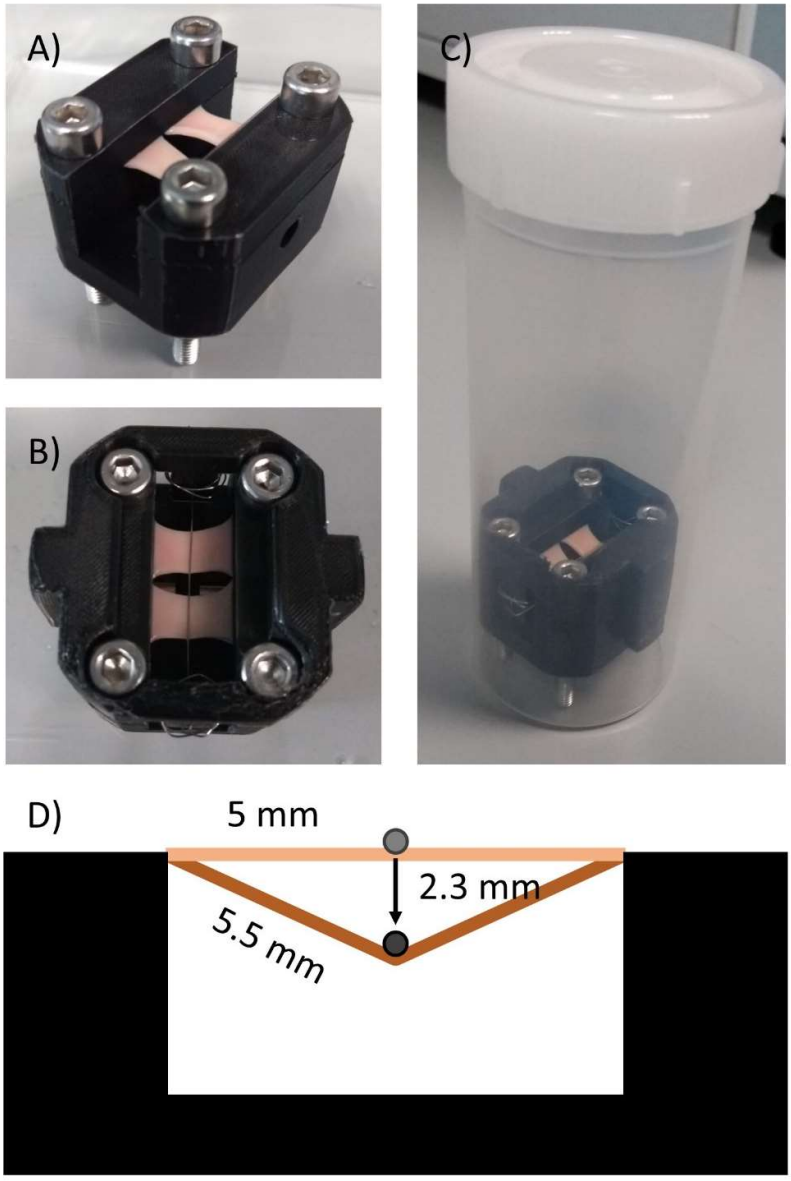

Figure 6.1: Images of static indentation device (A) Before application of stent strut (B)Top view with stent strut (C)In 120mL tube for addition of medium (D)Diagram showing 10% elongation of tissue strips from stent strut application.

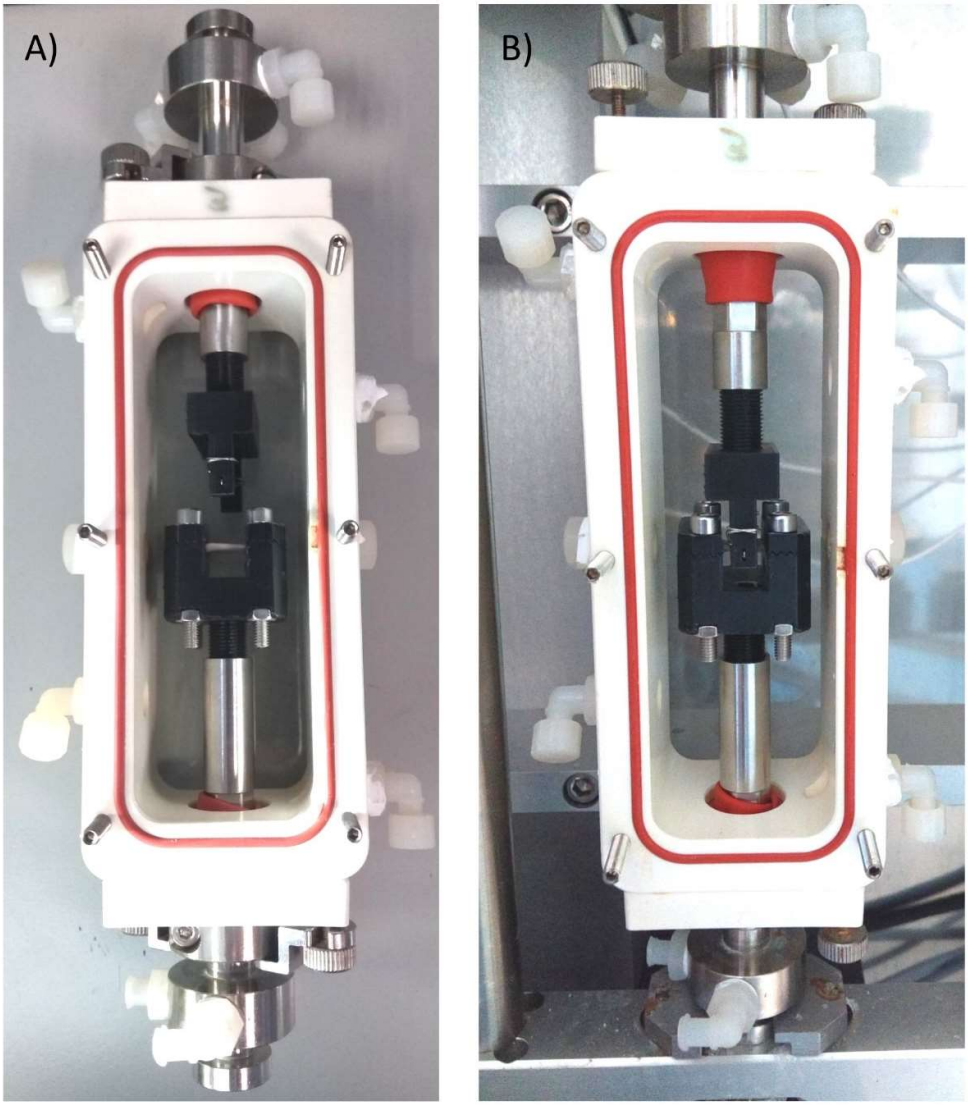

Figure 6.2: Images of the dynamic indentation device (A) with strips loaded into the Bose bioreactor chamber and (B) loaded into the Bose Biodynamic device with stent strut placed level with the top of the recellularized strips

6.2.4 Staining

To stain for collagen, strips were incubated in a 1:200 dilution of CNA35 in the medium used for strain application at 37ºC for 2 hours. PDMS strips were fixed in 10% formalin for greater than 24 hours at 4ºC. Strips were blocked and permeabilized in a solution of 5% BSA and 0.2% Triton-X 100 in PBS at room temperature for 40 minutes with agitation. Strips were then rinsed twice in PBS. Primary antibody solution was prepared in 0.5% BSA and 0.2% Triton-X 100 in PBS, with. Strips were incubated in 1:200 Ki67 antibody (Abcam ab15580) overnight at 4ºC. Strips were rinsed three times in PBS. Secondary antibody

solution was prepared 0.5% BSA and 0.2% Triton-X 100 in PBS with 1:1000 secondary antibody, 1:1000 DAPI and 1:500 rhodamine Phalloidin (for strips not previously stained with CNA35). Strips were incubated in secondary antibody solution in the dark at room temperature for 1 hour. Strips were rinsed three times in PBS and stored at 4ºC protected from light before imaging.

6.2.5 Imaging and Image Analysis

All images were taken on a Leica SP8 scanning confocal microscope at 20x. For each sample, a continuous area of at least 28 images was scanned with a z-stack taken at intervals of 10µm. The images were taken as 1024x1024 pixel images with a scan speed of 400 Hz. Nuclear analysis was performed with ImageJ particle analysis to get nuclear number, nuclear orientation, major and minor axis, and nuclear area as described in Chapter 4. Images where nuclei were too dense to separate using particle analysis were counted and percentage of images that couldn't be counted were calculated. Collagen alignment and actin alignment were both determined using the MatFiber MatLab program.[225] Ki67+ nuclei were determined by masking Ki67 with nuclear area, and then counting positive nuclei using ImageJ particle analysis as described in Chapter 4. Images where Ki67+ nuclei were too dense to separate using particle analysis were counted and percentage of images that couldn't be counted were calculated.

6.2.6 Statistics

Statistics were performed using GraphPad Prism version 8.2.1. Significance was determined using an ordinary one-way ANOVA for cell counts and Ki67+ nuclear counts with $n \geq 3$ samples. Collagen and F-actin alignment significance was determined using a 2-way ANOVA with a post-hoc Tukey test with $n \geq 3$ samples.

6.3 Results

In order to determine if loading with a simulated stent strut would cause realignment of collagen fibres, collagen in the recellularized strips was strained with CNA35 and imaged. Overall, all conditions showed collagen aligned primarily parallel to the direction of strain (Figure 6.3). Additionally, there was no evidence of any regional realignment of collagen as shown in the representative images of collagen structure (Figure 6.4).

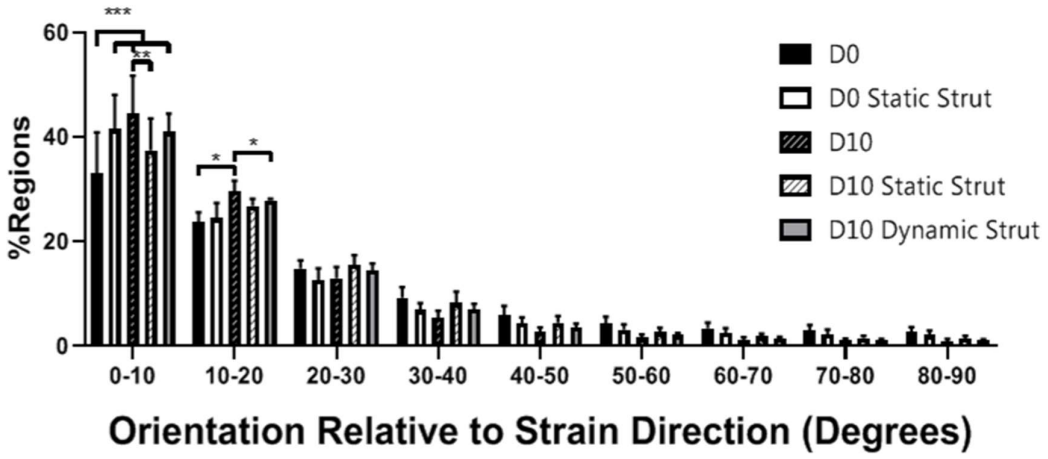

Figure 6.3: Orientation of collagen structure of decellularized porcine carotid artery relative to strain direction. (A) Fibre distribution changes after stent strut loading regimes. *p<0.05, **p<0.01, ***p<0.001, n ≥ 3

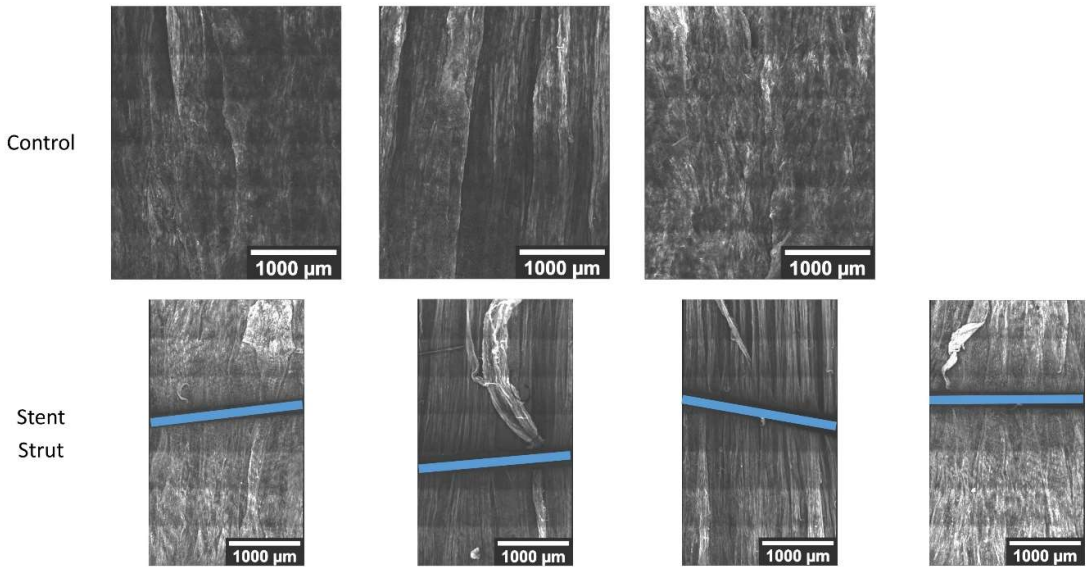

Figure 6.4: Images of collagen fibres from day 0 samples stained with CNA35. Blue lines indicate locations of wire strut. Scale bars = 1000µm

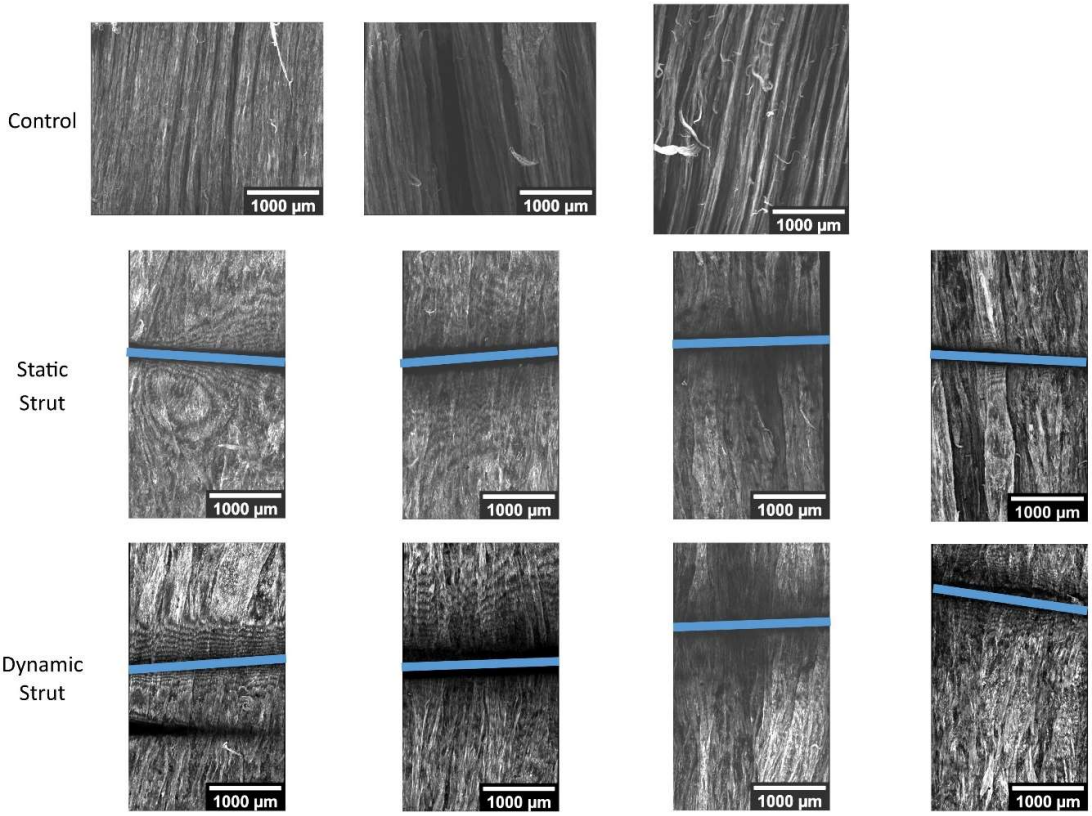

Figure 6.5: Images of collagen fibres from day 10 samples stained with CNA35. Blue lines indicate locations of wire strut. Scale bars = 1000µm

After ten days, cell alignment was evaluated using f-actin staining of cell actin cytoskeleton. Figure 6.5 demonstrates that ten days of loading with either a static or a dynamic stent strut decreased the alignment of cells parallel to the direction of the collagen fibres and strain.

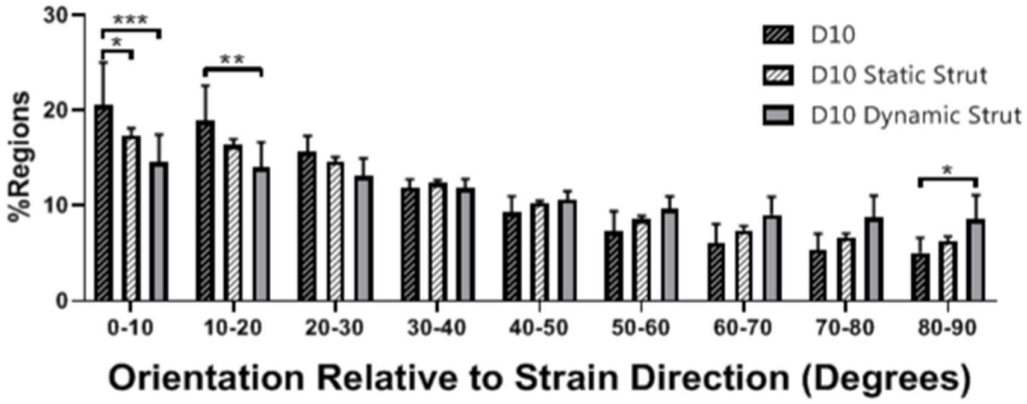

Figure 6.6: F-actin orientation of cells exposed to various loading regimes for 10 days. (A) Stent strut indentation decreases cell alignment in strain direction. *p<0.05, **p<0.01, ***p<0.001, n ≥ 3

In samples without a stent strut, cells remained aligned with the direction of collagen fibres (Figure 6.6A). In both statically loaded and dynamically loaded samples, cells aligned along the stent strut, perpendicular to the direction of the collagen fibres (Figure 6.6B, C). Further away from the stent, however, in statically loaded samples cells remained aligned with the underlying collagen fibres (Figure 6.6D), while in dynamically loaded samples, some regions showed cells aligning perpendicular to the direction of strain and collagen fibres (Figure 6.6E). Figure 6.7 shows the overall f-actin fibres.

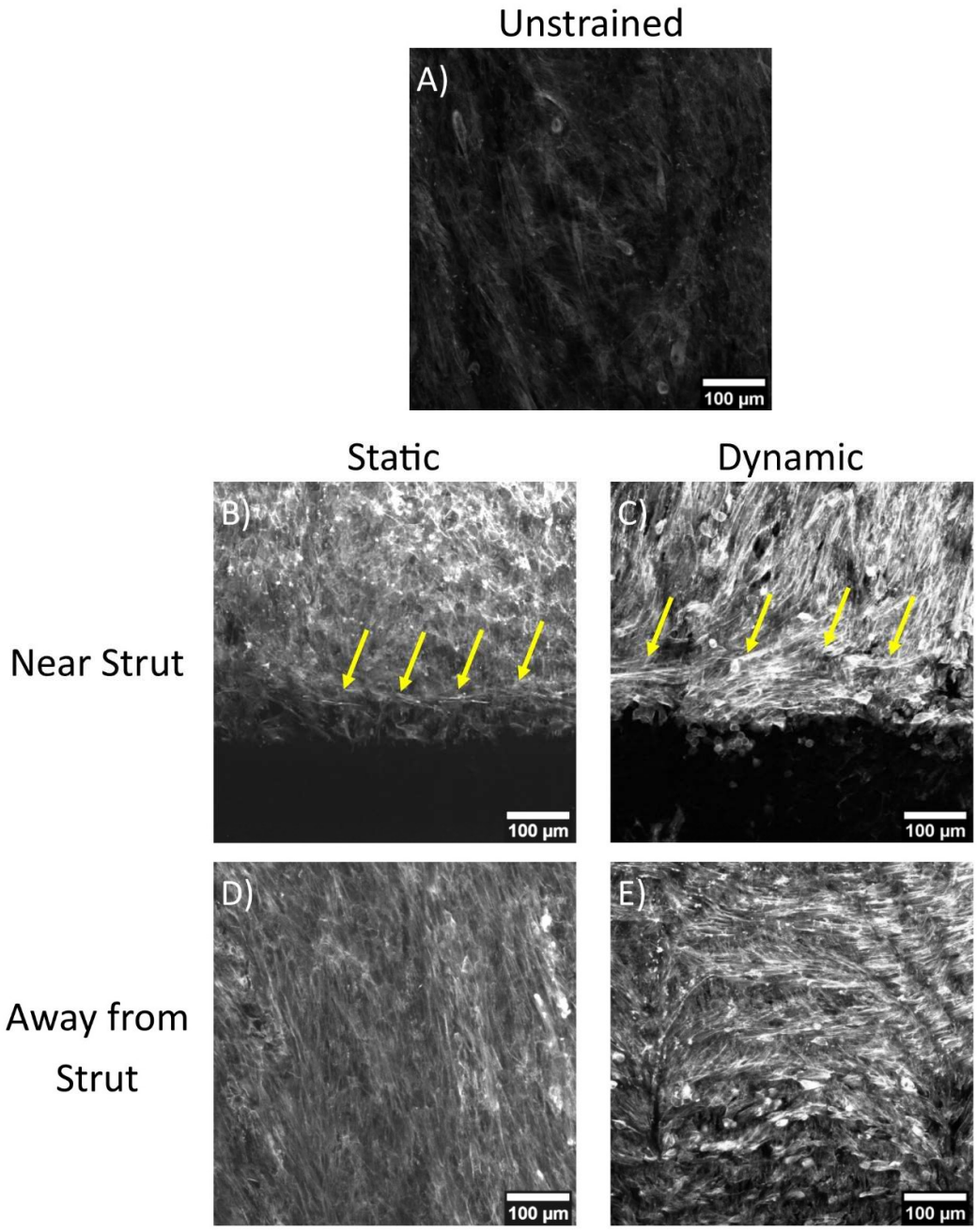

Figure 6.7: Representative images of cells stained for f-actin for unstrained (A) and statically (B, D) and dynamically (C, E) loaded cells, both near (B, C) and far (D, E) from stent strut. Yellow arrows indicate areas where cells aligned along the edge of the stent strut. Scale bar = 100 µm

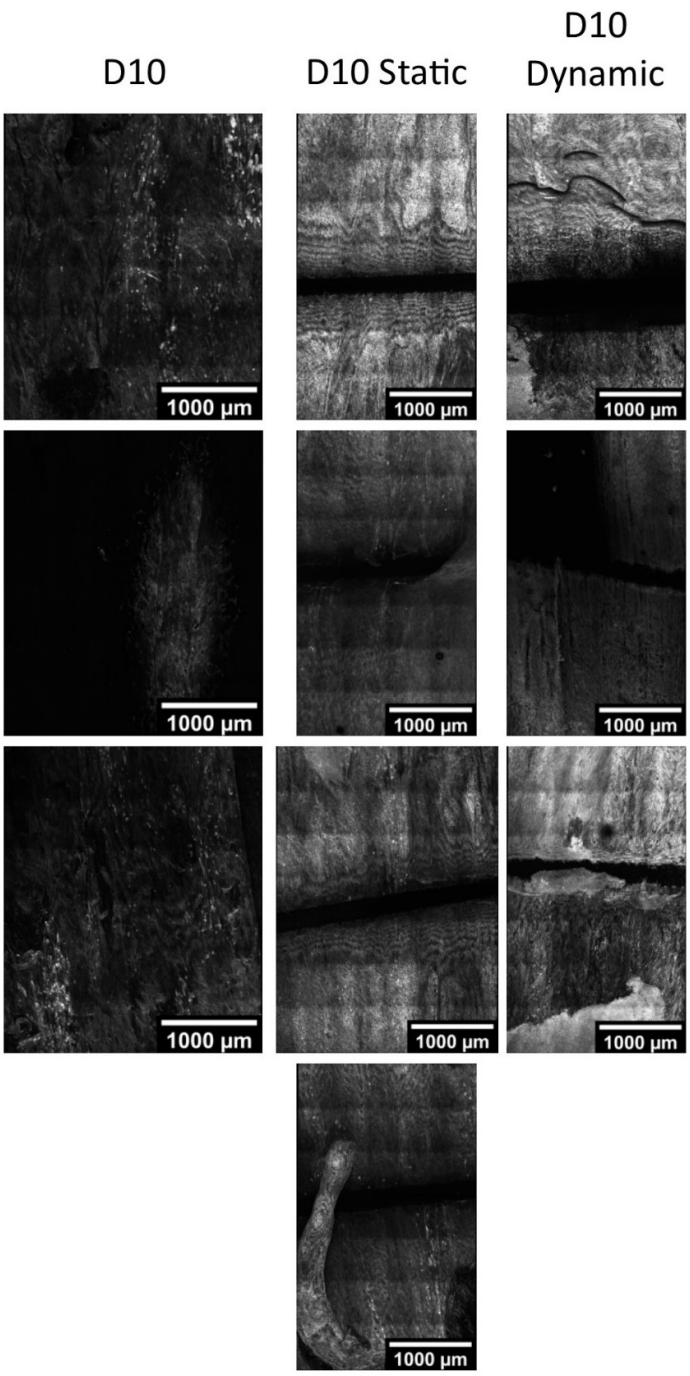

Figure 6.8: F-actin fibres for each sample shown in white. Stented samples show black line where stent was applied. Scale bar = 400 µm

Cell proliferation was evaluated both by cell count and by number of Ki67 positive, proliferative cells. While samples from day 0, and unstrained cells at day 10 showed countable numbers of nuclei, and Ki67+ cells (Figure 6.8A-C,F-H,K-M), samples that were exposed to a static stent strut for 10 days showed cell nuclei that had many frames

that were too dense to count (Figure 6.8D), and samples that were exposed to a dynamically loaded stent strut for 10 days showed both regions of nuclei, and regions of Ki67+ nuclei that were too dense to count (Figure 6.8E, J, O).

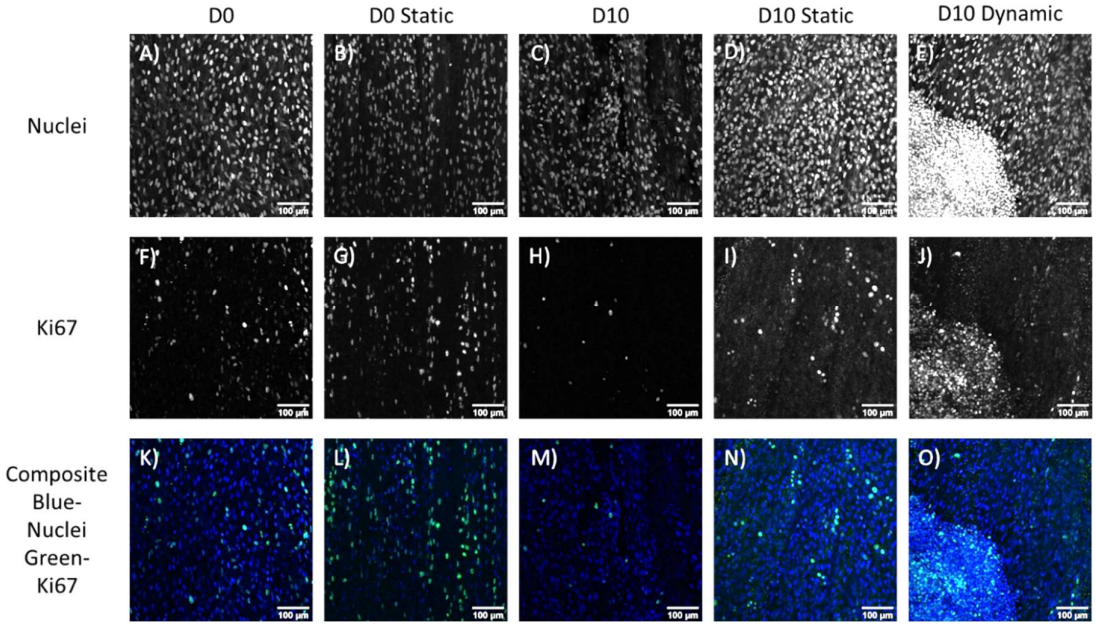

Figure 6.9: Representative images of nuclei and ki67 positive nuclei for different stent strut loading regimes. Scale bar = 100 µm

When the nuclear staining results were quantified, it was shown that neither cell number nor percentage of Ki67+ nuclei was significantly different between either of the day 0 conditions or day 10 samples that were left unstrained (Figure 6.9A, B). Both day 10 conditions that involved loading with a simulated stent strut showed regions that had cells that were too densely packed to count nuclei. The number of uncountable frames was slightly, but not significantly higher in the dynamically loaded samples than the statically loaded samples, however only dynamically loaded samples had regions where Ki67+ cells were too densely packed to count (Figure 6.9C). Most of the samples that were dynamically loaded had regions of densely packed and highly proliferative cells, while other samples showed more even cell distribution (Figure 6.10).

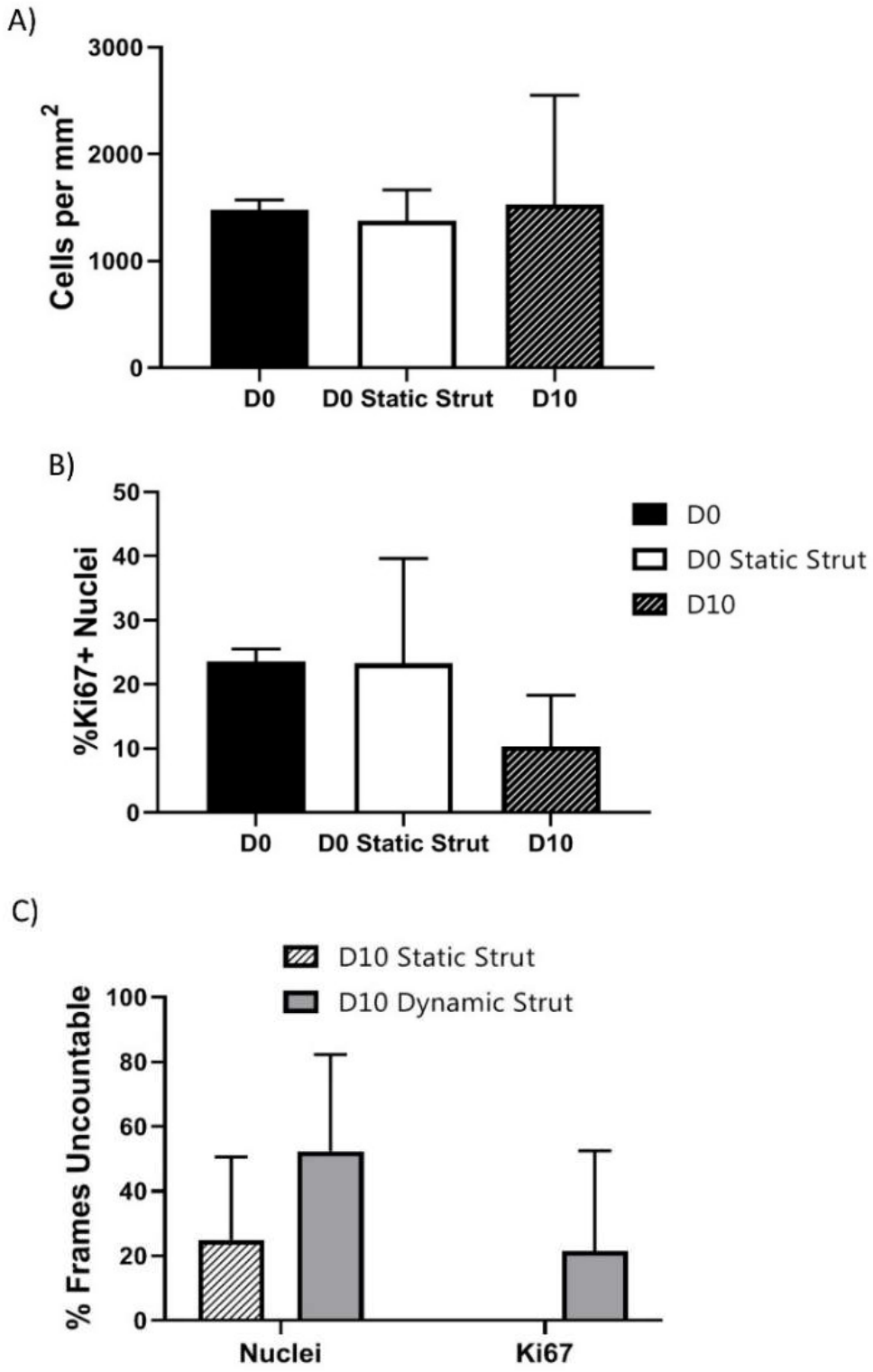

Figure 6.10: Cell number and proliferation. (A) Cell number for conditions with countable nuclei. (B) Percentage of Ki67+ nuclei for conditions with countable nuclei. (C) For conditions without countable nuclei, percentage of frames for which individual nuclei or Ki67+ nuclei cannot be counted. n ≥ 3

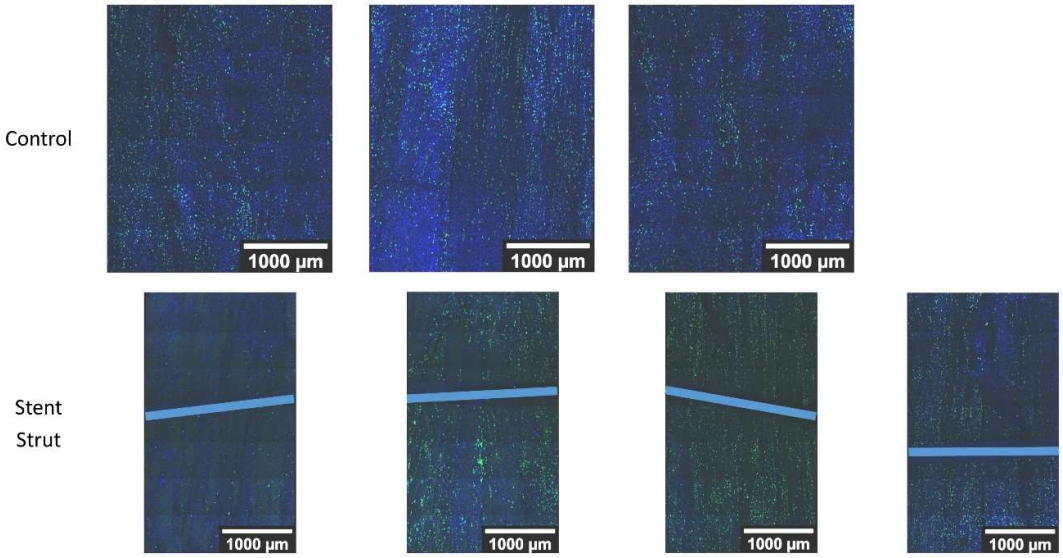

Figure 6.11: Images of day 0 samples showing nuclei and proliferative cells. Light blue lines indicate wire locations. Blue-Nuclei Green-Ki67 Scale bars = 1000µm

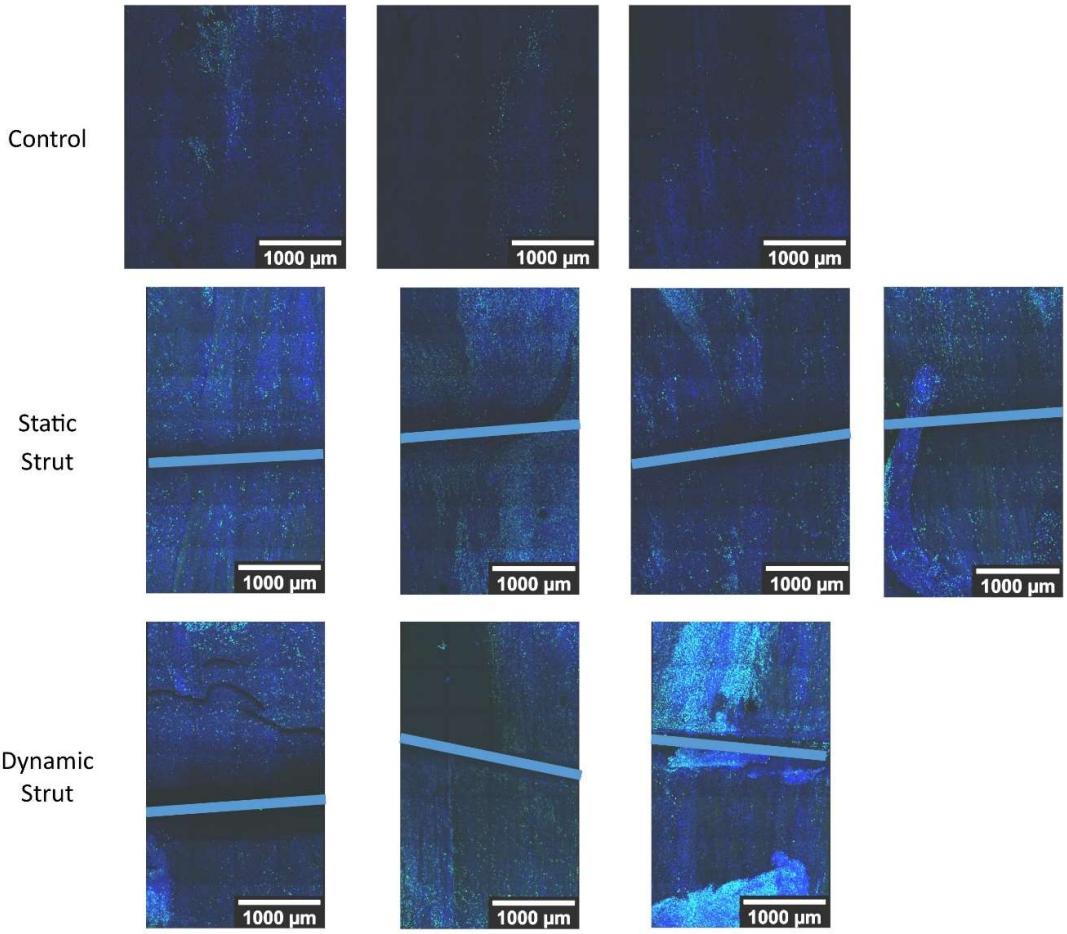

Figure 6.12: Images of day 10 samples showing nuclei and proliferative cells. Light blue lines indicate wire locations. Blue-Nuclei Green-Ki67 Scale bars = 1000µm

6.4 Discussion

Although previous experiments have shown some collagen reorientation in response to the loading of stent struts,[10,44] in this simulated stent loading regime, no collagen reorientation occurred. However, in previous experiments this reorientation occurred below the surface level of the vessel,[10] whereas this experiment only observed the surface layer of collagen. Mechanical models suggesting fibre-matrix shearing based reorientation of collagen have also shown that regions of high shear occur mainly deeper within the vessel wall.[45] As a result, it may be that the collagen reorientation is occurring at a deeper level where it would not affect the cells that were seeded only on the surface level of the vessel strips.

Even without collagen reorientation, cell realignment was observed in samples that were loaded by the simulated stent strut for 10 days. The cells that realigned along the length of the stent strut were likely aligned due to contact guidance. Because *in vivo* stenting causes deendothelialization, any cells that migrate to the intimal space could come in contact with the stent strut itself, changing the cellular orientation, this change in orientation could change how the cells experience strain. Chapter 5 showed how both MVSC and VSMC orientation relative to strain direction could influence cell number, with MVSC being less proliferative when oriented perpendicular to strain direction. This indicates that MVSC aligning with the stent strut orientation, perpendicular to the primary direction of strain, may limit MVSC proliferation, assuming this arrangement doesn't increase cyclic strain in other areas of the vessel. Under dynamic stent strut indentation, some regions of cells not near the stent strut realigned perpendicular to strain direction. As was described in Chapter 4, when MVSC aren't influenced by underlying microstructural cues, they will reorient perpendicular to strain direction. In regions where cells reoriented perpendicular to fibre and strain direction, the cells that remained in contact with the ECM structure remained oriented with the fibre direction, while the cells that had reoriented were layered over the top of other cells, so they were no longer sensing the microstructural cues from the underlying ECM. If MVSC are the primary driver of in-stent restenosis we would expect that the cells proliferating in in-stent restenosis would be in regions where there is ECM or other guidance oriented parallel to the direction of strain.

When samples were loaded with a stent strut for 10 days, both the static strut and the dynamic stent induced an increase in cell number versus unstrained samples. While static strain has not been investigated in MVSC specifically, static strain in intact tissue rings showed increased DNA synthesis, possibly indicating increased cell division, in medial

cells. [238] This could indicate the presence of MVSC in these intact tissue samples or indicate that VSMC respond differently to static strain than cyclic tensile strain. Previous studies have shown differing responses for VSMC between static and cyclic strain. VSMC under stationary strain increased MMP-2 and MMP-9 expression, while cyclic strain decreased production of these ECM degrading proteins.[146] In this experiment we see that static strain is causing an increased cell proliferation that is still qualitatively different than the proliferation seen in cyclically loaded samples.

Given the increased proliferation of MVSC when strained in the direction of cell alignment in Chapter 5, we would have expected to see the increase in MVSC when they were dynamically loaded parallel to strain direction. Additionally, when dynamically loaded, samples began to show regions of dense, highly proliferative cells. These areas mimic areas of in-stent restenosis which have both high cell density,[46] and high proliferation.[47] This study correlates with studies of various stent designs that indicate that designs that cause increased strains within the vessel caused increased in-stent restenosis.[48-50] Additionally, many parameters that might induce greater strains within the vessel have been shown to increase the extent of in-stent restenosis including more rigid stents,[52] and stents that are mismatched to the size of the artery.[53] The dynamic strut indentation would simulate a loading environment where there is high dynamic strain applied within the artery, which would be consistent with the regions that showed high in-stent restenosis.

While this research makes a strong argument for MVSC being a key player in in-stent restenosis, the device that was designed to provide stent strut indentation could be used to investigate many further parameters of stent design. Since strut thickness has been shown to influence the restenosis rate,[54] stent strut diameter and cross-sectional shape could be easily modified by substituting different wires into the indentation devices. In addition, stent struts are often oriented in directions other than axial to the vessel, and Chapter 5 clearly demonstrated that ECM and cell alignment relative to strain direction plays a vital role in how cells sense strain. By cutting decellularized tissue strips at angles other than circumferential to the artery, the effect of stent strut orientation could be easily studied allowing for a better understanding of how to control stent strut orientation in order to prevent in-stent restenosis. With some minor modifications to the static device, and only modifying input parameters on the dynamic device, indentation depth could be modified in order to apply different levels of strain to the strips. This would clearly be of interest given

that Chapter 4 demonstrated that different amplitudes of uniaxial strain can influence cell response to strain. This information could be used to help inform how to best expand stents as well as to design stents that apply the correct level of strain.

In addition to changing the strain conditions applied, the strain device could also be easily modified to investigate different potential factors in in-stent restenosis. As VSMC have also been implicated in in-stent restenosis[68,69] those cells could also be investigated for response to stent strut indentation. However, as described in Chapter 5, when exposed to 10% uniaxial strain in the direction of cell elongation VSMC cell number decreased, so it would be unlikely that VSMC exposed to the strain regime used in these experiments would exhibit significant proliferation. In addition to cells being tested individually, this model could easily accommodate full strips of vascular tissue, although they would have to be of a larger species such as porcine, bovine or human. This would allow a model that might be able to recapitulate how the different cell types interact with each other. It would also allow a model in which the smooth muscle cells are truly contractile, as opposed to cultured smooth muscle cells that adopt a synthetic phenotype. By creating a device that allows the application of both static and dynamic stent strut indentation, this chapter has demonstrated that MVSC are potentially a dominant cell type in in-stent restenosis.

Chapter 7 Final Discussion

Vascular disease is currently a large problem with over 17.6 million deaths caused per year.[1] While the prevalence has begun to decrease slightly, with a 0.8% age-adjusted decrease in prevalence and a 14.5% decrease in age adjusted death rate from 2006 to 2016, the overall number of people affected by cardiovascular disease only continues to rise, with a 26.7% increase between 2006 and 2016.[1] The prevalence of stents has followed a similar trend with cardiac stenting procedures per 10 000 population rising by 61% from 1999 to 2006, then declining by 27% between 2006 and 2009, however increasing population means the overall number of stents used has continued to rise.[1] With the increasing number of stents being used there is a driving need to develop stents that will avoid both the restenosis associated with bare metal stents, and the thrombosis associated with drug eluting stents. MVSC are a novel target for the prevention of in-stent restenosis, and the research presented in this thesis allow us to understand the role these cells could play in the development of this condition.

MVSC have been shown to play a role in vascular disease,[12] and may be a key player in in-stent restenosis. However, VSMC have also been implicated in this phenomenon. While VSMC mechanoresponse has already been extensively studied, there is no previous research on the response of MVSC to mechanical changes in blood vessels. Therefore it is important to understand MVSC behaviour when exposed to various mechanical and structural changes. Insight into this little-studied cell type will allow for the better development of treatments for in-stent restenosis as well as provide opportunities to design better stents in order to prevent the development of this complication.

In Chapter 3, when MVSC and VSMC were exposed to cyclic equiaxial tensile strain, MVSC and VSMC responded differently to the application of tensile strain. MVSC showed an increase in contractile phenotype in response to tensile strain, while VSMC showed no such response. These preliminary results showed the first evidence of differences in how MVSC and VSMC respond to tensile strain. This indicates that MVSC and VSMC may be playing different roles in the development of vascular disease. Because both of these cell types have been implicated in the development of intimal hyperplasia,[12,67] if these cell types respond differently to the application of tensile strain, then any vascular interventions

which change the mechanical environment within the vessel will have to account for the reactions of both cell types.

Chapter 3 also highlights the differences in cell phenotypes between MVSC and VSMC. The MVSC express much lower levels of contractile genes compared to VSMC. This study also demonstrates that the VSMC grown in culture are not fully contractile, because they can be induced into a more contractile phenotype by the addition of TGF-β1. VSMC grown *in vitro* are expected to be of a synthetic phenotype,[239] and these cells may be derived from a stem cell origin as they express neural stem cell markers.[106] In fact, experiments on cells freshly isolated from the medial layer of the porcine carotid artery described in Appendix V demonstrated that these cells had the potential to undergo both osteogenic and adipogenic differentiation. The fact that the VSMC are not fully contractile is one major limitation of this work, and, indeed, most current *in vitro* work on VSMC.

Chapter 4 comprehensively investigated how MVSC and VSMC responded to the more physiologically relevant uniaxial strain at three different strain levels and two different time points. Unlike what was shown in Chapter 3, when exposed to uniaxial strain, MVSC and VSMC behaved similarly. Both cell types exhibited strain avoidant realignment perpendicular to strain direction, an increasing amount of alignment as strain amplitude increased, and a decrease in cell number when cells were strained. There were, however, a few key differences between the two cell types. MVSC strain avoided more strongly at the early 24 hour time point, while VSMC reoriented more strongly at the later 72 hour timepoint. Additionally, MVSC and VSMC may have differing mechanotransduction mechanisms with MVSC showing a greater nuclear deformation in response to strain, and VSMC showing a greater actin cytoskeletal reorganization in response to strain.

This is consistent with mechanotransduction mechanisms seen in other populations of stem cells. In a study on embryonic stem cells, the nuclei stiffened as the stem cells differentiated.[231] Thus it could be the case that MVSC nuclei are less stiff than the more differentiated VSMC thus allowing greater deformation and increased nuclear mechanotransduction. In previous studies of CPCs, when these stem cells were left undifferentiated, they did not have a well-organized cytoskeleton and did not respond to tensile strain.[188] After the CPCs began to differentiate their cytoskeleton became better organized, and these differentiated cells then responded to strain.[188] This indicates that the MVSCs may be in a partially differentiated state that still have a less robust cytoskeleton

than the synthetic VSMCs used in the strain experiments. It further suggests that fully contractile VSMCs may have an even more robust actin cytoskeleton and thus stronger cytoskeletal mechanotransduction than the population of VSMC routinely used in *in vitro* experiments.

Chapter 5 examined how MVSC and VSMC respond when subjected to strain while constrained by a native ECM microstructure. When cells were grown on decellularized surfaces without the application of strain, these cells aligned with the direction of the underlying circumferentially aligned collagen fibres. Chapter 4 established that when exposed to strain, both MVSC and VSMC strain avoid perpendicular to the direction of strain. When cells experienced a microstructural cue that would cause alignment in one direction and strain that would cause alignment in a different direction, it was unclear which cue would dominate over the other.

Although Chapter 4 shows that, MVSC and VSMC react similarly to cyclic tensile strain on an unstructured surface, *in vivo*, vessels are constrained by circumferentially arranged collagen fibres. In Chapter 5, we begin to see large differences in how the two cell types react to uniaxial tensile strain. While MVSC alignment was determined solely by the underlying ECM structure alignment, VSMC showed some strain avoidant behaviour. Because VSMC are both larger[12] and more heterogeneous[104] than MVSC, the spacing between the collagen fibres in the decellularized tissue was likely too closely spaced to fully constrain the VSMC and prevent strain avoidance. Therefore, it appears that structure cues can dominate over strain cues in determining cell alignment, but only if the fibre spacing is the correct size for the cells. This has implications for tissue engineered blood vessels. In order to ensure that the cells are oriented in the correct direction, the engineered microstructure has to be of the correct size for the cell type used so that the cells remain oriented in the desired direction regardless of the strains applied to the tissue.

Cell alignment can be critical to obtaining the desired cell response. When the cells were not able to strain avoid, differences in proliferative responses between VSMC and MVSC emerged. When MVSC were strained parallel to cell orientation, cell proliferation increased. Conversely, VSMC aligned parallel to strain direction showed a large decrease in cell number. This would suggest that in a high strain situation, MVSC would proliferate and eventually be the dominant cell type as the VSMC die off. Interestingly, these strain-induced changes did not appear when the cells were aligned perpendicularly to the direction

of strain, showing that cell orientation relative to strain direction is critical to how the cells sense uniaxial tensile strain. A significant finding in this work is that cells only appear to sense the strain when they are aligned with the direction of the strain.

Ultimately this alignment-directed sensing of strain could be critical in understanding cell response in vascular disease. Both atherosclerosis[33,34] and stenting[44,45] have been shown to change the fibre structure so that collagen fibres no longer align circumferentially to the vessel. Ultimately, this could decrease the strain sensed by the VSMC and cause increased proliferation of these cell types, thus contributing to restenosis.

This also shows how critical cell alignment is in tissue engineering applications. In order to induce a specific behaviour in cells in response to tensile strain, the cells first have to sense the strain. This means that knowing the orientation of the cells within the tissue engineered construct is important in selecting the correct strain amplitude to apply to achieve the desired phenotypic and proliferative results. The combination of MVSC and VSMC sensitivity to strain amplitude described in Chapter 4, and strain orientation relative to cell orientation described in Chapter 5 means that the combination of the two can be used in order to direct vascular cell and tissue development into the desired structures. This could be combined with multi-scale mechanical modelling which could then predict how the mechanical properties of the vascular tissue change as the cells grow and differentiate in order to design a loading regime that would be able to adapt as the tissue matures.

In Chapter 6, a test rig was developed to simulate the indentation of a single stent strut. In stenting situations, tensile strain is much more complex that simple uniaxial loading. This device allowed for the generation of strains in vascular tissue more similar to those found in a stenting situation. Since Chapter 5 suggested that MVSC would be the proliferative cell type in a high strain situation, this device was then used in order to determine how MVSC would react in a simulated stenting situation. When exposed to dynamic stent indentation, MVSC proliferated as we would have expected from Chapter 5. They also developed regions of densely packed highly proliferative cells, which mimicked regions of in-stent restenosis. This clearly indicates that MVSC have the potential to develop an over-proliferative response when loaded in a manner consistent with stenting suggesting that this cell type is involved in the development of in-stent restenosis.

While only the dynamic stent indentation showed the development of dense highly proliferative cell regions, static stenting also showed an increase in overall cell number

compared to unstrained samples. This indicates that both types of loading would increase neointimal thickness to some degree. It is possible that the differences in how the cells perceive static vs cyclic strain are due to how the different types of strain affect mechanotransduction through the actin-cytoskeleton. In MSC, cyclic strain causes a greater rearrangement of the cytoskeleton of cells stretched statically to the same strain. [240] Thus, in VSMC,which have more developed contractile cytoskeletal structures, we might expect to see a larger difference between how they respond to static strain and dynamic strain than what is observed with MVSC.

These differences in static versus dynamic response have implications in stent design. Stents that allow the vessel to deform around the stent may be at higher risk of developing in-stent restenosis than stents that hold the blood vessel taught, if MVSC are the key cell type in neointimal formation.

However, as with any experimental based work there are some limitations to consider. Firstly, these cells were rat cells and rats do not naturally develop vascular disease in the same way that humans do. Whether the main findings translate to human cells and tissues certainly warrants further investigation. Additionally, the collagen template used to align the cells were obtained from decellularized porcine carotid arteries. This could result in a size mismatch between the rat cells and the porcine collagen structure, although this un unlikely to have influenced the main observations to any great extent.

There is also some uncertainty to the exact strain experienced by the cells. While the underlying substrates were strained using displacement controlled clamps, it is unclear how much of the strain for the underlying substrate is translated to the cells themselves. This is further complicated when the cells are strained on the decellularlised porcine carotid artery strips. Collagen itself has an intrinsic wavy configuration. Depending on the position along the collagen fibres where the cells attach, as the fibres are elongated with strain, the cells may be strained unevenly. Therefore, it's uncertain whether or not cells are experiencing the full 10% uniaxial strain applied to the strip as a whole. However, this problem could be overcome using a system where the cells and collagen are imaged as they are undergoing strain, which would allow for the calculation of strains on individual collagen fibres and allow for the understanding of how strain transfers to individual cells.

Another possible limitation of this work was the small size of the constructs being strained. This meant that only immunostaining could be used to verify any phenotypic changes in the cells. With a larger surface area, there would have been enough cells to measure any phenotypic changes using RT-qPCR for changes in mRNA expression, or Western blot for protein expression. These methods are more quantitative than measuring immunostaining intensity alone and may provide deeper insight into how tensile strain and aligned fibres modulate the phenotype of vascular cells. These more sensitive quantitative techniques may demonstrate phenotypic changes in these vascular cells, that we would expect to see with the differing proliferation rates observed.

However, as the first comprehensive study of the mechanical responses of the MVSC this thesis demonstrates the importance of this cell type in vascular disease. This body of research has established the importance of MVSC as a mechanosensitive vascular cell type. Furthermore, it establishes that this cell type may play a key role in in-stent restenosis. This clearly identifies a cell type that may be a potential therapeutic target for any vascular intervention and makes the case that this cell type needs extensive further study in order to understand and prevent in-stent restenosis.

Chapter 8 Concluding Remarks

Summary of Key Findings

This thesis aimed to explore the mechanical responses of MVSC as they pertained to the role of MVSC in the role of in-stent restenosis. These are amongst the first studies of the mechanosensitivity of this critical cell type. The key contributions that this work has made to the field of mechanobiology are listed below:

- These studies established the mechanosensitivity of MVSC, with this cell type showing phenotypic, proliferation, and alignment changes in response to various different types of mechanical loading.
- Under equiaxial strain MVSC and VSMC show different phenotypic responses, with MVSC showing an increased contractile phenotype in response to strain, while VSMC showed no change in phenotype.
- MVSC were evaluated for response to uniaxial tensile strain, comparing them to VSMC. MVSC were determined to demonstrate strain avoidant behaviour and that they strain avoid more strongly than VSMC at an early time point. There was also indication that MVSC and VSMC may have different mechanotransduction mechanisms.
- MVSC and VSMC proliferation response was determined in response to uniaxial tensile strain. This indicated a strain-induced loss of cells which was not attributable to decreased proliferation.
- MVSC response to underlying ECM structure was determined using a decellularized porcine carotid artery ECM structure. This showed that MVSC and VSMC will align with predominant direction of collagen fibres in vascular ECM.
- Using the decellularized matrix, the influence of MVSC and VSMC alignment on uniaxial strain response was investigated. MVSC remained aligned with the direction of strain, while VSMC realigned in some cases.
- MVSC aligned in the direction of strain increased in proliferation, while conversely, VSMC aligned in the direction of strain showed a decreased cell number
- Finally, indentation with a simulated stent strut demonstrated that MVSC will develop dense regions of highly proliferative cells, which mimic the behaviour of

cells involved in in-stent restenosis. This points to a critical role for MVSC in the biological response to stenting, and the importance of MVSC as a potential target for the prevention of restenosis.

Future Perspectives

Establishing MVSC as a mechanosensitive cell that could play a role in the development of in-stent restenosis has suggested several further avenues of study that could be further explored:

- Other important aspects of MVSC response to tensile strain cues can be investigated, such as extracellular matrix synthesis in response to strain, and the molecular mechanisms for MVSC reorientation and differentiation
- MVSC can be cultured in the presence of other vascular cell types such as VSMC or endothelial cells in order to understand the interaction between these cell types in the development of vascular disease.
- The developed bioreactor system for stent strut indentation could be used to measure the response of other cell types involved in in-stent restenosis such as VSMC or endothelial cells. Additionally, fresh tissue strips could be indented in order to understand how the multiple cell types within the vessel interact under a simulated stent loading situation.
- Full intact decellularized vessels with deployed stents could be used to investigate the response of individual cell types to stenting with both tensile strain and fluid flow relevant to physiological conditions
- Using the cell proliferation and alignment data, multiscale modelling can be used to further elucidate the role of MVSC and VSMC in various stent loading scenarios. This data could be used to optimize stent design in order to prevent over proliferation of both MVSC and VSMC.

Appendix I Strain Response of RASMC to Varying Strain Amplitudes

A1.1 Introduction

Vascular smooth muscle cells are a mechanically sensitive cell type, which have previously been shown to be responsive to equiaxial strain amplitude but not mean strain.[37] In this study, the effect of strain amplitude on RASMC phenotype was investigated as a preliminary study into how strain amplitude could affect medial vascular cells.

A1.2 Methods

A1.2.1 Cell Culture

RASMC were obtained from Cell Applications and cultured in DMEM with 10% FBS (Sigma) and 1% Penicillin/Streptomycin. Cells were used between p15-17.

A1.2.2 Tensile Strain

Cells were strained on the Flexcell® FX-5000™ Tension System. Cells were seeded at 10^5 cells per well in 6 well, pronectin coated Bioflex™ plates. Cells were allowed to adhere for 48 hours in their respective culture medium, then serum starved in DMEM with 0.2% FBS for 24 hours. At this point the strain regime was started. After serum starvation, cells were returned to DMEM with 10% FBS and were either started on strain, or left unstrained for the next 24 hours. Cells were strained at 1Hz equiaxially at three strain magnitudes with a mean strain of 5% strain: 2% strain amplitude (4-6% strain), 6% strain amplitude (2-8% strain), or 10% strain amplitude (0-10% strain).

A1.2.3 Immunocytochemistry

To assess cell morphology, cells were fixed in 4% formaldehyde for 20 minutes and then rinsed in deionized water. Cells were stained for f-actin and nuclei. Cells were incubated in a solution of 1:500 FITC-Phalloidin and 1:1000 DAPI (1mg/ml) in PBS for 1 hour, protected from light.

A1.1.4 Gene Expression

In Study 1, RNA was extracted using a MagCore® HF16 System with the MagCore® kit no. 610 as directed by the manufacturer. Gene expression was then determined using 1-step RT-qPCR using a Real Time Rotor-GeneRG-3000TM lightcycler. The Rotor-Gene SYBR® Green RT-PCR Kit (Qiagen) was used according to manufacturer's instructions with the following Quantitect Primer Assays (Qiagen): ACTA2: Mm_Acta2_1_SG

QT00140119, MYH11: Mm_Myh11_1_SG QT01060843, CNN1: Mm_Cnn1_1_SG QT00105420.

A1.3 Results

RASMC were strained at three strain amplitudes for 24 hours. As shown in Figure A1.1, 24 hours of 2% strain amplitude significantly increased the expression of MYH11 versus the unstrained control and 6% strain amplitude and significantly increased CNN1 versus all other strain conditions.

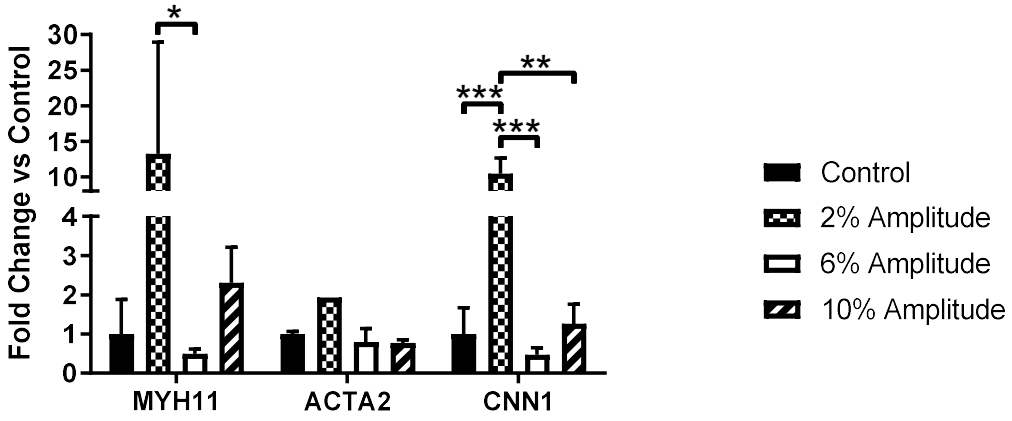

Figure A1.1: Gene expression of contractile genes normalized to control. RASMC were exposed to 24 hours of strain at 5% mean strain and varying amplitudes. MYH11 and CNN1 are significantly upregulated in response to 2% strain amplitude. *p<0.05, **p<0.01, ***p<0.001, ****p<0.0001

As shown in Figure A1.2, proliferation based on cell counts decreased for all levels of strain compared to unstrained cells. Differing strain amplitudes also resulted in differing morphologies of strained RASMC.

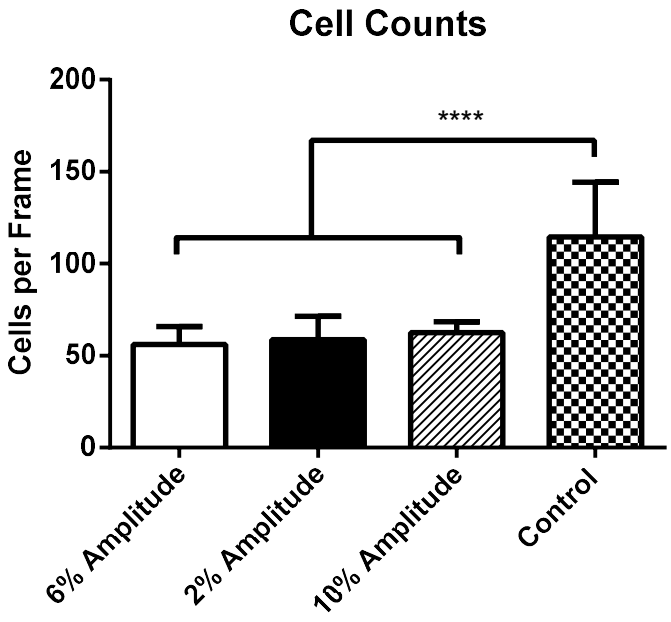

Figure A1.2: Cell counts of RASMC exposed to three amplitudes of strain for 24 hours. All strain conditions showed lower levels of proliferation than the unstrained control. *p<0.05, **p<0.01, ***p<0.001, ****p<0.0001

As seen in Figure A1.3, cells exposed to 2% amplitude strain showed a more organized actin structure than cells exposed to 6% amplitude, 10% amplitude, or no strain. This is consistent with the PCR data showing a greater contractile phenotype in cells exposed to 2% strain amplitude.

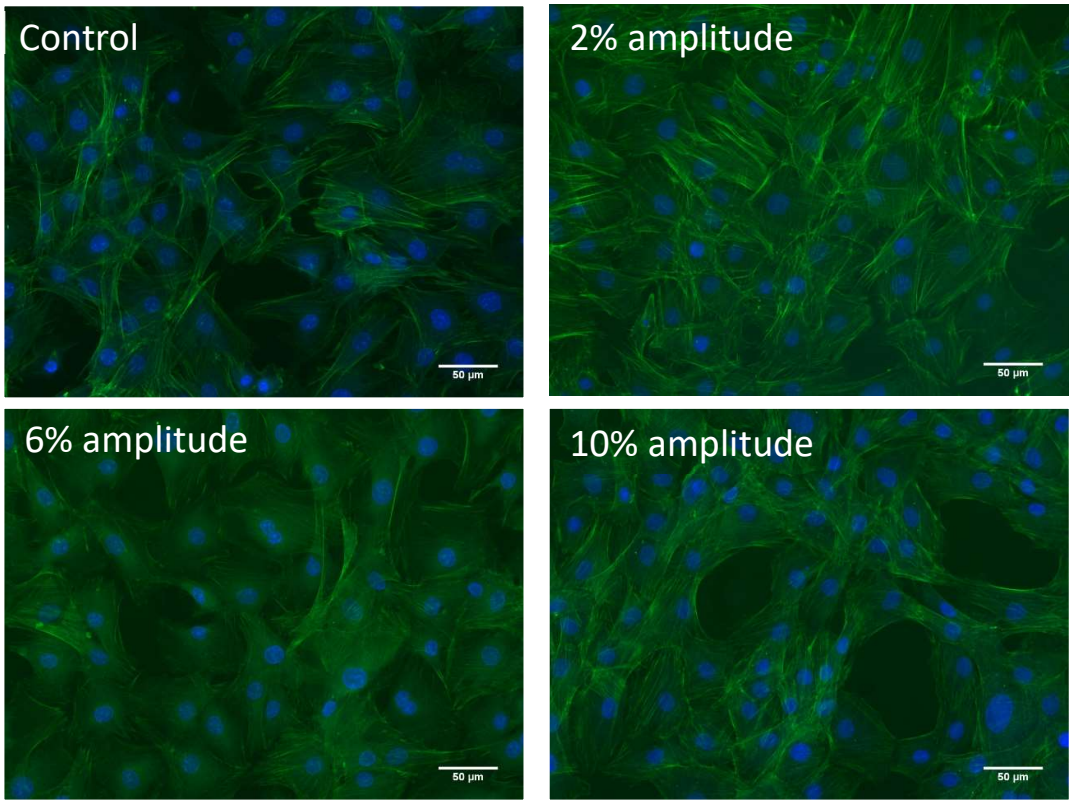

Figure A1.3: RASMC strained for 24 hours at 5% mean strain with varying strain amplitudes. Cells were stained with DAPI (blue) and Phalloidin (green). Cells strained at 2% amplitude show more developed f-actin filaments along the outside of the cells. Scale bars = 50µm

A1.4 Discussion

The results showed that 24 hours of 2% strain amplitude increased the contractile phenotype of RASMC based on gene expression and cytoskeletal morphology. Worth et al. had previously established that cytoskeletal changes can be indicative of a change between contractile and synthetic phenotype.[101] These results were unexpected because it was anticipated that the 2% strain amplitude would be most consistent with a stiffer blood vessel, such as one that is undergoing arteriosclerosis, atherosclerosis or stenting. Typically, under these conditions, VSMC are expected to start proliferating, which is associated with a synthetic phenotype.[67,98,241] However, this phenotype switch model may not fully explain what is happening during vascular disease. As described in Tang et al., the proliferating cells involved in vascular stenosis may, in fact, be a subpopulation of medial cells that are not SMC.[12] In that case, the absence of the shift may be a result of the lack of these cells in the RASMC population measured. Another possible reason for this discrepancy is that the gene expression is being measured after only 24 hours of strain. In

this case, we may be measuring the acute response of the RASMC to strain instead of the long term response that would occur after these cells are exposed to a stiffer environment for days, months or even years that would be seen in vascular disease. One more possibility for this discrepancy is that the strain levels used were based on a study on bovine cells done by Colombo *et al.* [37] Rat blood arteries, coming from smaller mammals, would naturally have a different *in vivo* strain amplitude and rate for a healthy vessel.

While strain amplitude did not seem to effect proliferation rate of RASMC between different strained samples, unstrained samples showed a larger increase in cell number. While this does not match with Colombo *et al.,* who showed that increased strain amplitude showed decreased proliferation, it still does show that unstrained cells show the largest amount of proliferation, which is consistent with Colombo *et al.*[37] It's possible that these inconsistencies with Colombo are based on the differences between bovine cells and rat cells.

Appendix II Flexcell FX-5000 Tension System Strain Calibration

A2.1 Introduction

The Flexcell FX-5000 Tension System is a bioreactor commonly used in tensile testing. It provides equiaxial strain by stretching an elastic membrane down over a post using a vacuum system. However, there is no feedback system within the device to ensure that the strain remains constant if the elastic surface deforms. Previous studies have shown that the Flexcell system can change in strain over time or due to changing the applied frequency.[242] Therefore, it was important to adequately calibrate the Flexcell system before using it in equiaxial strain testing.

A2.2 Methods

New, uncoated Bioflex plates were loaded into the Flexcell FX-5000 Tension System. 6 black dots were applied to the surface of the well in a two by three arrangement using permanent marker (Figure A2.1). Using a USB camera, images were obtained as the Flexcell was strained according to factory settings. A MatLab program was used to localize the six dots and determine the strain between each dot. Between time points, the Flexcell was run at 2-8% 1Hz equiaxial strain as determined by the Flexcell program. Vacuum pressures as measured by the Flexcell device were recorded in order to construct the strain curves necessary for to calibrate the Flexcell device. Two methods of constructing a strain to vacuum pressure curve were attempted. First, strain tests were run at 0-X% 1Hz equiaxial strain as described previously[242] every 24 hours, with X- values of 2, 4, 8, 10 and 16. . Secondly, strain tests were run at 5±X% 1Hz equiaxial strain every 24 hours with X values of 1-5. Polynomial curves were plot to fit to the camera measured strain values versus the vacuum pressure using a polynomial regression to provide a vacuum pressure to strain curve that could be input into the Flexcell software.

Figure A2.1 Flexcell plate well showing 6 dot pattern for strain testing

A2.3 Results

Strain curves were calculated every 24 hours starting at day 0. The curve calculated did not stay consistent over time (Figure A2.2). Additionally. When a 2-8% strain test was plotted on the curve, it did not fit on the curve calculated from the 0-X% strain values.

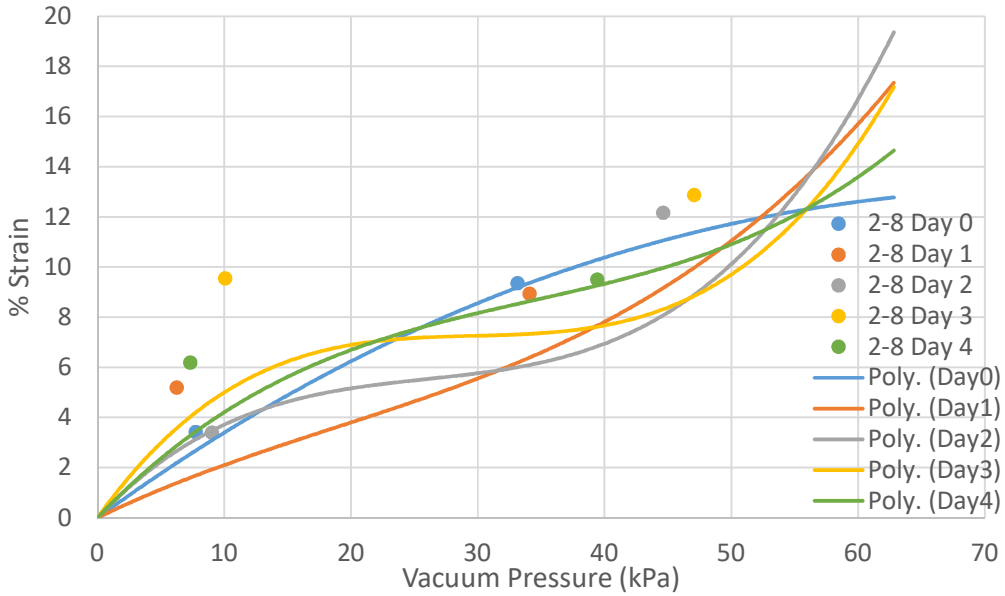

Figure A2.2: Polynomial curves fitted to the 0-X% cyclic strain measurements after 0-4 days of 2-8% strain as determined by Flexcell factory settings. Dots represent measurements from 2-8% strain tests, which do not line up well with the calculated curves.

To compensate for the fact that the vacuum pressure necessary might be different as the membrane relaxes, versus when it is strained, a strain curve was obtained by looking at 5±X% strain data points. These curves also changed over time (Figure A2.3). They also provided curves that would cause errors if input into the Flexcell system as they are not strictly increasing curves.

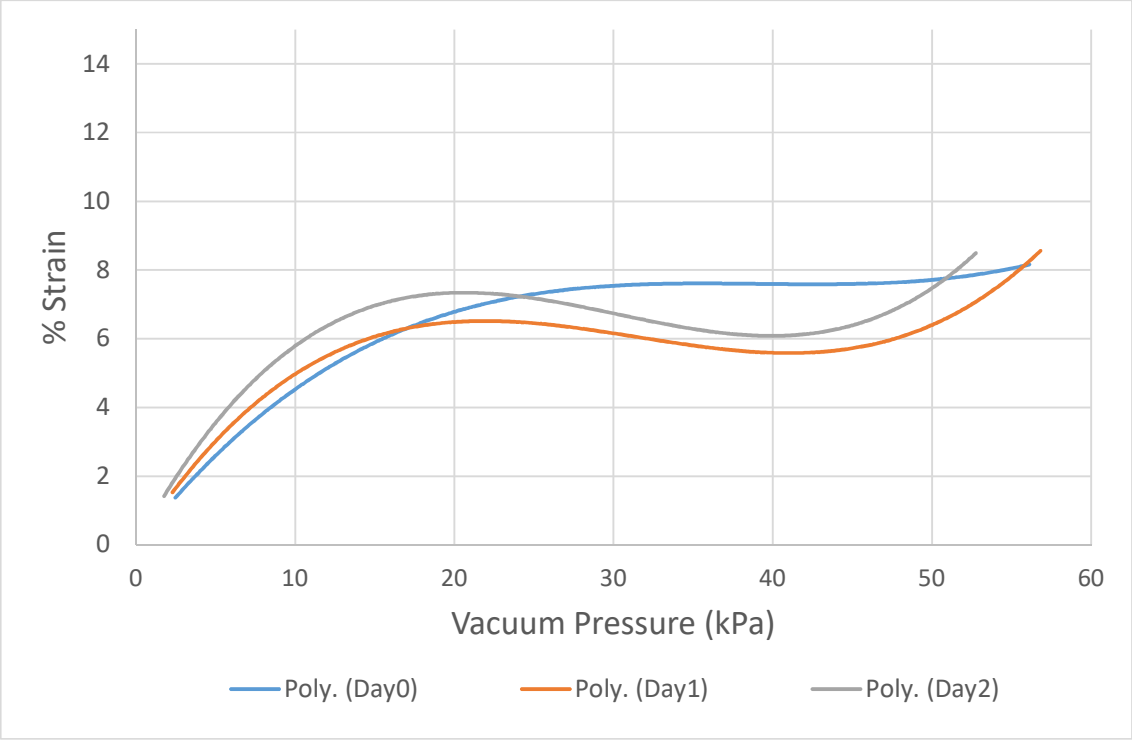

Figure A2.3: Polynomial curves fitted to the 5±X% cyclic strain measurements after 0, 1, or 2 days of 2-8% strain as determined by Flexcell factory settings.

A2.4 Discussion

Ultimately, the only calibration tests that provided curves that were usable by the Flexcell device, were the 0-X% strain tests at Day 0 and Day 1 and the 5±X% strain tests at Day 0. All other curves produced an inflection point in the curve and the Flexcell device could not support a curve that had a negative derivative at any point, as this would mean that a given strain value could pertain to multiple pressure values. Because of this, the equiaxial strain tests were confined to timepoints of 24 hours in order to ensure that the strains desired were the strains provided.

Appendix III Chapter 4 Supplemental Images

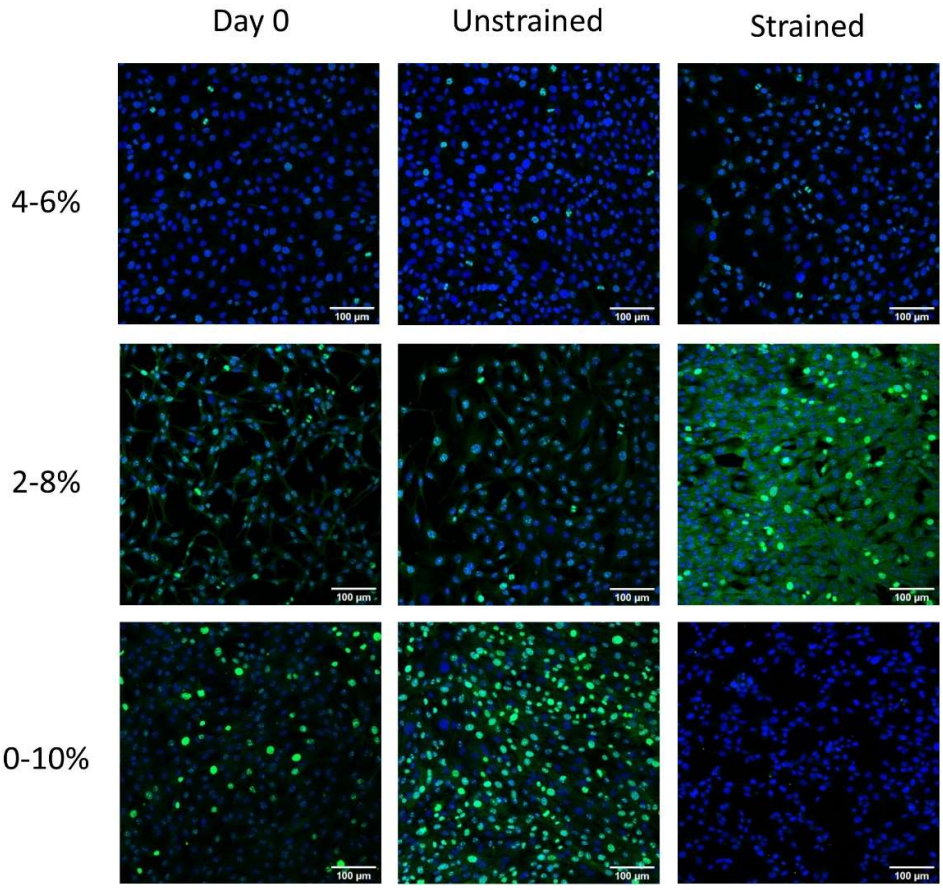

Figure A3.1: Representative images of rMVSC after 0 or 24 hours of no strain or 24 hours of 4-6%, 2-8%, or 0-10% 1 Hz cyclic tensile strain. Blue – DAPI nuclei, Green - Ki67.

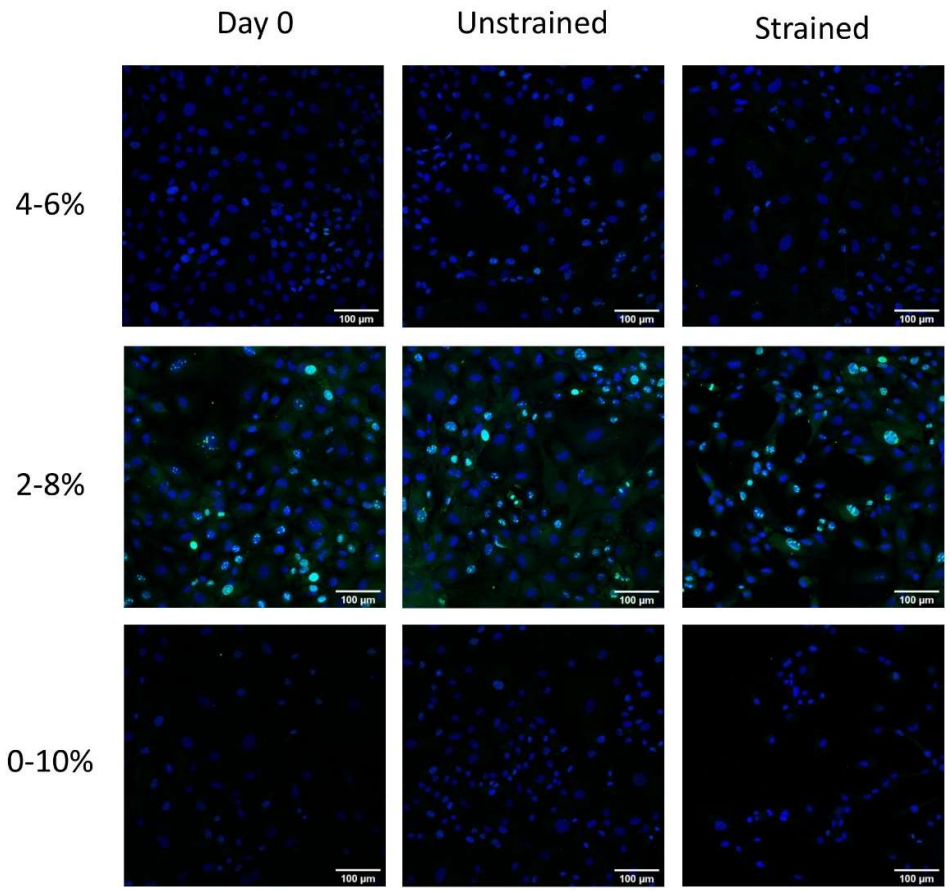

Figure A3.2: Representative images of RASMC after 0 or 24 hours of no strain or 24 hours of 4-6%, 2-8%, or 0-10% 1 Hz cyclic tensile strain. Blue – DAPI nuclei, Green - Ki67.

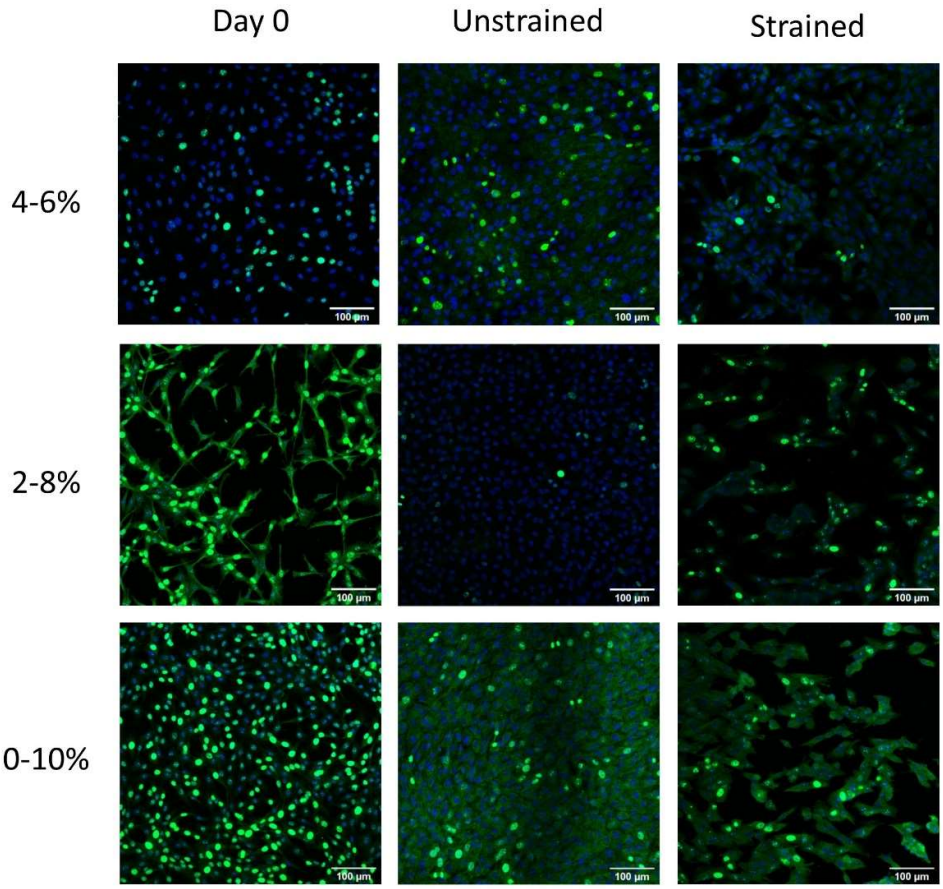

Figure A3.3: Representative images of rMVSC after 0 or 72 hours of no strain or 72 hours of 4-6%, 2-8%, or 0-10% 1 Hz cyclic tensile strain. Blue – DAPI nuclei, Green - Ki67.

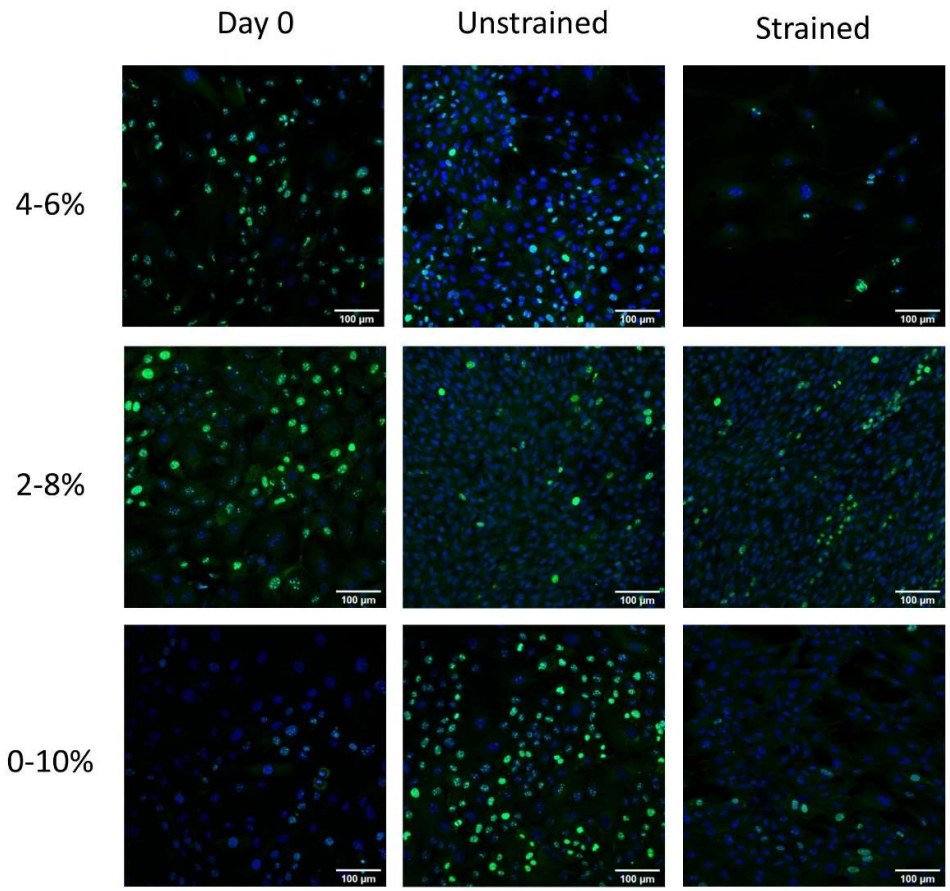

Figure A3.4: Representative images of RASMC after 0 or 72 hours of no strain or 72 hours of 4-6%, 2-8%, or 0-10% 1 Hz cyclic tensile strain. Blue – DAPI nuclei, Green - Ki67.

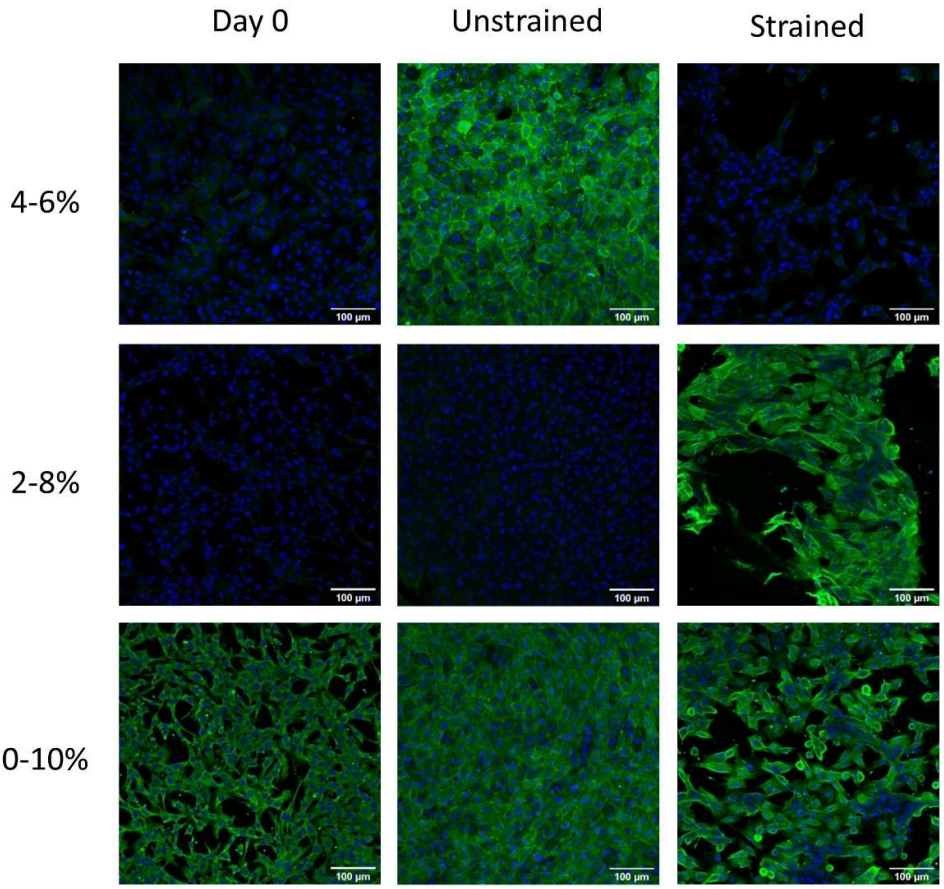

Figure A3.5: Representative images of rMVSC after 0 or 72 hours of no strain or 72 hours of 4-6%, 2-8%, or 0-10% 1 Hz cyclic tensile strain. Blue – DAPI nuclei, Green - αSMA.

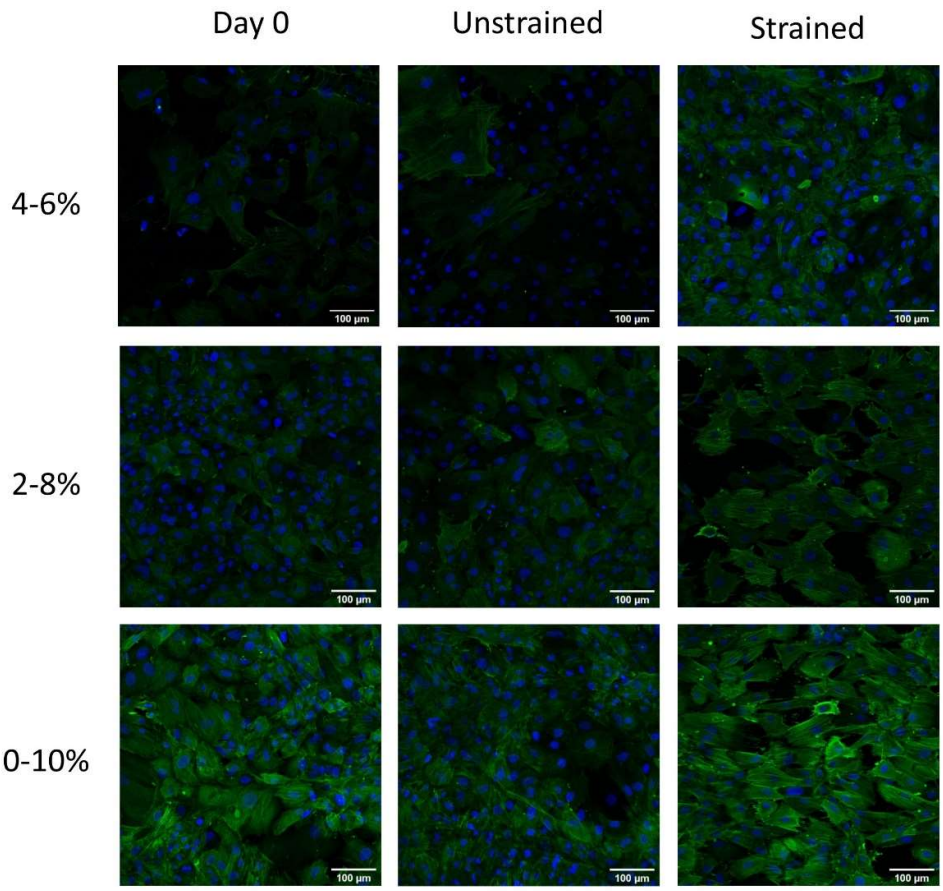

Figure A3.6: Representative images of RASMC after 0 or 72 hours of no strain or 72 hours of 4-6%, 2-8%, or 0-10% 1 Hz cyclic tensile strain. Blue – DAPI nuclei, Green - αSMA.

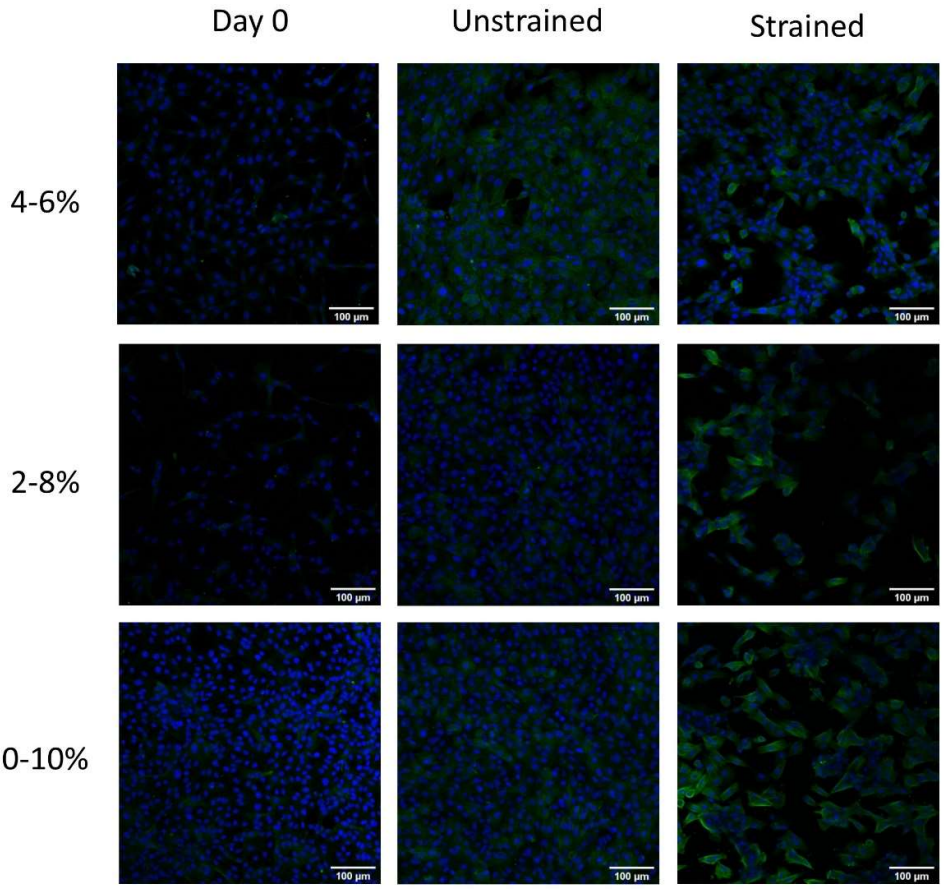

Figure A3.7: Representative images of rMVSC after 0 or 72 hours of no strain or 72 hours of 4-6%, 2-8%, or 0-10% 1 Hz cyclic tensile strain. Blue – DAPI nuclei, Green – Calponin 1.

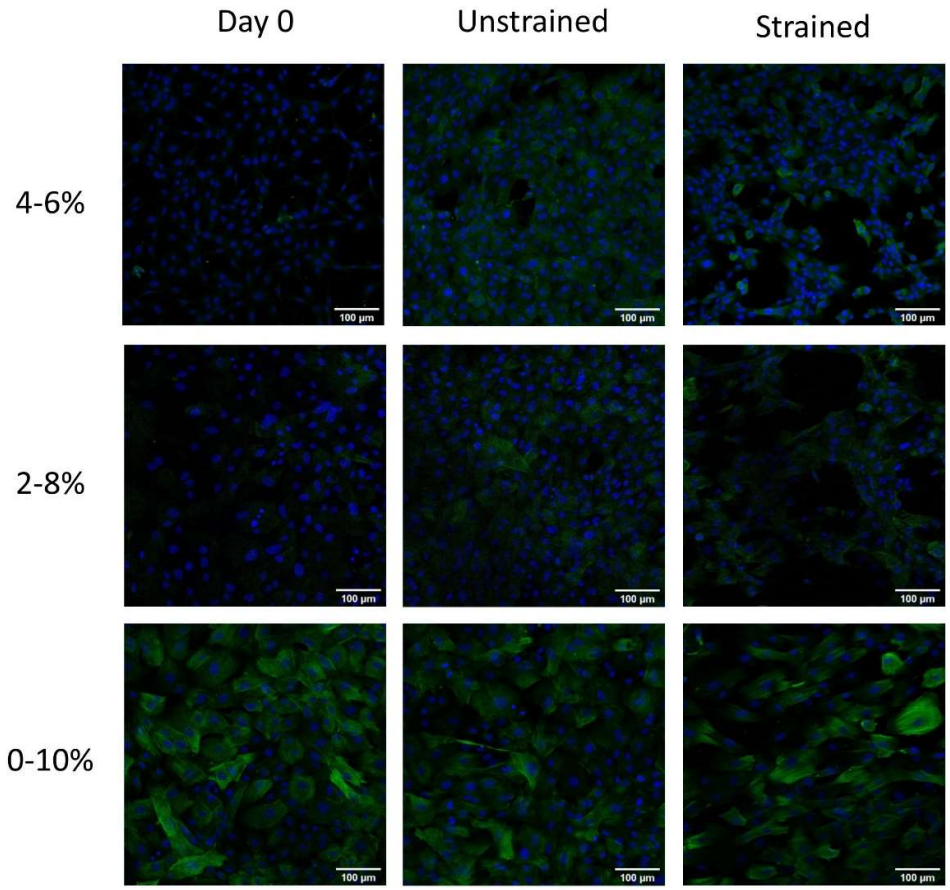

Figure A3.8: Representative images of RASMC after 0 or 72 hours of no strain or 72 hours of 4-6%, 2-8%, or 0-10% 1 Hz cyclic tensile strain. Blue – DAPI nuclei, Green – Calponin 1.

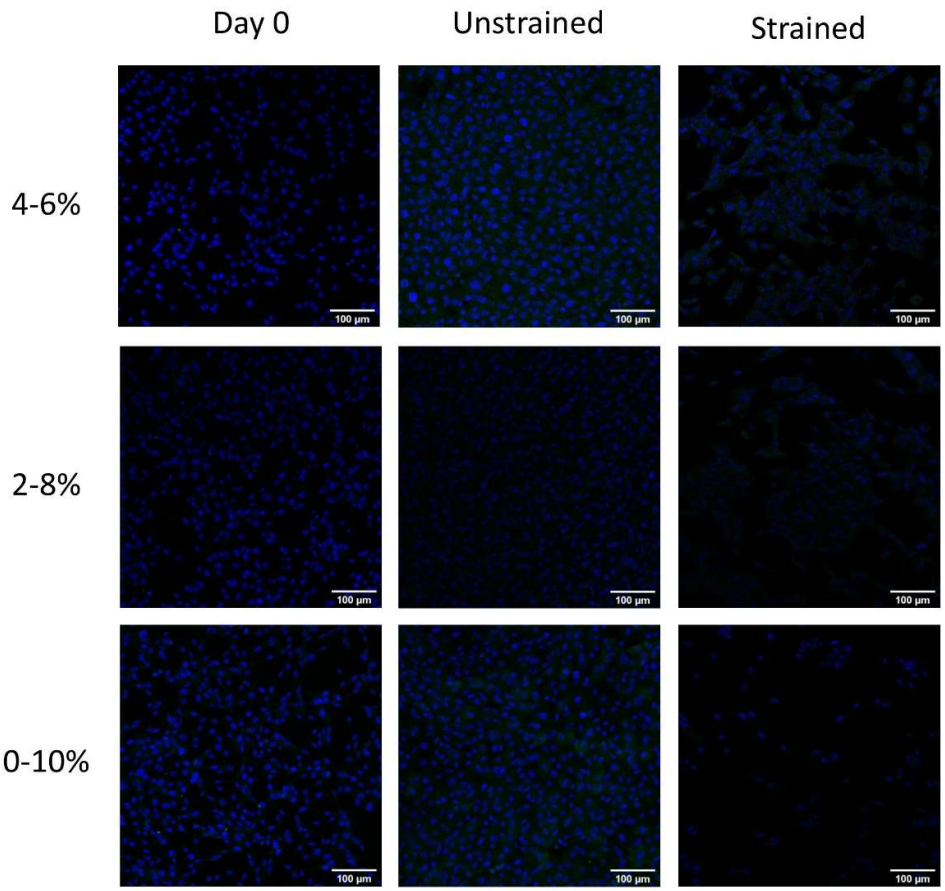

Figure A3.9: Representative images of rMVSC after 0 or 72 hours of no strain or 72 hours of 4-6%, 2-8%, or 0-10% 1 Hz cyclic tensile strain. Blue – DAPI nuclei, Green – SM-MHC.

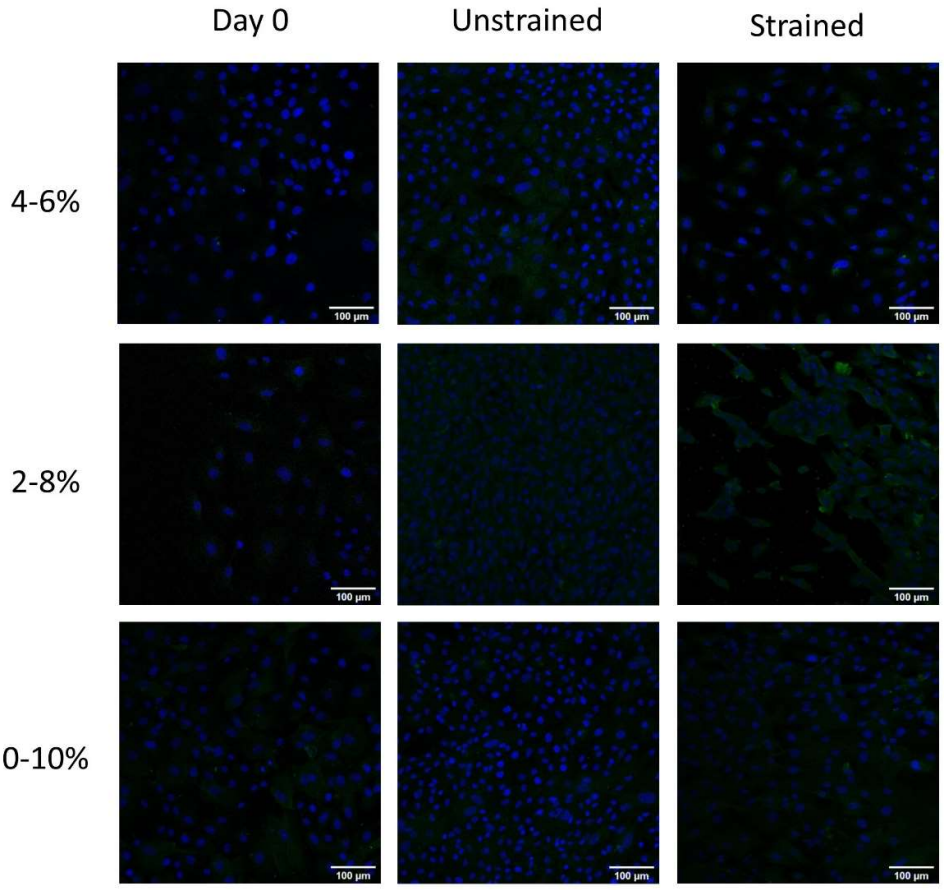

Figure A3.10: Representative images of RASMC after 0 or 72 hours of no strain or 72 hours of 4-6%, 2-8%, or 0-10% 1 Hz cyclic tensile strain. Blue – DAPI nuclei, Green – SM-MHC.

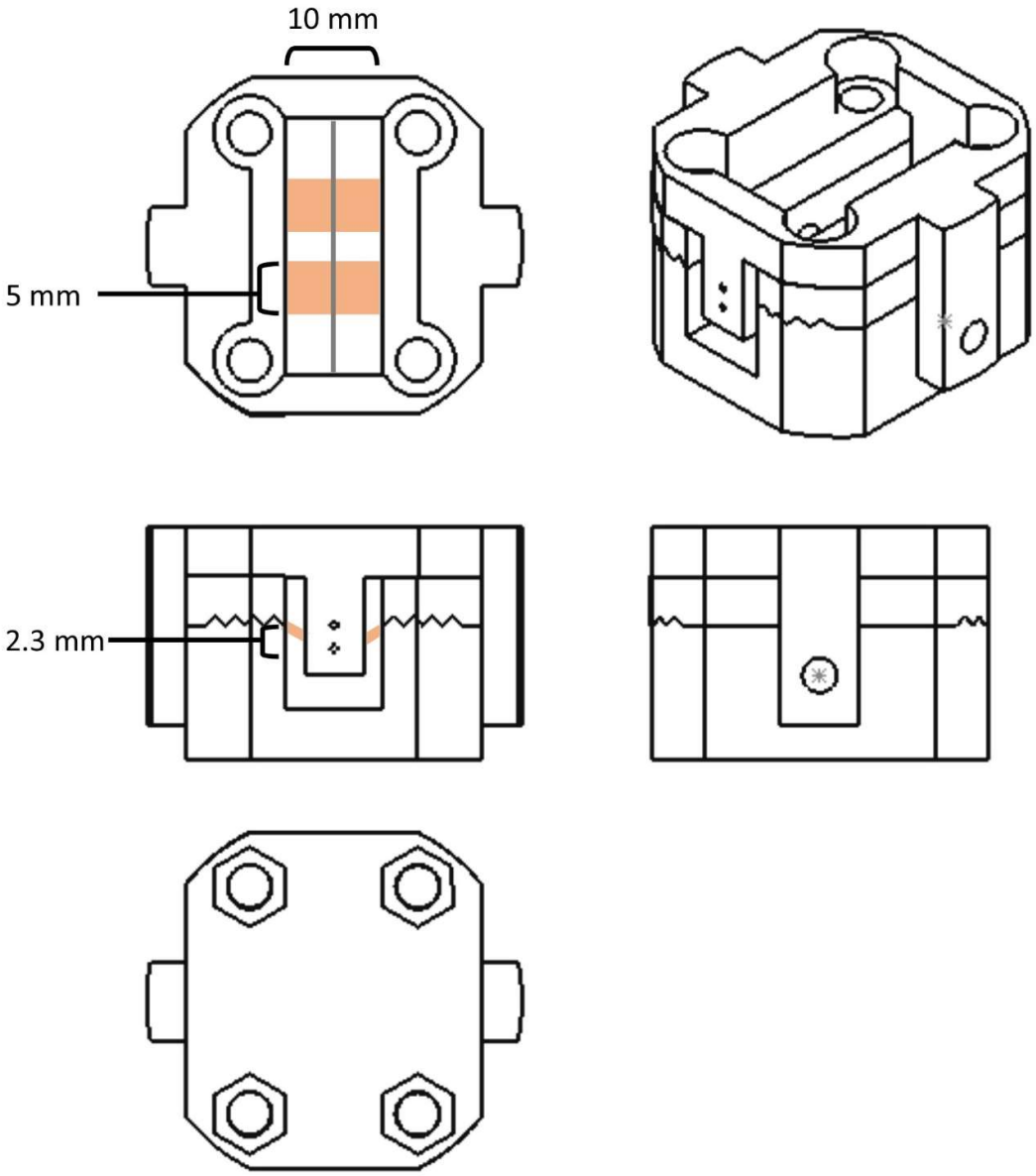

Figure A4.1: Schematic for static stent loading device showing two strips of recellularized tissue in pink and simulated stent strut in grey.

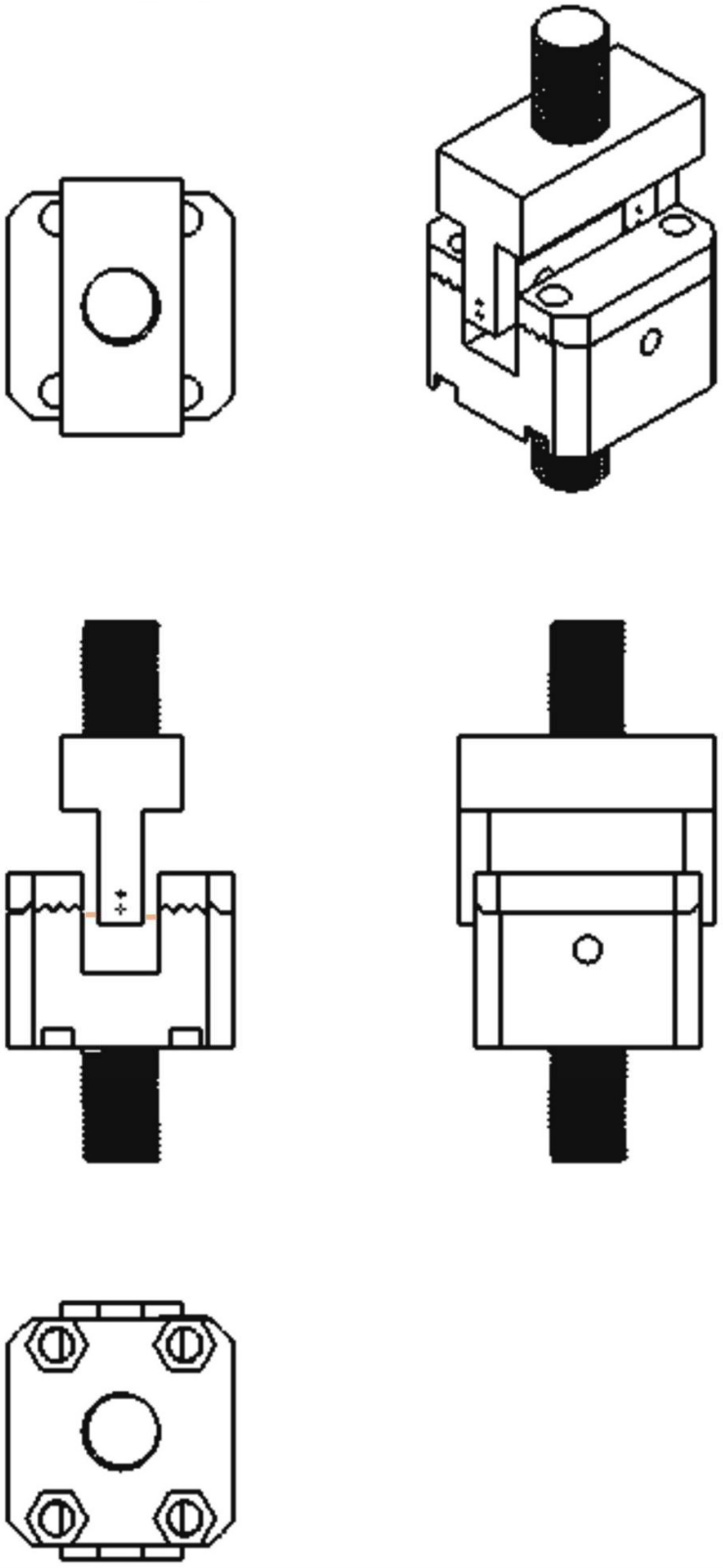

Figure A4.2: Schematic of dynamic stent loading device.

Appendix V Multipotentiality of Freshly Isolated Porcine Carotid Media Digest Cells

A5.1 Introduction

Vascular medial cells are known to be an inhomogeneous population [103]. Tang et al. isolated a population of multipotent vascular stem cells (MVSC) from rat aortic media that differentiated down VSMC, osteogenic, chondrogenic, adipogenic, and neural pathways.[12] MVSC may also be present within cultures of SMC *in vitro.* Most SMC cultures are established from a total digest of arterial media, which would not exclude MVSC. Several studies have shown evidence for MVSC or MVSC derived cells within SMC cultures. Kennedy *et al.* showed that commercially purchased rat, mouse and bovine SMC showed expression of both SMC and MVSC at high passages, but these cells underwent no osteogenic or adipogenic differentiation[106]. Therefore these cells are no longer fully MVSC, but they are likely of MVSC origin. Freshly isolated rat aortic SMC showed smooth muscle markers but not MVSC markers, therefore, it is likely that the Sox10 positive cells are overtaking the population[106]. In order to better understand the properties of the medial population of cells, porcine carotid digest cells (PCDC) were isolated and tested for contractile VSMC and stem cell markers in early and long term culture.

A5.2 Methods

A5.2.1 Cell Isolation and Culture

Porcine carotid digest cells (PCDC) were isolated as follows. Porcine carotid arteries were obtained from porcine necks obtained from an abattoir. Excess tissue was removed from the carotid, and the adventitia was removed from the artery. For digest culture, the carotid was then chopped into no larger than $1mm^3$ and placed in a solution of PBS with calcium and magnesium with 0.7mg/ml collagenase type 1A from Clostridium histolyticum (Sigma) and 0.25mg/ml elastase type III from porcine pancreas (Sigma). The tissue was digested at 37ºC under constant agitation, until totally digested (approximately 7 hours). The resulting cell suspension was spun at 400g and the digestion solution was removed. The cells were resuspended in expansion medium (XPAN) (hgDMEM with Glutamax (Thermo-Scientific) with 10% FBS (Gibco) and 2% penicillin and streptomycin (Thermo-Scientific)) and seeded on Nunclon culture flasks. Cells were cultured in XPAN and

medium was changed every 3-4 days. Cells were used at p5 (Early Passage) and p23 (Late Passage).

A5.2.2 Immunocytochemistry

Glass coverslips were seeded at 11,000 cells/cm^2 and allowed to culture for 4 days before fixation in order to assess cell phenotype. Cells were fixed in 10% formalin for 10 minutes and then rinsed twice with PBS. Cells were blocked and permeabilized in 5% BSA and 0.2% Triton X-100 for 30 minutes at room temperature. Primary antibody was used in PBS with 0.5% BSA and 0.2% Triton X-100 overnight at 4ºC at a concentration of 1:50 for Myosin11 (ab53219), and 1:200 for Calponin (ab46794) and SM22α (ab14106). Cells were incubated in secondary antibody (ab150073) 1:1000 in PBS with 0.5% BSA and 0.2% Triton X-100 for 1 hour at room temperature. Cells were then incubated in DAPI 1:1000 in PBS for 30 minutes at room temperature. Cells were rinsed in PBS between each incubation step. Cells were imaged using an Olympus IX83 epifluorescent inverted microscope using CellSens software.

A5.2.3 Differentiation Assay

Cells were seeded in 6 well plates at a density of 1x10^6 cells/well and allowed to grow to 80% confluence in XPAN. At this point, cells were cultured either in differentiation medium or XPAN for 21 days. Osteogenic differentiation medium (ODM) was composed of XPAN with 10nM dexamethasone, 10mM β-glycerol phosphate and 0.05mM ascorbic acid. Adipogenic differentiation medium (ADM) was composed of XPAN with 100nM dexamethasone, 0.5mM IBMX and 50µM indomethacin. Cells were then fixed in 10% formalin for 10 minutes. Osteogenesis was determined using Alizarin Red staining, and Adipogenesis was determined using Oil Red O staining.

A5.3 Results

Two passages of the same initial population of PCDC were used, p5 (early passage) or p23 (late passage). The phenotype of the populations was assessed for both differentiation potential and smooth muscle cell phenotype. Osteogenic and adipogenic differentiation potential was determined for both populations, as shown in Figure A5.1. After 21 days of culture in ODM, early passage cells showed high levels of calcium under Alizarin Red staining, while in XPAN medium they were still showing spontaneous osteogenic differentiation in the ridges of the over confluent culture. Late passage cells were showed a lower level of osteogenic differentiation in ODM, with no ridge formation or spontaneous

differentiation. After 21 days in ADM, early passage cells showed some adipogenic differentiation. They also showed some spontaneous differentiation. Late passage cells were still showing both induced and spontaneous adipogenic differentiation, see Figure A5.1.

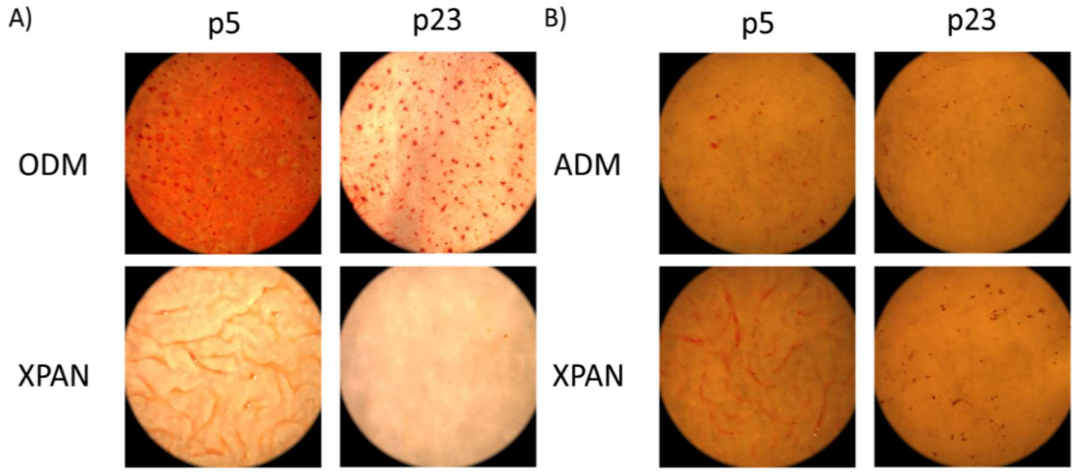

Figure A5.1: Digest cells after 21 days of differentiation. Cells at p5 show a greater level of osteogenic differentiation, and some spontaneous osteogenic differentiation, while p23 cells show some induced osteogenic differentiation, but no spontaneous differentiation. Cells at p5 show some induced and spontaneous adipogenic differentiation, while cells at p23 show less adipogenic differentiation.

Additionally, both populations of cells were also assessed for their expression of smooth muscle cell markers (Figure A5.2). For calponin 1, the cell population did not express it homogeneously at either passage (Figure A5.2A, B). More cells at early passage were calponin positive than late passage cells.

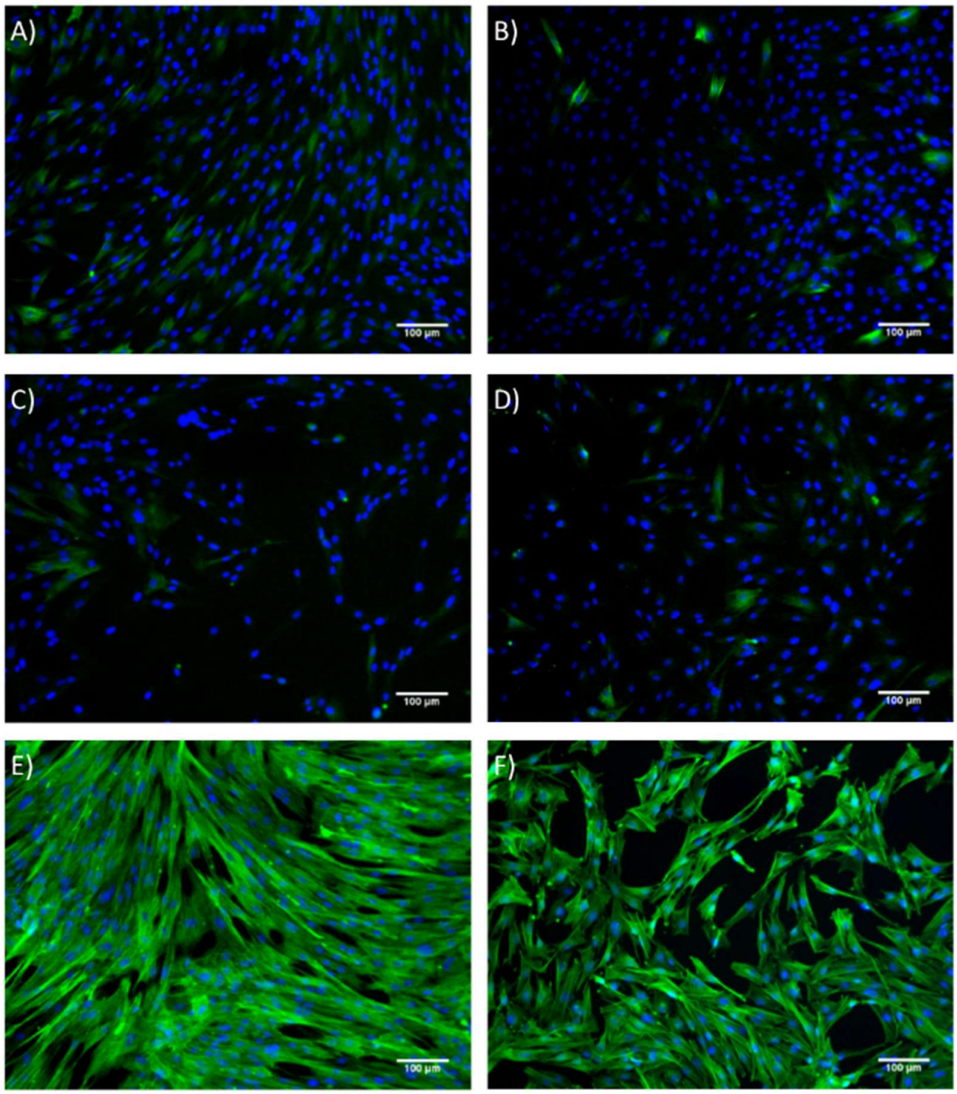

Figure A5.2: Smooth muscle markers in digest cells at low passage (A, C, E) vs high passage (B, D, F). Calponin 1 (A, B) shows slightly more cells expressing it at p5. Myosin 11 (C, D) shows a few cells expressing it at both passages. Both cell populations stain positive for SM22α (E, F). Scale bars = 100µm

Myosin was also not expressed homogeneously (Figure A5.2C, D). Both early and late passage cells showed a few positive cells. Both early and late passage cells stained positive for SM22α (Figure A5.2E, F). Quantitative cell counts from one slide each confirm that low passage cells express greater amounts of myosin 11 and calponin 1, while SM22α and Ki67 levels are similar between both passages (Figure A5.3).

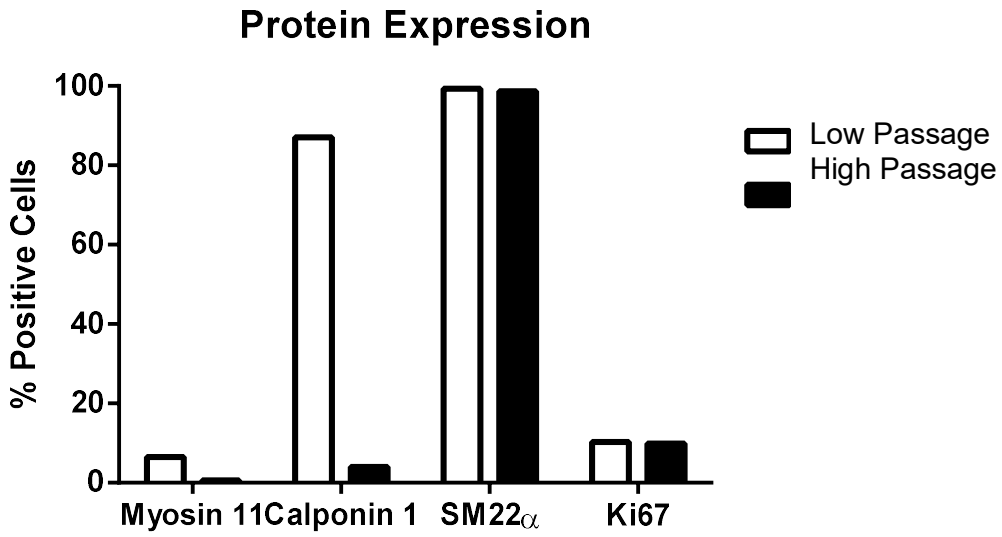

Figure A5.3: Quantification of low passage versus high passage immunostaining. Low passage cells show higher levels of Myosin 11 and Calponin 1, but not SM22α or Ki67.

A5.4 Discussion

This study shows that the multipotency observed in the porcine carotid vascular cells decreases as the cells are cultured, yet there is also a decrease in the number of cells expressing contractile markers, which suggests that these cells are becoming more differentiated but not towards contractile smooth muscle cells. Because total enzymatic digestion is typically used for isolating SMC, the differentiation potential of these cells may not at first seem congruous with cells from a medial digest. However, Tintut *et al.* described a population of calcifying vascular cells (CVC) derived from the media of a bovine aorta.[243] Like the cells isolated in this paper, CVC formed ridges in which the cells spontaneously produced calcium.[243] Zaniboni *et al.* also produced a population of medial cells from a partial medial digest that show multipotentiality.[107,108] While Zaniboni *et al.* described their population as MVSC, they did not test for MVSC markers such as Sox10 or S100β. They may have just found a similar population to the PCDC that we isolated.

This cell population at both early and late passage needs to be further characterized in order to better understand the phenotype of these cells. These cells should be assessed for myogenic differentiation potential. Furthermore cells could be further characterized by a full flow cytometric assessment of surface markers to better compare these cells to MVSC.

Additionally, in order to understand when the cells develop their differentiation characteristics, it would be useful to assess the phenotype of a group of digested medial cells immediately after digest, and then assess them as they undergo culture.

References

1 Benjamin, E. J. *et al.* Heart Disease and Stroke Statistics-2019 Update: A Report From the American Heart Association. *Circulation* **139**, e56-e528, doi:10.1161/cir.0000000000000659 (2019).

2 Auerbach, D., Maeda, J. & Steiner, C. Hospital Stays with Cardiac Stents, 2009. *Agency for Healthcare Research and Quality* **HCUP Statistical Brief #128** (2012).

3 Byrne, R. A., Joner, M. & Kastrati, A. Stent thrombosis and restenosis: what have we learned and where are we going? The Andreas Gruntzig Lecture ESC 2014. *Eur Heart J* **36**, 3320-3331, doi:10.1093/eurheartj/ehv511 (2015).

4 Kukreja, N. *et al.* The risk of stent thrombosis in patients with acute coronary syndromes treated with bare-metal and drug-eluting stents. *JACC Cardiovasc Interv* **2**, 534-541, doi:10.1016/j.jcin.2009.04.003 (2009).

5 Holmes, D. R., Camrud, A. R., Jorgenson, M. A., Edwards, W. D. & Schwartz, R. S. Polymeric stenting in the porcine coronary artery model: differential outcome of exogenous fibrin sleeves versus polyurethane-coated stents. *J Am Coll Cardiol* **24**, 525-531 (1994).

6 Zahedmanesh, H. & Lally, C. Determination of the influence of stent strut thickness using the finite element method: implications for vascular injury and in-stent restenosis. *Med Biol Eng Comput* **47**, 385-393, doi:10.1007/s11517-009-0432-5 (2009).

7 Nakano, M. *et al.* Human autopsy study of drug-eluting stents restenosis: histomorphological predictors and neointimal characteristics. *Eur Heart J* **7**, 3304-3313 (2013).

8 Holzapfel, G. A. in *Collagen* 285-324 (Springer, 2008).

9 Holzapfel, G. A. & Gasser, T. C. A new constitutive framework for arterial wall mechanics and a comparative study of material models. *Journal of Elasticity* (2000).

10 Khilji, H. In-Vitro Effects of Intravascular Stenting on Collagen Fiber Reorientation and Tissue Remodeling. *(Master's thesis)* (2017).

11 Ghazanfari, S. *et al.* In Vivo Collagen Remodeling in the Vascular Wall of Decellularized Stented Tissue-Engineered Heart Valves. *Tissue Eng Part A* **21**, 2206-2215, doi:10.1089/ten.TEA.2014.0417 (2015).

12 Tang, Z. *et al.* Differentiation of multipotent vascular stem cells contributes to vascular diseases. *Nat Commun* **3**, 875, doi:10.1038/ncomms1867 (2012).

13 Zhu, J. H. *et al.* Cyclic stretch stimulates vascular smooth muscle cell alignment by redox-dependent activation of Notch3. *Am J Physiol Heart Circ Physiol* **300**, H1770-1780, doi:10.1152/ajpheart.00535.2010 (2011).

14 Montenegro, M. F. *et al.* Nox4-dependent activation of cofilin mediates VSMC reorientation in response to cyclic stretching. *Free Radic Biol Med* **85**, 288-294, doi:10.1016/j.freeradbiomed.2015.05.011 (2015).

15 Li, W., Chen, Q., Mills, I. & Sumpio, B. E. Involvement of S6 kinase and p38 mitogen activated protein kinase pathways in strain-induced alignment and proliferation of bovine aortic smooth muscle cells. *J Cell Physiol* **195**, 202-209, doi:10.1002/jcp.10230 (2003).

16 Rodriguez, A. I. *et al.* MEF2B-Nox1 signaling is critical for stretch-induced phenotypic modulation of vascular smooth muscle cells. *Arterioscler Thromb Vasc Biol* **35**, 430-438, doi:10.1161/ATVBAHA.114.304936 (2015).

17 Houtchens, G. R., Foster, M. D., Desai, T. A., Morgan, E. F. & Wong, J. Y. Combined effects of microtopography and cyclic strain on vascular smooth muscle cell orientation. *J Biomech* **41**, 762-769, doi:10.1016/j.jbiomech.2007.11.027 (2008).

18 Kurpinski, K., Park, J., Thakar, R. G. & Li, S. Regulation of vascular smooth muscle cells and mesenchymal stem cells by mechanical strain. *Mol Cell Biomech* **3**, 21-34 (2006).

19 Fitzpatrick, E. Stem Cell Antigen 1 Positive Resident Vascular Stem Cells and their Contribution to Vascular Disease. *(PhD Thesis)* (2017).
20 Wagenseil, J. E. & Mecham, R. P. Vascular extracellular matrix and arterial mechanics. *Physiol Rev* **89**, 957-989, doi:10.1152/physrev.00041.2008 (2009).
21 in *Basic Physiology for Anaesthetists* (eds Christopher Huang, David Chambers, & Gareth Matthews) 155-157 (Cambridge University Press, 2019).
22 Roach, M. R. & Burton, A. C. The reason for the shape of the distensibility curves of arteries. *Canadian journal of biochemistry and physiology* **35**, 681-690 (1957).
23 Guo, X., Kono, Y., Mattrey, R. & Kassab, G. S. Morphometry and strain distribution of the C57BL/6 mouse aorta. *Am J Physiol Heart Circ Physiol* **283**, H1829-1837, doi:10.1152/ajpheart.00224.2002 (2002).
24 Park, H. E., Cho, G. Y., Kim, H. K., Kim, Y. J. & Sohn, D. W. Validation of circumferential carotid artery strain as a screening tool for subclinical atherosclerosis. *J Atheroscler Thromb* **19**, 349-356, doi:10.5551/jat.10686 (2012).
25 Karimi, A., Navidbakhsh, M., Shojaei, A. & Faghihi, S. Measurement of the uniaxial mechanical properties of healthy and atherosclerotic human coronary arteries. *Mater Sci Eng C Mater Biol Appl* **33**, 2550-2554, doi:10.1016/j.msec.2013.02.016 (2013).
26 Teng, Z. *et al.* Material properties of components in human carotid atherosclerotic plaques: a uniaxial extension study. *Acta Biomater* **10**, 5055-5063, doi:10.1016/j.actbio.2014.09.001 (2014).
27 He, C. M. & Roach, M. R. The composition and mechanical properties of abdominal aortic aneurysms. *J Vasc Surg* **20**, 6-13 (1994).
28 Vorp, D. A. *et al.* Wall strength and stiffness of aneurysmal and nonaneurysmal abdominal aorta. *Ann N Y Acad Sci* **800**, 274-276 (1996).
29 Chow, M. J., Mondonedo, J. R., Johnson, V. M. & Zhang, Y. Progressive structural and biomechanical changes in elastin degraded aorta. *Biomech Model Mechanobiol* **12**, 361-372, doi:10.1007/s10237-012-0404-9 (2013).
30 Ghazanfari, S. *et al.* A comparative analysis of the collagen architecture in the carotid artery: second harmonic generation versus diffusion tensor imaging. *Biochem Biophys Res Commun* **426**, 54-58, doi:10.1016/j.bbrc.2012.08.031 (2012).
31 Sugita, S. & Matsumoto, T. Heterogeneity of deformation of aortic wall at the microscopic level: contribution of heterogeneous distribution of collagen fibers in the wall. *Biomed Mater Eng* **23**, 447-461, doi:10.3233/BME-130771 (2013).
32 van Varik, B. J. *et al.* Mechanisms of arterial remodeling: lessons from genetic diseases. *Frontiers in genetics* **3**, 290, doi:10.3389/fgene.2012.00290 (2012).
33 Watson, S. R. *et al.* Comparison of Aortic Collagen Fiber Angle Distribution in Mouse Models of Atherosclerosis Using Second-Harmonic Generation (SHG) Microscopy. *Microsc Microanal* **22**, 55-62, doi:10.1017/S1431927615015585 (2016).
34 Pagiatakis, C., Galaz, R., Tardif, J. C. & Mongrain, R. A comparison between the principal stress direction and collagen fiber orientation in coronary atherosclerotic plaque fibrous caps. *Med Biol Eng Comput* **53**, 545-555, doi:10.1007/s11517-015-1257-z (2015).
35 Pahwa, R. & Jialal, I. in *StatPearls* (StatPearls Publishing

StatPearls Publishing LLC., 2019).
36 Ormiston, J. A. & Webster, M. W. Of Stents and Scaffolds: Trial Data and the Real World. *Circulation. Cardiovascular interventions* **9**, doi:10.1161/circinterventions.116.004249 (2016).
37 Colombo, A., Guha, S., Mackle, J. N., Cahill, P. A. & Lally, C. Cyclic strain amplitude dictates the growth response of vascular smooth muscle cells in vitro: role in in-stent restenosis and inhibition with a sirolimus drug-eluting stent. *Biomech Model Mechanobiol* **12**, 671-683, doi:10.1007/s10237-012-0433-4 (2013).

38 Vernhet, H. *et al.* Changes in wall mechanics after endovascular stenting in the rabbit aorta: comparison of three stent designs. *AJR. American journal of roentgenology* **176**, 803-807, doi:10.2214/ajr.176.3.1760803 (2001).

39 Garasic, J. M. *et al.* Stent and artery geometry determine intimal thickening independent of arterial injury. *Circulation* **101**, 812-818 (2000).

40 Lally, C., Dolan, F. & Prendergast, P. J. Cardiovascular stent design and vessel stresses: a finite element analysis. *J Biomech* **38**, 1574-1581, doi:10.1016/j.jbiomech.2004.07.022 (2005).

41 Rolland, P. H. *et al.* Hemodynamics and wall mechanics after stent placement in swine iliac arteries: comparative results from six stent designs. *Radiology* **213**, 229-246, doi:10.1148/radiology.213.1.r99oc26229 (1999).

42 Bedoya, J., Meyer, C. A., Timmins, L. H., Moreno, M. R. & Moore, J. E. Effects of stent design parameters on normal artery wall mechanics. *J Biomech Eng* **128**, 757-765, doi:10.1115/1.2246236 (2006).

43 Timmins, L. H., Meyer, C. A., Moreno, M. R. & Moore, J. E., Jr. Mechanical modeling of stents deployed in tapered arteries. *Ann Biomed Eng* **36**, 2042-2050, doi:10.1007/s10439-008-9582-0 (2008).

44 Ghazanfari, S., Driessen-Mol, A., Hoerstrup, S. P., Baaijens, F. P. & Bouten, C. V. Collagen Matrix Remodeling in Stented Pulmonary Arteries after Transapical Heart Valve Replacement. *Cells Tissues Organs* **201**, 159-169, doi:10.1159/000442521 (2016).

45 Nolan, D., Khilji, H. & Lally, C. in *8th World Congress of Biomechanics* (Dublin, Ireland, 2018).

46 Skowasch, D. *et al.* Presence of bone-marrow- and neural-crest-derived cells in intimal hyperplasia at the time of clinical in-stent restenosis. *Cardiovasc Res* **60**, 684-691 (2003).

47 Carter, A. J. *et al.* Morphologic characteristics of lesion formation and time course of smooth muscle cell proliferation in a porcine proliferative restenosis model. *J Am Coll Cardiol* **24**, 1398-1405, doi:10.1016/0735-1097(94)90126-0 (1994).

48 Timmins, L. H., Miller, M. W., Clubb, F. J., Jr. & Moore, J. E., Jr. Increased artery wall stress post-stenting leads to greater intimal thickening. *Lab Invest* **91**, 955-967, doi:10.1038/labinvest.2011.57 (2011).

49 Park, J. K. *et al.* Stent linker effect in a porcine coronary restenosis model. *J Mech Behav Biomed Mater* **53**, 68-77, doi:10.1016/j.jmbbm.2015.08.014 (2016).

50 Sullivan, T. M. *et al.* Effect of endovascular stent strut geometry on vascular injury, myointimal hyperplasia, and restenosis. *J Vasc Surg* **36**, 143-149, doi:10.1067/mva.2002.122878 (2002).

51 Freeman, J. W., Snowhill, P. B. & Nosher, J. L. A link between stent radial forces and vascular wall remodeling: the discovery of an optimal stent radial force for minimal vessel restenosis. *Connect Tissue Res* **51**, 314-326, doi:10.3109/03008200903329771 (2010).

52 Fontaine, A. B. *et al.* Stent-induced intimal hyperplasia: are there fundamental differences between flexible and rigid stent designs? *Journal of vascular and interventional radiology : JVIR* **5**, 739-744, doi:10.1016/s1051-0443(94)71593-1 (1994).

53 Chen, H. Y. *et al.* Mis-sizing of stent promotes intimal hyperplasia: impact of endothelial shear and intramural stress. *Am J Physiol Heart Circ Physiol* **301**, H2254-2263, doi:10.1152/ajpheart.00240.2011 (2011).

54 Briguori, C. *et al.* In-stent restenosis in small coronary arteries: impact of strut thickness. *J Am Coll Cardiol* **40**, 403-409, doi:10.1016/s0735-1097(02)01989-7 (2002).

55 Chhabra, L., Zain, M. A. & Siddiqui, W. J. in *StatPearls* (StatPearls Publishing StatPearls Publishing LLC., 2019).

56 Bennett, M. R., Sinha, S. & Owens, G. K. Vascular Smooth Muscle Cells in Atherosclerosis. *Circ Res* **118**, 692-702, doi:10.1161/CIRCRESAHA.115.306361 (2016).

57 Yuan, F. *et al.* Contribution of Vascular Cells to Neointimal Formation. *PLoS One* **12**, e0168914, doi:10.1371/journal.pone.0168914 (2017).

58 Kramann, R. *et al.* Adventitial MSC-like Cells Are Progenitors of Vascular Smooth Muscle Cells and Drive Vascular Calcification in Chronic Kidney Disease. *Cell Stem Cell* **19**, 628-642, doi:10.1016/j.stem.2016.08.001 (2016).

59 Wan, M. *et al.* Injury-activated transforming growth factor beta controls mobilization of mesenchymal stem cells for tissue remodeling. *Stem Cells* **30**, 2498-2511, doi:10.1002/stem.1208 (2012).

60 Cooley, B. C. *et al.* TGF-beta signaling mediates endothelial-to-mesenchymal transition (EndMT) during vein graft remodeling. *Sci Transl Med* **6**, 227ra234, doi:10.1126/scitranslmed.3006927 (2014).

61 Nemenoff, R. A. *et al.* SDF-1alpha induction in mature smooth muscle cells by inactivation of PTEN is a critical mediator of exacerbated injury-induced neointima formation. *Arterioscler Thromb Vasc Biol* **31**, 1300-1308, doi:10.1161/ATVBAHA.111.223701 (2011).

62 Herring, B. P., Hoggatt, A. M., Burlak, C. & Offermanns, S. Previously differentiated medial vascular smooth muscle cells contribute to neointima formation following vascular injury. *Vasc Cell* **6**, 21, doi:10.1186/2045-824X-6-21 (2014).

63 Chappell, J. *et al.* Extensive Proliferation of a Subset of Differentiated, yet Plastic, Medial Vascular Smooth Muscle Cells Contributes to Neointimal Formation in Mouse Injury and Atherosclerosis Models. *Circ Res* **119**, 1313-1323, doi:10.1161/CIRCRESAHA.116.309799 (2016).

64 Majesky, M. W. Adventitia and perivascular cells. *Arterioscler Thromb Vasc Biol* **35**, e31-35, doi:10.1161/ATVBAHA.115.306088 (2015).

65 Psaltis, P. J. & Simari, R. D. Vascular wall progenitor cells in health and disease. *Circ Res* **116**, 1392-1412, doi:10.1161/CIRCRESAHA.116.305368 (2015).

66 Owens, G. K. Regulation of differentiation of vascular smooth muscle cells. *Physiol Rev* **75**, 487-517, doi:10.1152/physrev.1995.75.3.487 (1995).

67 Rzucidlo, E. M., Martin, K. A. & Powell, R. J. Regulation of vascular smooth muscle cell differentiation. *J Vasc Surg* **45 Suppl A**, A25-32, doi:10.1016/j.jvs.2007.03.001 (2007).

68 Clowes, A. W. & Schwartz, S. M. Significance of quiescent smooth muscle migration in the injured rat carotid artery. *Circ Res* **56**, 139-145 (1985).

69 Newby, A. C. An overview of the vascular response to injury: a tribute to the late Russell Ross. *Toxicol Lett* **112-113**, 519-529 (2000).

70 Feil, S. *et al.* Transdifferentiation of vascular smooth muscle cells to macrophage-like cells during atherogenesis. *Circ Res* **115**, 662-667, doi:10.1161/CIRCRESAHA.115.304634 (2014).

71 Speer, M. Y. *et al.* Smooth muscle cells give rise to osteochondrogenic precursors and chondrocytes in calcifying arteries. *Circ Res* **104**, 733-741, doi:10.1161/CIRCRESAHA.108.183053 (2009).

72 Gomez, D., Shankman, L. S., Nguyen, A. T. & Owens, G. K. Detection of histone modifications at specific gene loci in single cells in histological sections. *Nat Methods* **10**, 171-177, doi:10.1038/nmeth.2332 (2013).

73 Owens, G. K., Kumar, M. S. & Wamhoff, B. R. Molecular regulation of vascular smooth muscle cell differentiation in development and disease. *Physiol Rev* **84**, 767-801, doi:10.1152/physrev.00041.2003 (2004).

74 Arimura, C. *et al.* Primary structure of chicken skeletal muscle and fibroblast alpha-actinins deduced from cDNA sequences. *Eur J Biochem* **177**, 649-655 (1988).

75 Babij, P., Kelly, C. & Periasamy, M. Characterization of a mammalian smooth muscle myosin heavy-chain gene: complete nucleotide and protein coding sequence and analysis of the 5' end of the gene. *Proc Natl Acad Sci U S A* **88**, 10676-10680 (1991).

76 Frid, M. G. *et al.* Myosin heavy-chain isoform composition and distribution in developing and adult human aortic smooth muscle. *J Vasc Res* **30**, 279-292 (1993).

77 Ferns, G. A. *et al.* Inhibition of neointimal smooth muscle accumulation after angioplasty by an antibody to PDGF. *Science* **253**, 1129-1132 (1991).

78 Miano, J. M., Cserjesi, P., Ligon, K. L., Periasamy, M. & Olson, E. N. Smooth muscle myosin heavy chain exclusively marks the smooth muscle lineage during mouse embryogenesis. *Circ Res* **75**, 803-812 (1994).

79 Duband, J. L., Gimona, M., Scatena, M., Sartore, S. & Small, J. V. Calponin and SM 22 as differentiation markers of smooth muscle: spatiotemporal distribution during avian embryonic development. *Differentiation* **55**, 1-11 (1993).

80 Miano, J. M., Carlson, M. J., Spencer, J. A. & Misra, R. P. Serum response factor-dependent regulation of the smooth muscle calponin gene. *J Biol Chem* **275**, 9814-9822 (2000).

81 Strasser, P., Gimona, M., Moessler, H., Herzog, M. & Small, J. V. Mammalian calponin. Identification and expression of genetic variants. *FEBS Lett* **330**, 13-18 (1993).

82 Gabbiani, G. *et al.* Vascular smooth muscle cells differ from other smooth muscle cells: predominance of vimentin filaments and a specific alpha-type actin. *Proc Natl Acad Sci U S A* **78**, 298-302 (1981).

83 Hungerford, J. E., Owens, G. K., Argraves, W. S. & Little, C. D. Development of the aortic vessel wall as defined by vascular smooth muscle and extracellular matrix markers. *Dev Biol* **178**, 375-392, doi:10.1006/dbio.1996.0225 (1996).

84 Mack, C. P. & Owens, G. K. Regulation of smooth muscle alpha-actin expression in vivo is dependent on CArG elements within the 5' and first intron promoter regions. *Circ Res* **84**, 852-861 (1999).

85 Kim, S., Ip, H. S., Lu, M. M., Clendenin, C. & Parmacek, M. S. A serum response factor-dependent transcriptional regulatory program identifies distinct smooth muscle cell sublineages. *Mol Cell Biol* **17**, 2266-2278 (1997).

86 Li, L., Miano, J. M., Cserjesi, P. & Olson, E. N. SM22 alpha, a marker of adult smooth muscle, is expressed in multiple myogenic lineages during embryogenesis. *Circ Res* **78**, 188-195 (1996).

87 Frid, M. G., Shekhonin, B. V., Koteliansky, V. E. & Glukhova, M. A. Phenotypic changes of human smooth muscle cells during development: late expression of heavy caldesmon and calponin. *Dev Biol* **153**, 185-193 (1992).

88 Sobue, K. & Sellers, J. R. Caldesmon, a novel regulatory protein in smooth muscle and nonmuscle actomyosin systems. *J Biol Chem* **266**, 12115-12118 (1991).

89 Yano, H. *et al.* Transcriptional regulation of the chicken caldesmon gene. Activation of gizzard-type caldesmon promoter requires a CArG box-like motif. *J Biol Chem* **270**, 23661-23666 (1995).

90 Layne, M. D. *et al.* Characterization of the mouse aortic carboxypeptidase-like protein promoter reveals activity in differentiated and dedifferentiated vascular smooth muscle cells. *Circ Res* **90**, 728-736 (2002).

91 Watanabe, M. *et al.* Regulation of smooth muscle cell differentiation by AT-rich interaction domain transcription factors Mrf2alpha and Mrf2beta. *Circ Res* **91**, 382-389 (2002).

92 Bolmont, C., Lilienbaum, A., Paulin, D. & Grimaud, J. A. Expression of desmin gene in skeletal and smooth muscle by in situ hybridization using a human desmin gene probe. *J Submicrosc Cytol Pathol* **22**, 117-122 (1990).

93 Mericskay, M. *et al.* An overlapping CArG/octamer element is required for regulation of desmin gene transcription in arterial smooth muscle cells. *Dev Biol* **226**, 192-208, doi:10.1006/dbio.2000.9865 (2000).

94 Gimona, M., Furst, D. O. & Small, J. V. Metavinculin and vinculin from mammalian smooth muscle: bulk isolation and characterization. *J Muscle Res Cell Motil* **8**, 329-341 (1987).

95 Herring, B. P., Lyons, G. E., Hoggatt, A. M. & Gallagher, P. J. Telokin expression is restricted to smooth muscle tissues during mouse development. *Am J Physiol Cell Physiol* **280**, C12-21 (2001).

96 van der Loop, F. T., Schaart, G., Timmer, E. D., Ramaekers, F. C. & van Eys, G. J. Smoothelin, a novel cytoskeletal protein specific for smooth muscle cells. *J Cell Biol* **134**, 401-411 (1996).

97 Li, S., Sims, S., Jiao, Y., Chow, L. H. & Pickering, J. G. Evidence from a novel human cell clone that adult vascular smooth muscle cells can convert reversibly between noncontractile and contractile phenotypes. *Circ Res* **85**, 338-348 (1999).

98 Beamish, J. A., He, P., Kottke-Marchant, K. & Marchant, R. E. Molecular regulation of contractile smooth muscle cell phenotype: implications for vascular tissue engineering. *Tissue Eng Part B Rev* **16**, 467-491, doi:10.1089/ten.TEB.2009.0630 (2010).

99 Owens, G. K. & Thompson, M. M. Developmental changes in isoactin expression in rat aortic smooth muscle cells in vivo. Relationship between growth and cytodifferentiation. *J Biol Chem* **261**, 13373-13380 (1986).

100 Orlandi, A., Ropraz, P. & Gabbiani, G. Proliferative activity and alpha-smooth muscle actin expression in cultured rat aortic smooth muscle cells are differently modulated by transforming growth factor-beta 1 and heparin. *Exp Cell Res* **214**, 528-536, doi:10.1006/excr.1994.1290 (1994).

101 Worth, N. F., Rolfe, B. E., Song, J. & Campbell, G. R. Vascular smooth muscle cell phenotypic modulation in culture is associated with reorganisation of contractile and cytoskeletal proteins. *Cell Motil Cytoskeleton* **49**, 130-145, doi:10.1002/cm.1027 (2001).

102 Frid, M. G., Moiseeva, E. P. & Stenmark, K. R. Multiple phenotypically distinct smooth muscle cell populations exist in the adult and developing bovine pulmonary arterial media in vivo. *Circ Res* **75**, 669-681 (1994).

103 Frid, M. G., Dempsey, E. C., Durmowicz, A. G. & Stenmark, K. R. Smooth muscle cell heterogeneity in pulmonary and systemic vessels. Importance in vascular disease. *Arterioscler Thromb Vasc Biol* **17**, 1203-1209 (1997).

104 Hao, H. *et al.* Heterogeneity of smooth muscle cell populations cultured from pig coronary artery. *Arterioscler Thromb Vasc Biol* **22**, 1093-1099 (2002).

105 Hao, H., Gabbiani, G. & Bochaton-Piallat, M. L. Arterial smooth muscle cell heterogeneity: implications for atherosclerosis and restenosis development. *Arterioscler Thromb Vasc Biol* **23**, 1510-1520, doi:10.1161/01.ATV.0000090130.85752.ED (2003).

106 Kennedy, E. *et al.* Adult vascular smooth muscle cells in culture express neural stem cell markers typical of resident multipotent vascular stem cells. *Cell Tissue Res* **358**, 203-216, doi:10.1007/s00441-014-1937-2 (2014).

107 Zaniboni, A. *et al.* Cells derived from porcine aorta tunica media show mesenchymal stromal-like cell properties in in vitro culture. *Am J Physiol Cell Physiol* **306**, C322-333, doi:10.1152/ajpcell.00112.2013 (2014).

108 Zaniboni, A. *et al.* In vitro differentiation of porcine aortic vascular precursor cells to endothelial and vascular smooth muscle cells. *Am J Physiol Cell Physiol* **309**, C320-331, doi:10.1152/ajpcell.00049.2015 (2015).

109 Tang, Z., Wang, A., Wang, D. & Li, S. Smooth muscle cells: to be or not to be? Response to Nguyen et Al. *Circ Res* **112**, 23-26, doi:10.1161/CIRCRESAHA.112.281055 (2013).

110 Curtis, B. M. *et al.* Slow and sustained nitric oxide releasing compounds inhibit multipotent vascular stem cell proliferation and differentiation without causing cell death. *Biochem Biophys Res Commun* **450**, 208-212, doi:10.1016/j.bbrc.2014.05.087 (2014).
111 Kokkinopoulos, I. *et al.* Adventitial SCA-1(+) Progenitor Cell Gene Sequencing Reveals the Mechanisms of Cell Migration in Response to Hyperlipidemia. *Stem Cell Reports* **9**, 681-696, doi:10.1016/j.stemcr.2017.06.011 (2017).
112 Li, C. & Xu, Q. Mechanical stress-initiated signal transductions in vascular smooth muscle cells. *Cell Signal* **12**, 435-445 (2000).
113 Hu, Y. *et al.* Abundant progenitor cells in the adventitia contribute to atherosclerosis of vein grafts in ApoE-deficient mice. *J Clin Invest* **113**, 1258-1265, doi:10.1172/JCI19628 (2004).
114 Mayr, M. *et al.* Proteomic and metabolomic analysis of smooth muscle cells derived from the arterial media and adventitial progenitors of apolipoprotein E-deficient mice. *Circ Res* **102**, 1046-1056, doi:10.1161/CIRCRESAHA.108.174623 (2008).
115 Chen, Y. *et al.* Adventitial stem cells in vein grafts display multilineage potential that contributes to neointimal formation. *Arterioscler Thromb Vasc Biol* **33**, 1844-1851, doi:10.1161/ATVBAHA.113.300902 (2013).
116 Tigges, U., Komatsu, M. & Stallcup, W. B. Adventitial pericyte progenitor/mesenchymal stem cells participate in the restenotic response to arterial injury. *J Vasc Res* **50**, 134-144, doi:10.1159/000345524

000345524 (2013).
117 Albarran-Juarez, J., Kaur, H., Grimm, M., Offermanns, S. & Wettschureck, N. Lineage tracing of cells involved in atherosclerosis. *Atherosclerosis* **251**, 445-453, doi:10.1016/j.atherosclerosis.2016.06.012 (2016).
118 Yang, P. *et al.* Preexisting smooth muscle cells contribute to neointimal cell repopulation at an incidence varying widely among individual lesions. *Surgery* **159**, 602-612, doi:10.1016/j.surg.2015.08.015 (2016).
119 Tanaka, K., Sata, M., Hirata, Y. & Nagai, R. Diverse contribution of bone marrow cells to neointimal hyperplasia after mechanical vascular injuries. *Circ Res* **93**, 783-790, doi:10.1161/01.RES.0000096651.13001.B4 (2003).
120 Song, H. *et al.* Inhibitory role of reactive oxygen species in the differentiation of multipotent vascular stem cells into vascular smooth muscle cells in rats: a novel aspect of traditional culture of rat aortic smooth muscle cells. *Cell Tissue Res* **362**, 97-113, doi:10.1007/s00441-015-2193-9 (2015).
121 Kwak, B. R. *et al.* Biomechanical factors in atherosclerosis: mechanisms and clinical implications. *Eur Heart J* **35**, 3013-3020, 3020a-3020d, doi:10.1093/eurheartj/ehu353 (2014).
122 Ruiter, M. S. & Pesce, M. Mechanotransduction in Coronary Vein Graft Disease. *Front Cardiovasc Med* **5**, 20, doi:10.3389/fcvm.2018.00020 (2018).
123 Li, J., Wu, M., Chu, J., Sochol, R. & Patel, S. Engineering micropatterned surfaces to modulate the function of vascular stem cells. *Biochem Biophys Res Commun* **444**, 562-567, doi:10.1016/j.bbrc.2014.01.100 (2014).
124 Halka, A. T. *et al.* The effects of stretch on vascular smooth muscle cell phenotype in vitro. *Cardiovasc Pathol* **17**, 98-102, doi:10.1016/j.carpath.2007.03.001 (2008).
125 Haga, J. H., Li, Y. S. & Chien, S. Molecular basis of the effects of mechanical stretch on vascular smooth muscle cells. *J Biomech* **40**, 947-960, doi:10.1016/j.jbiomech.2006.04.011 (2007).
126 Jakkaraju, S., Zhe, X. & Schuger, L. Role of stretch in activation of smooth muscle cell lineage. *Trends Cardiovasc Med* **13**, 330-335 (2003).

127 Cappadona, C. *et al.* Phenotype dictates the growth response of vascular smooth muscle cells to pulse pressure in vitro. *Exp Cell Res* **250**, 174-186, doi:10.1006/excr.1999.4502 (1999).

128 Qiu, J. *et al.* Biomechanical regulation of vascular smooth muscle cell functions: from in vitro to in vivo understanding. *J R Soc Interface* **11**, 20130852, doi:10.1098/rsif.2013.0852 (2014).

129 Tock, J., Van Putten, V., Stenmark, K. R. & Nemenoff, R. A. Induction of SM-alpha-actin expression by mechanical strain in adult vascular smooth muscle cells is mediated through activation of JNK and p38 MAP kinase. *Biochem Biophys Res Commun* **301**, 1116-1121 (2003).

130 Yao, Q. P. *et al.* The role of SIRT6 in the differentiation of vascular smooth muscle cells in response to cyclic strain. *Int J Biochem Cell Biol* **49**, 98-104, doi:10.1016/j.biocel.2014.01.016 (2014).

131 Butcher, J. T., Barrett, B. C. & Nerem, R. M. Equibiaxial strain stimulates fibroblastic phenotype shift in smooth muscle cells in an engineered tissue model of the aortic wall. *Biomaterials* **27**, 5252-5258, doi:10.1016/j.biomaterials.2006.05.040 (2006).

132 Lee, J., Wong, M., Smith, Q. & Baker, A. B. A novel system for studying mechanical strain waveform-dependent responses in vascular smooth muscle cells. *Lab Chip* **13**, 4573-4582, doi:10.1039/c3lc50894c (2013).

133 Chapman, G. B., Durante, W., Hellums, J. D. & Schafer, A. I. Physiological cyclic stretch causes cell cycle arrest in cultured vascular smooth muscle cells. *Am J Physiol Heart Circ Physiol* **278**, H748-754 (2000).

134 Kona, S., Chellamuthu, P., Xu, H., Hills, S. R. & Nguyen, K. T. Effects of cyclic strain and growth factors on vascular smooth muscle cell responses. *Open Biomed Eng J* **3**, 28-38, doi:10.2174/1874120700903010028 (2009).

135 Morrow, D. *et al.* Biomechanical regulation of hedgehog signaling in vascular smooth muscle cells in vitro and in vivo. *Am J Physiol Cell Physiol* **292**, C488-496, doi:10.1152/ajpcell.00337.2005 (2007).

136 Qi, Y. X. *et al.* Cyclic strain modulates migration and proliferation of vascular smooth muscle cells via Rho-GDIalpha, Rac1, and p38 pathway. *J Cell Biochem* **109**, 906-914, doi:10.1002/jcb.22465 (2010).

137 Mills, I. *et al.* Strain activation of bovine aortic smooth muscle cell proliferation and alignment: study of strain dependency and the role of protein kinase A and C signaling pathways. *J Cell Physiol* **170**, 228-234, doi:10.1002/(SICI)1097-4652(199703)170:3<228::AID-JCP2>3.0.CO;2-Q (1997).

138 Seo, K. W. *et al.* Mechanical stretch increases MMP-2 production in vascular smooth muscle cells via activation of PDGFR-beta/Akt signaling pathway. *PLoS One* **8**, e70437, doi:10.1371/journal.pone.0070437 (2013).

139 O'Callaghan, C. J. & Williams, B. Mechanical strain-induced extracellular matrix production by human vascular smooth muscle cells: role of TGF-beta(1). *Hypertension* **36**, 319-324 (2000).

140 Tamura, K. *et al.* Molecular mechanism of fibronectin gene activation by cyclic stretch in vascular smooth muscle cells. *J Biol Chem* **275**, 34619-34627, doi:10.1074/jbc.M004421200 (2000).

141 Na, S. *et al.* Time-dependent changes in smooth muscle cell stiffness and focal adhesion area in response to cyclic equibiaxial stretch. *Ann Biomed Eng* **36**, 369-380, doi:10.1007/s10439-008-9438-7 (2008).

142 Zampetaki, A., Zhang, Z., Hu, Y. & Xu, Q. Biomechanical stress induces IL-6 expression in smooth muscle cells via Ras/Rac1-p38 MAPK-NF-kappaB signaling pathways. *Am J Physiol Heart Circ Physiol* **288**, H2946-2954, doi:10.1152/ajpheart.00919.2004 (2005).

143 Standley, P. R., Cammarata, A., Nolan, B. P., Purgason, C. T. & Stanley, M. A. Cyclic stretch induces vascular smooth muscle cell alignment via NO signaling. *Am J Physiol Heart Circ Physiol* **283**, H1907-1914, doi:10.1152/ajpheart.01043.2001 (2002).

144 Greiner, A. M., Biela, S. A., Chen, H., Spatz, J. P. & Kemkemer, R. Featured Article: Temporal responses of human endothelial and smooth muscle cells exposed to uniaxial cyclic tensile strain. *Exp Biol Med (Maywood)* **240**, 1298-1309, doi:10.1177/1535370215570191 (2015).

145 Liu, B. *et al.* Role of cyclic strain frequency in regulating the alignment of vascular smooth muscle cells in vitro. *Biophys J* **94**, 1497-1507, doi:10.1529/biophysj.106.098574 (2008).

146 Asanuma, K., Magid, R., Johnson, C., Nerem, R. M. & Galis, Z. S. Uniaxial strain upregulates matrix-degrading enzymes produced by human vascular smooth muscle cells. *Am J Physiol Heart Circ Physiol* **284**, H1778-1784, doi:10.1152/ajpheart.00494.2002 (2003).

147 McKnight, N. L. & Frangos, J. A. Strain rate mechanotransduction in aligned human vascular smooth muscle cells. *Ann Biomed Eng* **31**, 239-249 (2003).

148 Kanda, K., Matsuda, T. & Oka, T. Mechanical stress induced cellular orientation and phenotypic modulation of 3-D cultured smooth muscle cells. *ASAIO J* **39**, M686-690 (1993).

149 Kim, B. S. & Mooney, D. J. Scaffolds for engineering smooth muscle under cyclic mechanical strain conditions. *J Biomech Eng* **122**, 210-215 (2000).

150 Liao, S. W., Hida, K., Park, J. S. & Li, S. Mechanical regulation of matrix reorganization and phenotype of smooth muscle cells and mesenchymal stem cells in 3D matrix. *Conf Proc IEEE Eng Med Biol Soc* **7**, 5024-5027, doi:10.1109/IEMBS.2004.1404388 (2004).

151 Sharifpoor, S., Simmons, C. A., Labow, R. S. & Santerre, J. P. A study of vascular smooth muscle cell function under cyclic mechanical loading in a polyurethane scaffold with optimized porosity. *Acta Biomater* **6**, 4218-4228, doi:10.1016/j.actbio.2010.06.018 (2010).

152 Sharifpoor, S., Simmons, C. A., Labow, R. S. & Paul Santerre, J. Functional characterization of human coronary artery smooth muscle cells under cyclic mechanical strain in a degradable polyurethane scaffold. *Biomaterials* **32**, 4816-4829, doi:10.1016/j.biomaterials.2011.03.034 (2011).

153 Kim, B. S., Nikolovski, J., Bonadio, J. & Mooney, D. J. Cyclic mechanical strain regulates the development of engineered smooth muscle tissue. *Nat Biotechnol* **17**, 979-983, doi:10.1038/13671 (1999).

154 Nikolovski, J., Kim, B. S. & Mooney, D. J. Cyclic strain inhibits switching of smooth muscle cells to an osteoblast-like phenotype. *Faseb J* **17**, 455-457, doi:10.1096/fj.02-0459fje (2003).

155 Hipper, A. & Isenberg, G. Cyclic mechanical strain decreases the DNA synthesis of vascular smooth muscle cells. *Pflugers Arch* **440**, 19-27 (2000).

156 Cheng, W. P., Hung, H. F., Wang, B. W. & Shyu, K. G. The molecular regulation of GADD153 in apoptosis of cultured vascular smooth muscle cells by cyclic mechanical stretch. *Cardiovasc Res* **77**, 551-559, doi:10.1093/cvr/cvm057 (2008).

157 Morrow, D. *et al.* Cyclic strain inhibits Notch receptor signaling in vascular smooth muscle cells in vitro. *Circ Res* **96**, 567-575, doi:10.1161/01.RES.0000159182.98874.43 (2005).

158 Iwasaki, H., Yoshimoto, T., Sugiyama, T. & Hirata, Y. Activation of cell adhesion kinase beta by mechanical stretch in vascular smooth muscle cells. *Endocrinology* **144**, 2304-2310, doi:10.1210/en.2002-220939 (2003).

159 Chen, Q., Li, W., Quan, Z. & Sumpio, B. E. Modulation of vascular smooth muscle cell alignment by cyclic strain is dependent on reactive oxygen species and P38 mitogen-activated protein kinase. *J Vasc Surg* **37**, 660-668, doi:10.1067/mva.2003.95 (2003).
160 Chaqour, B., Howard, P. S., Richards, C. F. & Macarak, E. J. Mechanical stretch induces platelet-activating factor receptor gene expression through the NF-kappaB transcription factor. *J Mol Cell Cardiol* **31**, 1345-1355, doi:10.1006/jmcc.1999.0967 (1999).
161 Julien, M. A., Wang, P., Haller, C. A., Wen, J. & Chaikof, E. L. Mechanical strain regulates syndecan-4 expression and shedding in smooth muscle cells through differential activation of MAP kinase signaling pathways. *Am J Physiol Cell Physiol* **292**, C517-525, doi:10.1152/ajpcell.00093.2006 (2007).
162 Sotoudeh, M. *et al.* Induction of apoptosis in vascular smooth muscle cells by mechanical stretch. *Am J Physiol Heart Circ Physiol* **282**, H1709-1716, doi:10.1152/ajpheart.00744.2001 (2002).
163 Ma, Y. H., Ling, S. & Ives, H. E. Mechanical strain increases PDGF-B and PDGF beta receptor expression in vascular smooth muscle cells. *Biochem Biophys Res Commun* **265**, 606-610, doi:10.1006/bbrc.1999.1718 (1999).
164 Jiang, M. J., Yu, Y. J., Chen, Y. L., Lee, Y. M. & Hung, L. S. Cyclic strain stimulates monocyte chemotactic protein-1 mRNA expression in smooth muscle cells. *J Cell Biochem* **76**, 303-310 (1999).
165 Pittenger, M. F. *et al.* Multilineage potential of adult human mesenchymal stem cells. *Science* **284**, 143-147 (1999).
166 Chen, Y. J. *et al.* Effects of cyclic mechanical stretching on the mRNA expression of tendon/ligament-related and osteoblast-specific genes in human mesenchymal stem cells. *Connect Tissue Res* **49**, 7-14, doi:10.1080/03008200701818561 (2008).
167 Altman, G. H. *et al.* Cell differentiation by mechanical stress. *Faseb J* **16**, 270-272, doi:10.1096/fj.01-0656fje (2002).
168 Even-Ram, S., Artym, V. & Yamada, K. M. Matrix control of stem cell fate. *Cell* **126**, 645-647, doi:10.1016/j.cell.2006.08.008 (2006).
169 Engler, A. J., Sen, S., Sweeney, H. L. & Discher, D. E. Matrix elasticity directs stem cell lineage specification. *Cell* **126**, 677-689, doi:10.1016/j.cell.2006.06.044 (2006).
170 Gong, Z. & Niklason, L. E. Use of human mesenchymal stem cells as alternative source of smooth muscle cells in vessel engineering. *Methods Mol Biol* **698**, 279-294, doi:10.1007/978-1-60761-999-4_21 (2011).
171 Huang, Y. *et al.* Effect of cyclic strain on cardiomyogenic differentiation of rat bone marrow derived mesenchymal stem cells. *PLoS One* **7**, e34960, doi:10.1371/journal.pone.0034960 (2012).
172 Ku, C. H. *et al.* Collagen synthesis by mesenchymal stem cells and aortic valve interstitial cells in response to mechanical stretch. *Cardiovasc Res* **71**, 548-556, doi:10.1016/j.cardiores.2006.03.022 (2006).
173 Haghighipour, N., Heidarian, S., Shokrgozar, M. A. & Amirizadeh, N. Differential effects of cyclic uniaxial stretch on human mesenchymal stem cell into skeletal muscle cell. *Cell Biol Int* **36**, 669-675, doi:10.1042/CBI20110400 (2012).
174 Delaine-Smith, R. M. & Reilly, G. C. Mesenchymal stem cell responses to mechanical stimuli. *Muscles Ligaments Tendons J* **2**, 169-180 (2012).
175 Guilak, F. *et al.* Control of stem cell fate by physical interactions with the extracellular matrix. *Cell Stem Cell* **5**, 17-26, doi:10.1016/j.stem.2009.06.016 (2009).
176 Reilly, G. C. & Engler, A. J. Intrinsic extracellular matrix properties regulate stem cell differentiation. *J Biomech* **43**, 55-62, doi:10.1016/j.jbiomech.2009.09.009 (2010).
177 Dumas, V. *et al.* Extracellular matrix produced by osteoblasts cultured under low-magnitude, high-frequency stimulation is favourable to osteogenic differentiation of

mesenchymal stem cells. *Calcif Tissue Int* **87**, 351-364, doi:10.1007/s00223-010-9394-8 (2010).

178 Jang, J. Y. *et al.* Combined effects of surface morphology and mechanical straining magnitudes on the differentiation of mesenchymal stem cells without using biochemical reagents. *J Biomed Biotechnol* **2011**, 860652, doi:10.1155/2011/860652 (2011).

179 Mehlhorn, A. T. *et al.* Differential expression pattern of extracellular matrix molecules during chondrogenesis of mesenchymal stem cells from bone marrow and adipose tissue. *Tissue Eng* **12**, 2853-2862, doi:10.1089/ten.2006.12.2853 (2006).

180 Hamilton, D. W., Maul, T. M. & Vorp, D. A. Characterization of the response of bone marrow-derived progenitor cells to cyclic strain: implications for vascular tissue-engineering applications. *Tissue Eng* **10**, 361-369, doi:10.1089/107632704323061726 (2004).

181 Yao, R. & Wong, J. Y. The effects of mechanical stimulation on controlling and maintaining marrow stromal cell differentiation into vascular smooth muscle cells. *J Biomech Eng* **137**, 020907, doi:10.1115/1.4029255 (2015).

182 Park, J. S. *et al.* Differential effects of equiaxial and uniaxial strain on mesenchymal stem cells. *Biotechnol Bioeng* **88**, 359-368, doi:10.1002/bit.20250 (2004).

183 Kurpinski, K., Chu, J., Wang, D. & Li, S. Proteomic Profiling of Mesenchymal Stem Cell Responses to Mechanical Strain and TGF-beta1. *Cell Mol Bioeng* **2**, 606-614, doi:10.1007/s12195-009-0090-6 (2009).

184 Kurpinski, K., Chu, J., Hashi, C. & Li, S. Anisotropic mechanosensing by mesenchymal stem cells. *Proc Natl Acad Sci U S A* **103**, 16095-16100, doi:10.1073/pnas.0604182103 (2006).

185 Park, J. S. *et al.* The effect of matrix stiffness on the differentiation of mesenchymal stem cells in response to TGF-beta. *Biomaterials* **32**, 3921-3930, doi:10.1016/j.biomaterials.2011.02.019 (2011).

186 Suzuki, S. *et al.* Effects of extracellular matrix on differentiation of human bone marrow-derived mesenchymal stem cells into smooth muscle cell lineage: utility for cardiovascular tissue engineering. *Cells Tissues Organs* **191**, 269-280, doi:10.1159/000260061 (2010).

187 Wang, D., Li, L. K., Dai, T., Wang, A. & Li, S. Adult Stem Cells in Vascular Remodeling. *Theranostics* **8**, 815-829, doi:10.7150/thno.19577 (2018).

188 Mauretti, A. *et al.* Cardiomyocyte progenitor cell mechanoresponse unrevealed: strain avoidance and mechanosome development. *Integr Biol (Camb)* **8**, 991-1001, doi:10.1039/c6ib00117c (2016).

189 French, K. M. *et al.* Fibronectin and Cyclic Strain Improve Cardiac Progenitor Cell Regenerative Potential In Vitro. *Stem Cells Int* **2016**, 8364382, doi:10.1155/2016/8364382 (2016).

190 Shimizu, N. *et al.* Cyclic strain induces mouse embryonic stem cell differentiation into vascular smooth muscle cells by activating PDGF receptor beta. *J Appl Physiol (1985)* **104**, 766-772, doi:10.1152/japplphysiol.00870.2007 (2008).

191 Qin, H. *et al.* Effects of extracellular matrix on phenotype modulation and MAPK transduction of rat aortic smooth muscle cells in vitro. *Exp Mol Pathol* **69**, 79-90, doi:10.1006/exmp.2000.2321 (2000).

192 Yamamoto, M., Yamamoto, K. & Noumura, T. Type I collagen promotes modulation of cultured rabbit arterial smooth muscle cells from a contractile to a synthetic phenotype. *Exp Cell Res* **204**, 121-129, doi:10.1006/excr.1993.1016 (1993).

193 Beamish, J. A. *et al.* The influence of RGD-bearing hydrogels on the re-expression of contractile vascular smooth muscle cell phenotype. *Biomaterials* **30**, 4127-4135, doi:10.1016/j.biomaterials.2009.04.038 (2009).

194 Elliott, J. T. *et al.* Vascular smooth muscle cell response on thin films of collagen. *Matrix Biol* **24**, 489-502, doi:10.1016/j.matbio.2005.07.005 (2005).
195 Peyton, S. R., Raub, C. B., Keschrumrus, V. P. & Putnam, A. J. The use of poly(ethylene glycol) hydrogels to investigate the impact of ECM chemistry and mechanics on smooth muscle cells. *Biomaterials* **27**, 4881-4893, doi:10.1016/j.biomaterials.2006.05.012 (2006).
196 Sazonova, O. V. *et al.* Extracellular matrix presentation modulates vascular smooth muscle cell mechanotransduction. *Matrix Biol* **41**, 36-43, doi:10.1016/j.matbio.2014.11.001 (2015).
197 Li, S. *et al.* Genomic analysis of smooth muscle cells in 3-dimensional collagen matrix. *Faseb J* **17**, 97-99, doi:10.1096/fj.02-0256fje (2003).
198 Redecker-Beuke, B., Thie, M., Rauterberg, J. & Robenek, H. Aortic smooth muscle cells in a three-dimensional collagen lattice culture. Evidence for posttranslational regulation of collagen synthesis. *Arterioscler Thromb* **13**, 1572-1579 (1993).
199 Ryan, A. J. & O'Brien, F. J. Insoluble elastin reduces collagen scaffold stiffness, improves viscoelastic properties, and induces a contractile phenotype in smooth muscle cells. *Biomaterials* **73**, 296-307, doi:10.1016/j.biomaterials.2015.09.003 (2015).
200 Schlumberger, W., Thie, M., Rauterberg, J. & Robenek, H. Collagen synthesis in cultured aortic smooth muscle cells. Modulation by collagen lattice culture, transforming growth factor-beta 1, and epidermal growth factor. *Arterioscler Thromb* **11**, 1660-1666 (1991).
201 Nagayama, K., Uchida, K. & Sato, A. A novel micro-grooved collagen substrate for inducing vascular smooth muscle differentiation through cell tissue arrangement and nucleus remodeling. *J Mech Behav Biomed Mater* **90**, 295-305, doi:10.1016/j.jmbbm.2018.10.005 (2019).
202 Vernon, R. B., Gooden, M. D., Lara, S. L. & Wight, T. N. Microgrooved fibrillar collagen membranes as scaffolds for cell support and alignment. *Biomaterials* **26**, 3131-3140, doi:10.1016/j.biomaterials.2004.08.011 (2005).
203 Yim, E. K. *et al.* Nanopattern-induced changes in morphology and motility of smooth muscle cells. *Biomaterials* **26**, 5405-5413, doi:10.1016/j.biomaterials.2005.01.058 (2005).
204 Thakar, R. G. *et al.* Cell-shape regulation of smooth muscle cell proliferation. *Biophys J* **96**, 3423-3432, doi:10.1016/j.bpj.2008.11.074 (2009).
205 Alford, P. W., Nesmith, A. P., Seywerd, J. N., Grosberg, A. & Parker, K. K. Vascular smooth muscle contractility depends on cell shape. *Integr Biol (Camb)* **3**, 1063-1070, doi:10.1039/c1ib00061f (2011).
206 Cao, Y. *et al.* Regulating orientation and phenotype of primary vascular smooth muscle cells by biodegradable films patterned with arrays of microchannels and discontinuous microwalls. *Biomaterials* **31**, 6228-6238, doi:10.1016/j.biomaterials.2010.04.059 (2010).
207 Nivison-Smith, L. & Weiss, A. S. Alignment of human vascular smooth muscle cells on parallel electrospun synthetic elastin fibers. *J Biomed Mater Res A* **100**, 155-161, doi:10.1002/jbm.a.33255 (2012).
208 Agrawal, A. *et al.* Smooth Muscle Cell Alignment and Phenotype Control by Melt Spun Polycaprolactone Fibers for Seeding of Tissue Engineered Blood Vessels. *Int J Biomater* **2015**, 434876, doi:10.1155/2015/434876 (2015).
209 Glawe, J. D., Hill, J. B., Mills, D. K. & McShane, M. J. Influence of channel width on alignment of smooth muscle cells by high-aspect-ratio microfabricated elastomeric cell culture scaffolds. *J Biomed Mater Res A* **75**, 106-114, doi:10.1002/jbm.a.30403 (2005).
210 Sarkar, S., Dadhania, M., Rourke, P., Desai, T. A. & Wong, J. Y. Vascular tissue engineering: microtextured scaffold templates to control organization of vascular smooth muscle cells and extracellular matrix. *Acta Biomater* **1**, 93-100, doi:10.1016/j.actbio.2004.08.003 (2005).

211 Biela, S. A., Su, Y., Spatz, J. P. & Kemkemer, R. Different sensitivity of human endothelial cells, smooth muscle cells and fibroblasts to topography in the nano-micro range. *Acta Biomater* **5**, 2460-2466, doi:10.1016/j.actbio.2009.04.003 (2009).

212 Parandakh, A., Anbarlou, A., Tafazzoli-Shadpour, M., Ardeshirylajimi, A. & Khani, M. M. Substrate topography interacts with substrate stiffness and culture time to regulate mechanical properties and smooth muscle differentiation of mesenchymal stem cells. *Colloids Surf B Biointerfaces* **173**, 194-201, doi:10.1016/j.colsurfb.2018.09.066 (2019).

213 Li, X. *et al.* Uniaxial mechanical strain modulates the differentiation of neural crest stem cells into smooth muscle lineage on micropatterned surfaces. *PLoS One* **6**, e26029, doi:10.1371/journal.pone.0026029 (2011).

214 Li, X., Chu, J. S., Yang, L. & Li, S. Anisotropic effects of mechanical strain on neural crest stem cells. *Ann Biomed Eng* **40**, 598-605, doi:10.1007/s10439-011-0403-5 (2012).

215 Wang, D. *et al.* Proteomic profiling of bone marrow mesenchymal stem cells upon transforming growth factor beta1 stimulation. *J Biol Chem* **279**, 43725-43734, doi:10.1074/jbc.M407368200 (2004).

216 Kinner, B., Zaleskas, J. M. & Spector, M. Regulation of smooth muscle actin expression and contraction in adult human mesenchymal stem cells. *Exp Cell Res* **278**, 72-83 (2002).

217 Kurpinski, K. *et al.* Transforming growth factor-beta and notch signaling mediate stem cell differentiation into smooth muscle cells. *Stem Cells* **28**, 734-742, doi:10.1002/stem.319 (2010).

218 Narita, Y., Yamawaki, A., Kagami, H., Ueda, M. & Ueda, Y. Effects of transforming growth factor-beta 1 and ascorbic acid on differentiation of human bone-marrow-derived mesenchymal stem cells into smooth muscle cell lineage. *Cell Tissue Res* **333**, 449-459, doi:10.1007/s00441-008-0654-0 (2008).

219 Dartsch, P. C., Hammerle, H. & Betz, E. Orientation of cultured arterial smooth muscle cells growing on cyclically stretched substrates. *Acta Anat (Basel)* **125**, 108-113 (1986).

220 Ritchie, A. C., Wijaya, S., Ong, W. F., Zhong, S. P. & Chian, K. S. Dependence of alignment direction on magnitude of strain in esophageal smooth muscle cells. *Biotechnol Bioeng* **102**, 1703-1711, doi:10.1002/bit.22190 (2009).

221 Takemasa, T., Sugimoto, K. & Yamashita, K. Amplitude-dependent stress fiber reorientation in early response to cyclic strain. *Exp Cell Res* **230**, 407-410, doi:10.1006/excr.1996.3428 (1997).

222 Neidlinger-Wilke, C., Grood, E. S., Wang, J.-C., Brand, R. A. & Claes, L. Cell alignment is induced by cyclic changes in cell length: studies of cells grown in cyclically stretched substrates. *J Orthop Res* **19**, 286-293, doi:10.1016/S0736-0266(00)00029-2 (2001).

223 Kennedy, E. *et al.* Embryonic rat vascular smooth muscle cells revisited - a model for neonatal, neointimal SMC or differentiated vascular stem cells? *Vasc Cell* **6**, 6, doi:10.1186/2045-824x-6-6 (2014).

224 Colombo, A., Zahedmanesh, H., Toner, D. M., Cahill, P. A. & Lally, C. A method to develop mock arteries suitable for cell seeding and in-vitro cell culture experiments. *J Mech Behav Biomed Mater* **3**, 470-477, doi:10.1016/j.jmbbm.2010.04.003 (2010).

225 Fomovsky, G. M. & Holmes, J. W. Evolution of scar structure, mechanics, and ventricular function after myocardial infarction in the rat. *Am J Physiol Heart Circ Physiol* **298**, H221-228, doi:10.1152/ajpheart.00495.2009 (2010).

226 Sato, K., Adachi, T., Matsuo, M. & Tomita, Y. Quantitative evaluation of threshold fiber strain that induces reorganization of cytoskeletal actin fiber structure in osteoblastic cells. *J Biomech* **38**, 1895-1901, doi:10.1016/j.jbiomech.2004.08.012 (2005).

227 Kaunas, R., Nguyen, P., Usami, S. & Chien, S. Cooperative effects of Rho and mechanical stretch on stress fiber organization. *Proc Natl Acad Sci U S A* **102**, 15895-15900, doi:10.1073/pnas.0506041102 (2005).

228 Greiner, A. M., Chen, H., Spatz, J. P. & Kemkemer, R. Cyclic tensile strain controls cell shape and directs actin stress fiber formation and focal adhesion alignment in spreading cells. *PLoS One* **8**, e77328, doi:10.1371/journal.pone.0077328 (2013).
229 Hsu, H. J., Lee, C. F. & Kaunas, R. A dynamic stochastic model of frequency-dependent stress fiber alignment induced by cyclic stretch. *PLoS One* **4**, e4853, doi:10.1371/journal.pone.0004853 (2009).
230 Grootaert, M. O. J. *et al.* Vascular smooth muscle cell death, autophagy and senescence in atherosclerosis. *Cardiovasc Res* **114**, 622-634, doi:10.1093/cvr/cvy007 (2018).
231 Pajerowski, J. D., Dahl, K. N., Zhong, F. L., Sammak, P. J. & Discher, D. E. Physical plasticity of the nucleus in stem cell differentiation. *Proc Natl Acad Sci U S A* **104**, 15619-15624, doi:10.1073/pnas.0702576104 (2007).
232 Aureille, J., Belaadi, N. & Guilluy, C. Mechanotransduction via the nuclear envelope: a distant reflection of the cell surface. *Curr Opin Cell Biol* **44**, 59-67, doi:10.1016/j.ceb.2016.10.003 (2017).
233 Driscoll, T. P., Cosgrove, B. D., Heo, S. J., Shurden, Z. E. & Mauck, R. L. Cytoskeletal to Nuclear Strain Transfer Regulates YAP Signaling in Mesenchymal Stem Cells. *Biophys J* **108**, 2783-2793, doi:10.1016/j.bpj.2015.05.010 (2015).
234 Guilluy, C. & Burridge, K. Nuclear mechanotransduction: forcing the nucleus to respond. *Nucleus* **6**, 19-22, doi:10.1080/19491034.2014.1001705 (2015).
235 Zahedmanesh, H. & Lally, C. A multiscale mechanobiological modelling framework using agent-based models and finite element analysis: application to vascular tissue engineering. *Biomech Model Mechanobiol* **11**, 363-377, doi:10.1007/s10237-011-0316-0 (2012).
236 Campbell, E. M., Cahill, P. A. & Lally, C. Investigation of a small-diameter decellularised artery as a potential scaffold for vascular tissue engineering; biomechanical evaluation and preliminary cell seeding. *J Mech Behav Biomed Mater* **14**, 130-142, doi:10.1016/j.jmbbm.2012.06.001 (2012).
237 Wall, M. E., Weinhold, P. S., Siu, T., Brown, T. D. & Banes, A. J. Comparison of cellular strain with applied substrate strain in vitro. *J Biomech* **40**, 173-181, doi:10.1016/j.jbiomech.2005.10.032 (2007).
238 Weiser, M. C., Majack, R. A., Tucker, A. & Orton, E. C. Static tension is associated with increased smooth muscle cell DNA synthesis in rat pulmonary arteries. *Am J Physiol* **268**, H1133-1138, doi:10.1152/ajpheart.1995.268.3.H1133 (1995).
239 Sandison, M. E., Dempster, J. & McCarron, J. G. The transition of smooth muscle cells from a contractile to a migratory, phagocytic phenotype: direct demonstration of phenotypic modulation. *J Physiol* **594**, 6189-6209, doi:10.1113/JP272729 (2016).
240 Goli-Malekabadi, Z., Tafazzoli-Shadpour, M., Rabbani, M. & Janmaleki, M. Effect of uniaxial stretch on morphology and cytoskeleton of human mesenchymal stem cells: static vs. dynamic loading. *Biomed Tech (Berl)* **56**, 259-265, doi:10.1515/bmt.2011.109 (2011).
241 Worth, N. F., Rolfe, B. E., Song, J. & Campbell, G. R. Vascular smooth muscle cell phenotypic modulation in culture is associated with reorganisation of contractile and cytoskeletal proteins. *Cell Motil Cytoskeleton* **49**, 130-145, doi:10.1002/cm.1027 (2001).
242 Colombo, A., Cahill, P. A. & Lally, C. An analysis of the strain field in biaxial Flexcell membranes for different waveforms and frequencies. *Proc Inst Mech Eng H* **222**, 1235-1245 (2008).
243 Tintut, Y. *et al.* Multilineage potential of cells from the artery wall. *Circulation* **108**, 2505-2510, doi:10.1161/01.CIR.0000096485.64373.C5 (2003).